MONITORING AND MODELLING COMPONENTS OF THE WATER BALANCE IN A GRASSLAND CATCHMENT IN THE SUMMER RAINFALL AREA OF SOUTH AFRICA

by

CS Everson, GL Molefe & TM Everson

CSIR Environmentek
% Department of Agronomy
University of Natal
Private Bag X01
Scottsville
Pietermaritzburg
3209

Final report to the Water Research Commission

WRC Report No: 493/1/98

ISBN No 1 86845 443 6

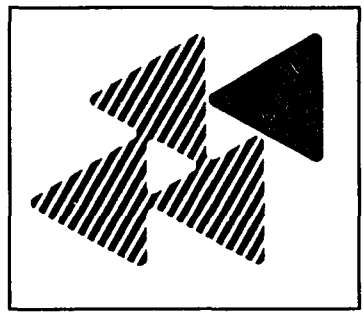

CSIR

Table of Contents

CHAPTER 4

EXECUTIVE SUMMARY

1. Motivation

To meet rising demands for water from all sectors of society, there is a need to optimize the yield of water from South African catchments. With increasing demands for grazing land and afforestation these catchments may be targeted for different land management practices. There is growing concern that such changes in the land management of the traditionally conserved grassland areas will result in reduced water yield from catchments. Estimates of the water use of grassland in mountain catchments are necessary to provide a sound baseline of natural water yields under grassland. An understanding of the principal factors (meteorological, plant and soil) affecting the water balance of a grassland catchment is necessary for planning future water supplies.

Traditionally, estimates of water use of vegetation in gauged catchments are made by determining the difference between precipitation and streamflow. However, these estimates are not precise enough to enable accurate predictions of water yield from hydrological models. Since the water use of natural grassland largely depends on available energy, accurate estimates of evaporation from the vegetation can only be made by quantifying the catchment energy budget. This study uses the Bowen ratio energy balance technique to measure the water use of a grassland catchment. This is the first long term study in South Africa in which all the components of the catchment water balance are measured simultaneously.

One of the most difficult hydrological processes to measure and monitor is soil water content. With continual advances in soil water measurement, there are a number of new techniques available to the scientist. This study tests two technologies that are currently used in hydrological research: the soil moisture capacitance technique and time domain reflectometry.

2. Objectives

2.1 *Project aims*:

(i) To quantify the spatial and temporal patterns of evaporation and soil water within a grassland catchment.

(ii) To describe these processes in terms of the controlling environmental variables.

(iii) To provide a modelling framework for the catchment water balance for use in water resource management planning.

2.2 Background

As large areas of grassland are being converted to forest and crops there is a need to determine the changes in water yield associated with different land management practices. In catchments where rainfall is seasonal, the distribution of streamflow over the year may change, leading to flooding where the grassland is over grazed and to shortages of water during dry periods. Reliable estimates of the rate of evaporation during wet and dry seasons is necessary to aid planners in policy decisions.

Because adequate hydrological measurements seldom take place where the decisions are most needed, hydrological models are developed to predict changes in water yield. Simulation models, which predict hydrological processes from a catchment to a regional scale, often represent hydrological processes in a vertical dimension and are driven by input which is only from a point. Water managers are therefore faced with the problem of accounting for soil water flow down a slope. This problem is overcome using distributed hydrological models which can determine hydrological flux in the second and third dimensions of catchments. Micrometeorological methods have the advantage that evapotranspiration may be established from relatively simple meteorological parameters (e.g. radiation, temperature, humidity and wind speed) over short periods of time. In this study weather and streamflow data were collected over a five year period in a 97 ha grassland catchment to test the reliability of existing hydrological

models (TOPOG and ACRU). This period represented a range hydrological years, including the driest year on record and a very wet year.

3. Results and conclusions

3.1 Evaporation

Total evaporation was measured using the Bowen ratio energy balance technique and compared to evaporation estimated from annual precipitation and discharge data. Results show that in normal years precipitation is equally split between evaporation and streamflow. In dry years evaporation is the dominant component of the water balance. The data were used to develop expressions to calculate annual streamflow and evaporation from the ratio of precipitation to potential evaporation.

The average annual evaporation over the study period was 695 mm. Mean annual rainfall is 1299 mm and therefore approximately 54% of the annual rainfall is evaporated back into the atmosphere and is not available for streamflow generation. The low variation in evaporation, irrespective of the high variability in rainfall, indicates that in the Drakensberg soil moisture is not the main factor limiting evaporation. Low rainfall years (<1100 mm) were generally associated with high incoming radiation (> 6150 MJ $^{-2}$).

This study showed that evaporation from the riparian zone was significantly higher (33%) than the north facing site. This can be attributed to the presence of open water at the riparian site which is freely evaporated (potential evaporation). Evaporation models may therefore under-estimate water losses from catchments with extensive riparian zones.

Slope and aspect had a negligible effect on evaporation in winter when there is a low evaporative demand. However, aspect induced differences were apparent in summer where evaporation from the north site was 10% higher than the east and west facing aspects.

The results of this study indicate that the evaporation rate of grassland catchments can be accurately modelled by using the Penman-Monteith combination equation. Although this is an elaborate model and requires detailed climatic data (net radiation, air temperature, vapour

pressure and wind speed) its accuracy far outweighs these considerations. Net radiation is the only parameter that is not routinely measured at South African weather stations. It can, however, be easily estimated from solar radiation which is measured at most weather stations, provided the correct value of albedo is used.

3.2 Soil water

Soil water is a critical variable in the modelling of infiltration, flux and redistribution of water in catchments. Accurate measurement of soil water is therefore an important factor in estimating water budgets. The comparative study of the capacitance probe, neutron probe and time domain reflectometry techniques for measuring soil water indicated that the most accurate results were obtained with the neutron probe and time domain reflectometry. Time domain reflectometry has the advantage that it does not require calibration, is easily automated and can be used to collect hourly or daily data.

Changes in the soil water storage of catchment VI were measured over four years and used to model the temporal and spatial distribution of soil water on a hillslope. Soil moisture changes in the grassland catchment of this study varied significantly with season. The annual cycle of soil moisture approximated a sine wave with a maximum in February and a minimum in July. In the dry season there was a gradient of increasing moisture content downslope from the ridge. This indicates that the stream was fed by moisture moving slowly downslope under conditions of unsaturated flow. The lower part of the slope therefore produced runoff early in the storm period while infiltration was still occurring on the upper section of the hillslope transect. The saturated area of the riparian zone increased or decreased in size depending on rainfall amount and antecedent wetness of the soil. This zone therefore produced a quick release of water during storms.

Subsurface stormflow was a major component of total stormflow from these grassland catchments. Part of the baseflow from the catchment originated from the deep coarse-textured soils. During the dry winter period baseflow was sustained by the slow drainage of the unsaturated soil at the upper part of the hillslope. The high water levels in the saturated zone were maintained by subsurface flow from the up slope parts of the catchment.

The results of this study indicate that unsaturated subsurface flow of water in the soil is an important component of the hydrology of these catchments. Therefore lumped type models are unlikely to accurately determine the complex moisture conditions found on the hillslope of this study. Models that account for the spatial distribution of soil moisture within a catchment are likely to be the most accurate.

3.3 Water balance

All components of the water balance equation were measured in catchment VI from 1990/91 to 1994/95 (Table I). Differences between the measured runoff and that calculated using the water balance equation were small (<4.1% of mean annual rainfall). This close agreement shows that the water balance was successfully determined and confirms the validity of the data collected in this study.

Table I. Components of the water balance equation measured in catchment VI (1990/91 to 1993/94). P = precipitation; E_a = actual evaporation; SS = soil storage; Q = streamflow calculated using the water balance equation; and Q_a = actual streamflow.

Year	P	-	E_a	-	SS	=	Q	Q_a	Difference	% of P
1990/91	1223	-	681	-	(-11)	=	553	603	-50 mm	4.100
1991/92	1092	-	752	-	(-45)	=	385	366	+19 mm	1.700
1992/93	1093	-	698	-	(+07)	=	388	391	-03 mm	0.003
1993/94	1469	-	651	-	(-14)	=	822	863	-41 mm	0.030

3.4 Model testing

The data collected in this study were used to test two hydrological models, TOPOG (a distributed model) and ACRU (a one dimensional model).The study has shown that the practical difficulties of computational analysis using TOPOG will limit the implementation of this model. The ACRU model generally predicted streamflow well except in wet years. The model was successfully validated against the catchment VI data set. One of the limitations of ACRU is its inability to account for subsurface soil water flow in a catchment.

4. Extent to which contract objectives have been met

* *To quantify the spatial and temporal patterns of evaporation and soil water within a grassland catchment.*

Evaporation and soil water were monitored continuously over a five year period in the remote catchment VI study site. This is a unique data set which makes a significant contribution to our understanding of the hydrological processes that operate in montane grassland catchments.

* *To describe these processes in terms of the controlling environmental variables.*

The study showed that the Penman-Monteith equation was suitable for describing the effect of environmental variables on evaporation.

Soil water was modelled in four dimensions and showed the complex distribution of volumetric soil water within the hillslope. The ability to extrapolate soil moisture on a hillslope in time and space provides a powerful tool for landscape management.

* *To provide a modelling framework for the catchment water balance for use in water resource management planning.*

The initial simulation undertaken with the ACRU model indicates that hydrological processes in catchment VI can be modelled successfully. Refinements may be necessary to reduce the 15% under-estimation of streamflow.

5. Useful contributions in the report

* The intensive long-term monitoring of all the components of the water balance of a catchment provides a unique data set for future research.
* The five-year hydrological data set enabled validation of ACRU for the Natal Drakensberg catchments.

* The study pioneered the use of the Bowen ratio technique for routine monitoring of evaporation in remote sites in South Africa.
* Testing of the time domain reflectometry technique in South Africa.
* The development of four dimensional maps of soil water content.
* The development of a model to predict evaporation and streamflow from rainfall.

6. Future research

6.1 *The effect of degradation on hillslope hydrology*

This study was undertaken in an undisturbed area of the Natal Drakensberg. There are large tracts of land in the Drakensberg and its foothills which are under the communal land system. This generally results in overgrazing and severe soil erosion which changes the hydrological response of these catchments. The data from this study provide a means for comparison with the degraded catchments which are such a common feature of the South African landscape. If the areas under this severe pressure are to be managed wisely then an understanding of the altered hydrological processes needs to be understood.

6.2 *Soils of the Drakensberg*

In this study and a number of previous studies the soils of the Little Berg have been shown to have some unusual features which appear to make them unique in the South African context. These features are low bulk densities (± 0.8) and very high water holding capacities. Current hydrological models are unable to cope with these soils and their geographical extent needs to be established.

6.3 *Establish linkages*

This research has concentrated on the measurement of the hydrological variables in a catchment. The next step is to link the driving variables of rainfall and evaporation to the soil water content and streamflow.

6.4 *Refinement of ACRU*

The development of the ACRU model is a dynamic process requiring ongoing

refinement. The present study provides a unique long term data set for continued development and improvement of the ACRU model.

7. Acknowledgements

We gratefully acknowledge the Water Research Commission for funding this study. The following members of the steering committee are thanked for their support and contributions:

Dr GC Green	Water Research Commission
Mr H. Maaren	Water Research Commission
Prof BE Kelbe	University of Zululand
Prof M Savage	University of Natal
Prof JF Botha	University of the Orange Free State
Prof JM de Jager	University of the Orange Free State
Mr DB Versfeld	CSIR
Mr D Huyser	Water Research Commission (secretary)

Sincere thanks are given to Peter Clarke, Mike Johnston, Andrew Pike, Mike Savage, Bruce Metelerkamp and Roland Schulze for their assistance in the project.

Staff of the Department of Water Affairs and Forestry are thanked for their help in calibrating the weirs and their persistence in drilling the boreholes. The Forestry branch is also thanked for their initial funding of the project.

The technical support of members of the project team, Karen Hudson, Alison Misselhorn and Phillip Vilakazi, was invaluable. Mark Gush is thanked for his artistic expertise with many of the diagrams.

CHAPTER 1

INTRODUCTION

1.1 Motivation

South Africa has a highly variable rainfall and hydrology. As the rapidly expanding population puts pressure on the water resources, water deficits are becoming severe. Because of the variation in rainfall over the country it is necessary to move water from high rainfall catchments to areas where water resources are poor. Optimizing the yield of water from catchments is therefore becoming an important issue in catchment management.

The major catchment areas for South Africa's water resources are covered by natural grasslands which occupy approximately 29% (350 000 km^2) of the country. These areas are relatively cool, and have an annual rainfall between 600 and 1 200 mm. These areas coincide with the afforestation zones for commercial exotic tree species, whose site requirements for growth are most limited by the availability of soil water. Given that strategic planners envisage the establishment of 16 000 hectares of forests per annum to supply commercial timber (Anon, 1996), and the increased demand for timber products resulting from the impact of the RDP, there can be no doubt that afforestation will have a further impact on the country's already scarce water supplies. Growing demands for water by all sectors is also placing pressure on water resources. Quantitative information on the effect of different land management practices on the water balance is critical in land management planning. Most of the research into predicting hydrological change due to afforestation, has been to quantify the water use of the commercial trees. Very little research has been directed at determining the water loss from natural communities. To quantify the effects of afforestation and agriculture, it is necessary to have information on the evaporation losses from natural vegetation to provide a management baseline.

The aim of this study was to identify and quantify the principal factors (meteorological, plant and soil) controlling the processes of water loss in montane grasslands. New techniques for measuring soil water are tested and the results are used to test existing hydrological models. This

is the first study in South Africa in which all the components of the catchment water balance are measured simultaneously.

1.2 Background and Justification

In the Republic of South Africa, where at least two thirds of the area may be classified as arid or semi-arid, the need for conserving water is of national importance (Dyer 1963). One of the most strategically important catchment areas in South Africa is the KwaZulu Natal Drakensberg mountain range which gives rise to many of the rivers that are so important to the economy of the country. The prime objective in managing these grassland catchments is to maintain a sustained yield of water supply for the country. With increasing demands for grazing land and afforestation these catchments may be targeted for different land management practices. There is growing concern that such changes in the land management of the traditionally conserved grassland areas will result in reduced water yield from catchments. Information on the hydrological cycle, particularly the changes in water and sediment production in response to changes in land use or management will aid planners in policy decisions.

Water balance is a relation between the water balance components which are random variables in time and space, with usually unknown probability distributions. The independent input variable is rainfall, which is transformed in the hydrological system into the dependent output variables evaporation, streamflow and change in soil storage (Figure 1.1). Because adequate hydrological measurements seldom take place where the decisions are most needed, simulation models are developed to predict hydrological processes from a catchment to a regional scale (Hewlett & Hibbert 1967). These models must be sensitive enough to enable managers to predict changes in land use realistically.

In order to develop physically based water balance models which reflect the dynamic interchange of energy at the atmospheric-soil-vegetation interface, it is important to accurately determine soil water content. In spite of the continual improvements in the neutron moderation technique for measuring water content, the fact that it cannot be automated and is labour intensive severely limits its usefulness in remote sites. There is clearly a need for improved methods of measuring soil water content. Time domain reflectometry (TDR) has been successfully used for *in situ* measurement of soil-water content. This study will investigate the usefulness of TDR and the

recently developed capacitance probe in the measurement of soil moisture.

1.3 Objectives

(i) To quantify the spatial and temporal patterns of evaporation and soil water within a grassland catchment.

(ii) To describe these processes in terms of the controlling environmental variables.

(iii) To provide a modelling framework for the catchment water balance for use in water resource management planning.

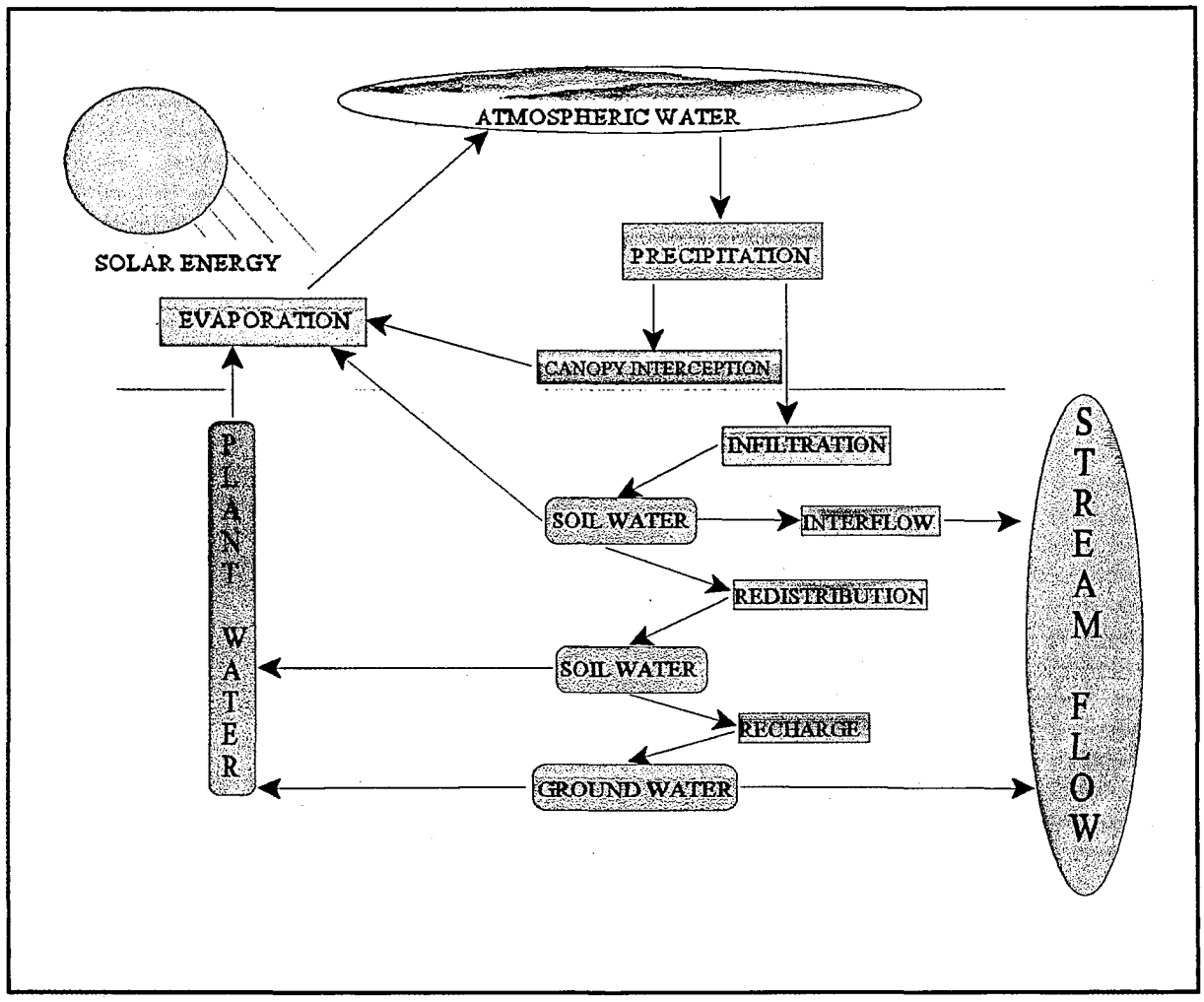

Figure 1.1 Schematic representation of the catchment water balance as undertaken at Cathedral Peak.

CHAPTER 2

DESCRIPTION OF STUDY SITE

2.1 Research location and physiography

The Drakensberg Mountains in KwaZulu Natal form a continuous crescent-shaped escarpment situated between 160 and 240 km inland of the east coast of South Africa. The area varies in altitude from 1 847 to 2076 m. The escarpment creates a natural boundary between South Africa and Lesotho (between latitudes 28° 30′S and 30° 30′S, and longitudes 28° 30′E and 29° 30′E). The study was carried out at the Cathedral Peak Forestry Research Station which lies in the northern part of the crescent in a conserved area of the Natal Drakensberg Park (29° 00′S, 29° 15′E, Figure 2.1).

The Cathedral Peak Research Station is the main centre for hydrological research in the mountainous summer rainfall region of southern Africa. It was established in 1935 to examine the influences of various management practices on the vegetation and water yield of the local mountain catchments. The fifteen research catchments (numbered I to XV) are situated at the head of three isolated Little Berg spurs at an altitude of approximately 1 890 m (Everson & Tainton, 1984). Each of these catchments receives a specific treatment (eg. afforestation, protection from fire, etc.). Most of the experiments in the present study were carried out in catchment six (VI), a grassland catchment receiving a biennial spring burn treatment.

2.2 Description of Catchment VI

Catchment VI is 0.677 km^2 in extent and is moderately dissected by streams (stream density 3.25 km/km^2). The origins of the streams are obscured beneath soil and boulders, and are believed to rise above non-amygdaloidal layers of basalt. A topographic map of Catchment VI is shown in Figure 2.2. Elevations range from 1 860 m a.s.l. at the basin outlet to 2 070 m a.s.l. at the highest point. The terrain has a slope of 19 %. Two large saturated zone areas exist in the catchment. The upper zone exists on a topographic convergence midway in the catchment and the other where the stream flattens before the catchment outlet. Their maximum axial extent is approximately 150 m. The former was chosen as a study site in this investigation.

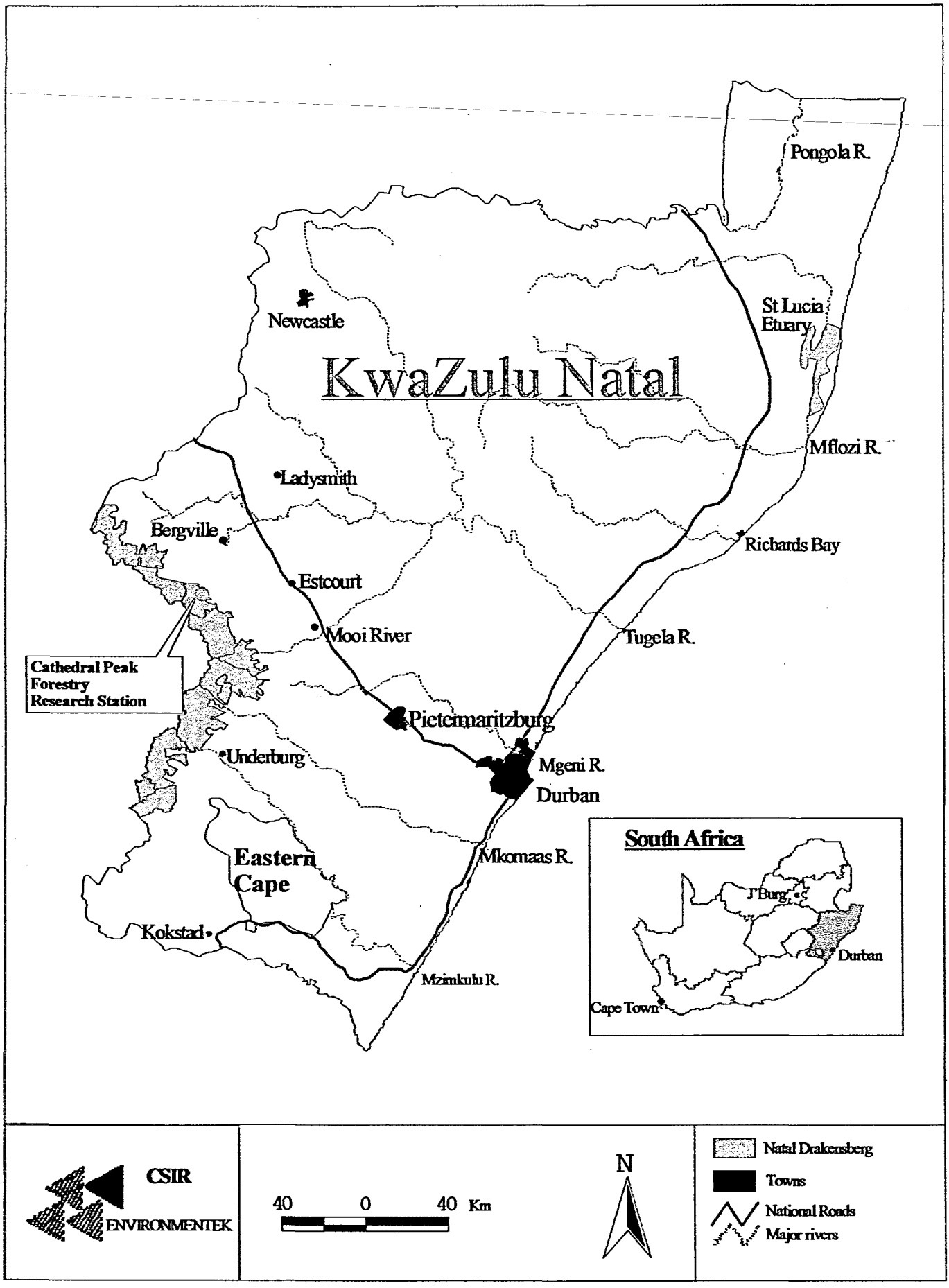

Figure 2.1 The locality of the Cathedral Peak Forest Research Station in the Natal Drakensberg Park.

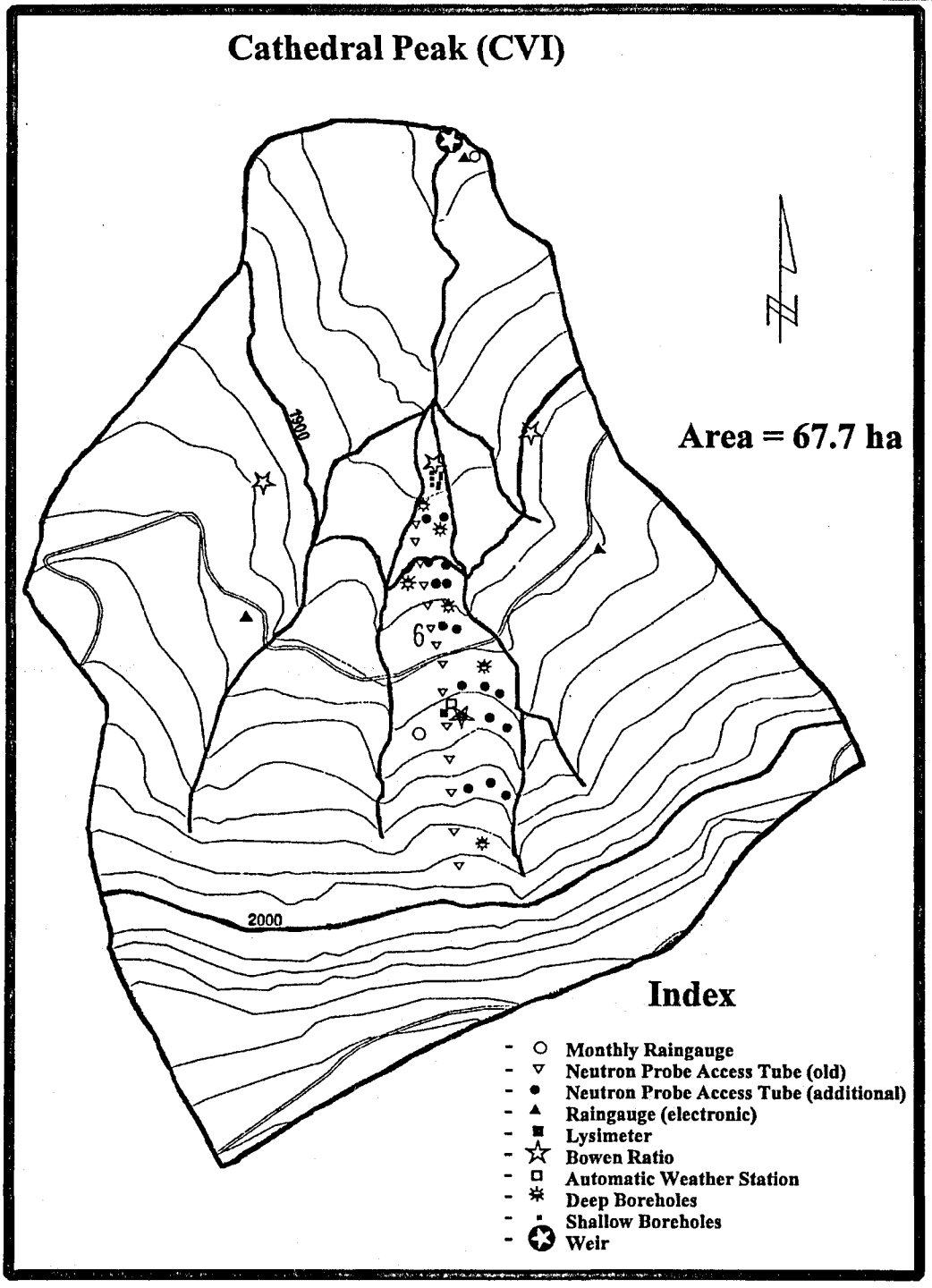

Figure 2.2 Topographic map of Catchment VI showing the location of the various monitoring sites.

2.3 Vegetation and land use

Grassland covers the greater part of the Drakensberg. Nearly all the grasses are tufted in habit and give the appearance of a continuous cover. Fire is a natural ecological factor in the Drakensberg. After the first winter frosts in May, the above-ground herbage dries out, increasing the flammability of the fuel.

The Natal Drakensberg is the highest mountain range in South Africa giving rise to many of the major rivers of the country. The upper reaches of the catchments which feed these rivers largely fall under the control of the Natal Parks Board. The prime objective in managing these catchments is to maintain a sustained yield of water with the lowest possible levels of silt and other contaminants, while conservation of the flora and fauna and recreation are compatible supplementary objectives (Bainbridge 1987).

2.4 Soil characteristics of study sites

The soils of the catchment are classified as Lateritic Red and Yellow earths, grading into heavy black soils (Katspruit and Champagne) in the saturated zones and along the stream banks (Granger 1976). They are of residual and colluvial origin and derived from basalt. Characteristically these soils are acidic, highly leached and structureless. The topsoils are of friable consistence and well suited for rapid infiltration and storage of water. The organic content of the top soil is high (6%-10%), resulting in a high water holding capacity of the soils. By contrast, the subsoils have a very high clay content and poor infiltration.

2.5 Climate

The weather parameters recorded during the study period were organized into hydrological years from 1 October - 30 September. The data for the five year study period (1990/91-1994/95) and for the 42 year period from 1949 to 1991 are summarized in climatic diagrams (Figure 2.3).

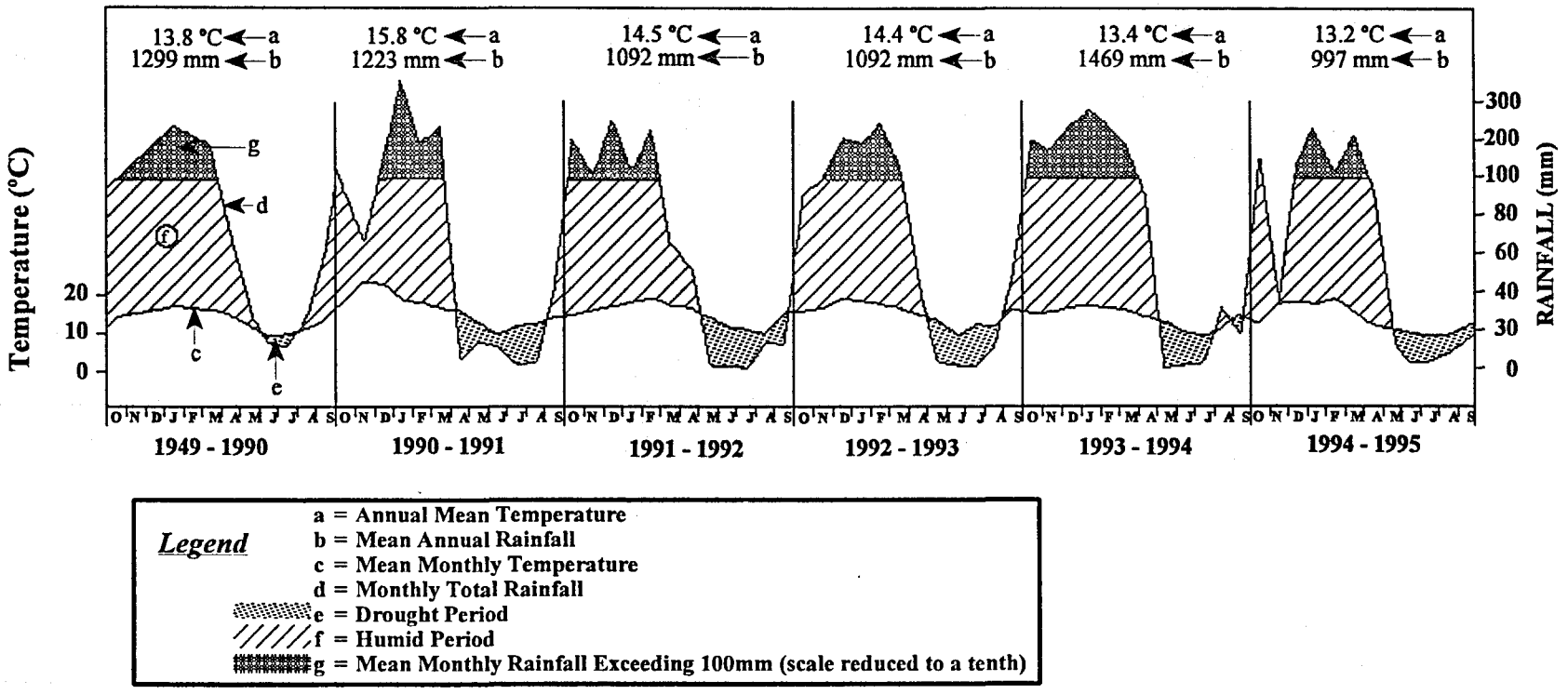

Figure 2.3 A long-term climatic diagram for Cathedral Peak (1949-1990), and annual climatic diagrams for 1990-1995.

2.5.1 *Rainfall*

The Cathedral Peak research area lies in the summer rainfall zone of South Africa where summers are wet and humid, and the winters are dry and cold. The long term average annual rainfall is 1 299 mm. Precipitation during the study period was 1 223, 1 092, 1 092, 1 469 and 997 mm for 1990/91, 1991/92, 1992/93, 1993/94 and 1994/95 respectively. The study period was therefore represented by dry (1994/95), average (1990/91-1992/93) and wet (1993/94) years.

Drought periods (dotted areas in Figure 2.3) are typically recorded in winter during June and July (see long-term climatic diagram). In spite of receiving an average rainfall during most of the study, extended drought periods were recorded in every year of the study. For example, in 1990/91and1991/92 drought was experienced for five months of the year from April to September (Figure 2.3). Even in the wet year drought conditions were recorded in four months of the year. This indicates that monthly distribution of rainfall is an important factor determining the occurrence of drought conditions.

2.5.2 *Temperature and humidity*

Air temperatures are never excessively high at Cathedral Peak. The mean annual temperatures from 1990/91 to 1994/95 were 15.8, 14.5, 14.4, 13.4 and 13.2 °C (Figure 2.3). With the exception of 1990/91, mean temperature did not differ markedly from the long term average of 13.8 °C. The highest temperatures (approximately 35 °C) are usually recorded in November before the rainy season properly sets in.

2.5.3 *Radiation*

Fluctuations in the components of the water balance are determined by the incident solar radiation. Radiation patterns at Cathedral Peak in summer (December and January) are poorly defined. High solar altitudes together with the prevailing overcast conditions in the afternoons largely obliterate topographically induced radiation differences (Granger & Schulze 1977). Therefore variation in steepness of slope, rather than the different aspects, exhibit greater spatial variation of radiation receipt.

Despite longer average daylight hours in summer (14 hours) than in winter (11 hours), the total number of daily sunshine hours in summer is 2.5-3.5 hours less than in winter. This is due to the characteristically cloudy and rainy conditions that reduce sunshine during the summer months (Granger 1976).

2.5.4 *Wind direction and wind speed*

Wind is an important climatic variable in the Drakensberg because it is prevalent during the dry season when fire hazard is at a maximum (Everson, van Wilgen & Everson 1988). Throughout the year the winds blow from the west to northwest, responding to high pressure circulation over the Lesotho plateau. Below the escarpment topographically-induced wind systems and gradient winds of the Indian Ocean prevail. Föhne or Berg winds are a characteristic feature of the Drakensberg (Tyson, Preston & Schulze, 1976), occurring in late winter and early spring (August and September). These winds, which are hot and dry, have been recorded at Cathedral Peak at speeds of up to 100 km h^{-1}. Extreme fire hazard conditions are strongly associated with Berg winds.

Windspeeds during the study were variable ranging from an annual windrun of 50 635 km in 1990/91 to 116 827 km in 1992/93. Annual wind runs can therefore vary by up to 43% between years. Wind runs were low during the wet season (October to March) and increased from April onwards (e.g. the 91/92 year, Figure 2.4). High winds were maintained until September.

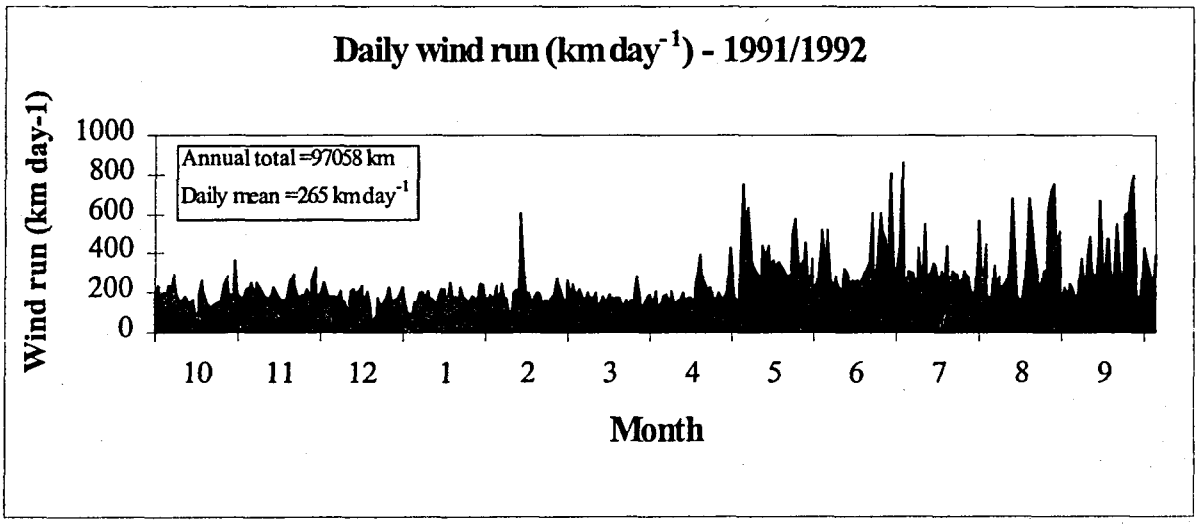

Figure 2.4 Daily wind run in catchment VI for the 1991/92 hydrological year.

CHAPTER 3

GRASSLAND EVAPORATION

3.1 Introduction

One of the most important factors in quantifying catchment water budgets is accurate estimates of evaporation. Methods for evaporation measurement include soil based, plant (heat pulse, sap flow, porometry) and aerodynamic techniques (Savage, Everson & Metelerkamp 1991). Soil and plant based techniques for estimating evaporation have a high temporal resolution, ranging from about one day for soil moisture measurements to a season for catchment water balance studies (Ward & Robinson 1990). By contrast, aerodynamic techniques such as the Bowen ratio energy balance are relatively simple and have a high resolution of 15 minutes to one hour. The Bowen ratio technique has traditionally been used over uniform agricultural crops on homogeneous terrain (Thom 1975). The application of this technique in mountain catchments formed a separate component of this study (Savage, Everson & Metelerkamp 1991). The authors showed that the Bowen ratio energy balance technique has distinct advantages for the field measurement of evaporation and compares favourably with lysimetric measurements of evaporation. The influence of advection was insignificant indicating that the technique is reliable for measuring grassland evaporation over rough terrain.

The present study used the Bowen ratio method to determine daily estimates of evaporation in a grassland catchment over five years. These long term data provide a unique data set of the evaporation component of the water balance of a montane grassland catchment.

3.2 Field instrumentation and methods

Weather data were obtained from an on-site automatic weather station. The weather station was linked to a ground surface raingauge (0.1 mm tip) and a MCS 160 tipping bucket raingauge (MC Systems, CT, SA) to provide precipitation measurements. Solar radiation (Kipp solarimeter, Kipp & Zonen, Holland), albedo, the reflection coefficient of shortwave radiation (Middleton

Instruments, Model CN1, Australia) and PAR (LI- 190 SB quantum sensor, LI-COR Inc., Lincoln, Nebraska, USA) were measured from the weather station and combined with the net irradiance from the Bowen ratio systems (Q*6 REBS net radiometer, REBS, Seatttle, WA, USA) to provide a comprehensive set of radiation measurements. Wind speed (2.0 m height) was measured with a cup anemometer, as well as with two 3-way anemometers (1.5 and 2.0m height) (Model SS-PA, SAFDY systems, Silverton, SA). Wind direction was monitored with a MCS 176 wind direction sensor. Air temperature and relative humidity were measured with a MCS 174-02 temperature and humidity sensor. All sensors were averaged or totalled at 20 minute intervals.

3.2.1 *Bowen ratio instrumentation*

Details of the theory of the technique and its accuracy are outlined in a report entitled "Evaporation measurement above vegetated surfaces using micro-meteorological techniques" (Savage, Everson & Metlerkamp 1995). Specifications of the instrumentation that apply to the present study are given below.

The sensors of the Bowen ratio systems used to determine surface evaporation were placed approximately one meter above the grassland canopy (Figure 3.1). Net irradiance R_n (Wm^{-2}) was measured with two net radiometers (one Middleton and one Fritschen type). The net radiometers were placed 1,0 m above ground on a north-south axis with the radiometer support on the south side to avoid shading of the ground surface. Soil heat flux density F_s(Wm^{-2}) and soil temperature T_{soil}(°C) were measured with four soil heat flux plates (Middleton- type) and eight soil temperature sensors. The soil heat flux plates were buried at a depth of 80 mm, on a north-south axis together with several meters of extra lead to reduce the influence of heat conduction along the exposed leads to the sensors. Four soil temperature sensors (type E thermocouples mounted in tubes) were buried at depths of 20 mm and 60 mm below the soil surface. These sensors were connected in parallel to produce a spatially averaged soil temperature measurement for the two depths for the two different positions. Net irradiance and soil heat flux density were used to calculate the Bowen ratio latent heat flux density L_vF_w(Wm^{-2}). In this report L_vF_w values were converted to millimetres of water. Soil water content in the 80 mm layer was measured gravimetrically every week.

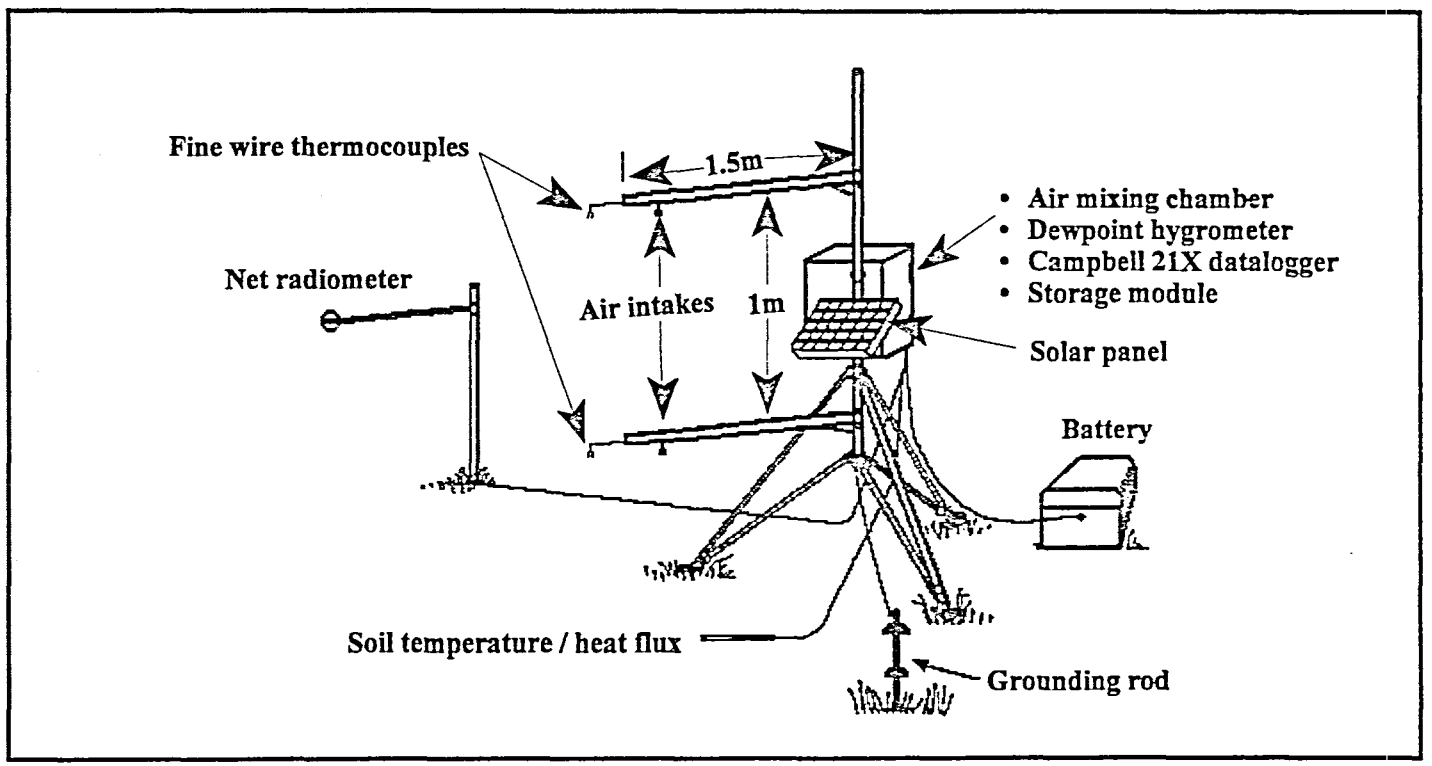

Figure 3.1 A typical Bowen ratio installation as supplied by Campbell Scientific Incorporated.

In the Bowen ratio system, a single cooled dewpoint hygrometer was employed to measure the dewpoint T_{dp} (°C) of air drawn in from the sensors situated 0,8m and 1,8m above ground. Air temperature at 0.8 m and the air temperature difference between 0,8 and 1,8 m was measured using two bare,76μm gauge type E-thermocouples. Parallel connections ensure that this stytem functions even if one of the thermocouples is damaged.

All sensors were connected to a Campbell 21X datalogger, one datalogger being used for each of the Bowen ratio systems. A frequent measurement period of 1 s for dewpoint and air temperatures was employed and 10 s for all other sensors. The dewpoint temperature was averaged for a period of 80 s (after a mirror stabilization time of 20 s), converted to water vapour pressure and then the datalogger switched a solenoid to sample the other level. Every 20 minutes the datalogger transferred an average of the output storage values to final storage. Weekly, the data were transferred to computer and the data checked for errors (normally caused by broken thermocouples or battery problems). Fuchs & Tanner (1970) provide an analysis of errors in Bowen ratio calculations. Fuchs (1973) suggests that daily estimates of the latent heat of evaporation cannot be made directly from daily average net radiation plus soil heat flux and daily average β. However, 20-60 minute estimates of the latent heat of evaporation over the day will yield the best results. In the present study the daily evaporation for the catchment was calculated from the sum of all the 20 minute data during periods when the net radiation was positive.

The monitoring network was expanded in 1992 to include the measurement of evaporation on different aspects within the research catchment. Three independent Bowen ratio units were used. The control was located on the original north facing site on which an automatic weather station was established. A second Bowen ratio system was set up in the riparian zone. A third unit was alternated between sites having similar slopes but different aspects. This unit was moved at approximately 2 weekly intervals.

3.3 Results and Discussion

3.3.1 *Solar radiation and soil heat flux*

Solar radiation is the most important component of the energy balance as it drives the processes of evaporation and heating of the air and soil. While most energy budgets require information on net radiation (the energy available at the ground surface), this is seldom routinely measured at weather stations. In the present study incoming solar radiation was monitored and tested against algorithms for predicating net radiation.

The seasonal trend in solar radiation followed a similar pattern throughout the four years of the study period (Figure 3.2). Daily totals of solar radiation on clear days varied between 10 MJ m^{-2} day^{-1} in winter (July) and 33 MJ $m^{-2}day^{-1}$ in summer (January). The lower daily values in winter are attributed to the low solar altitudes, short days and longer nights at this time of the year. The predominance of cloudy days in the summer rainy season is depicted by the numerous peaks and troughs in the radiation values. Winter is characterized by more consistent incoming radiation. The years with lower solar radiation coincided with the wetter years of the study period (1990/91 and 1993/94).

Annual totals of solar radiation ranged from 5 663 MJ m^{-2} in 1990/91 to 6 306 MJ m^{-2} in 1992/93. Assuming that an average radiation value of 20 MJ m^{-2} day^{-1} is required for a daily evaporation of 3 mm, then the 643 MJ m^{-2} difference between radiation in wet and dry years represents approximately 96 mm of evaporation. This value is close to the 101mm difference observed between evaporation in wet and dry years of the study period (section 3.3.2). These results confirm that the driving force of evaporation in these catchments is solar radiation.

A portion of the total solar radiation that reaches the atmosphere and the earth is reflected back into space. The degree of reflection is a function of wavelength within this range. The term "albedo" is used to describe the reflection of the solar beam (0.3 - 4.0 μm) regardless of wavelength. A number of factors affect the determination of albedo including the moisture status of the leaves, degree of ground cover and time of day (Rosenberg, Blad & Verma 1983). A plot of shortwave albedo in catchment VI (Figure 3.3) indicated that reflectance was highly seasonal. During the winter of 1992 the albedo values increased from 0.25 to a maximum of 0.42

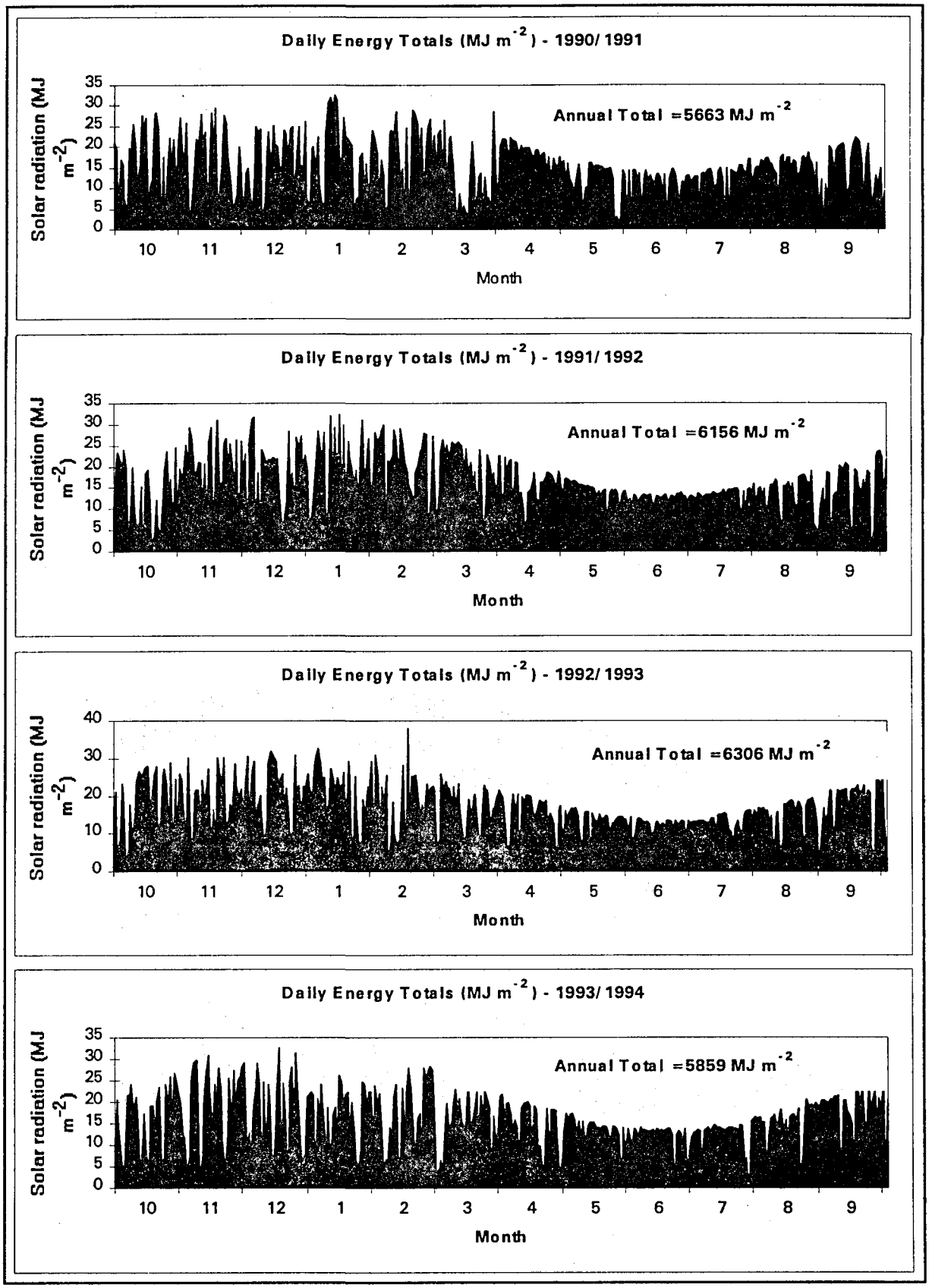

Figure 3.2 The daily total of solar radiation (MJ m^{-2}) for the 1990/91 to 1993/94 hydrological years.

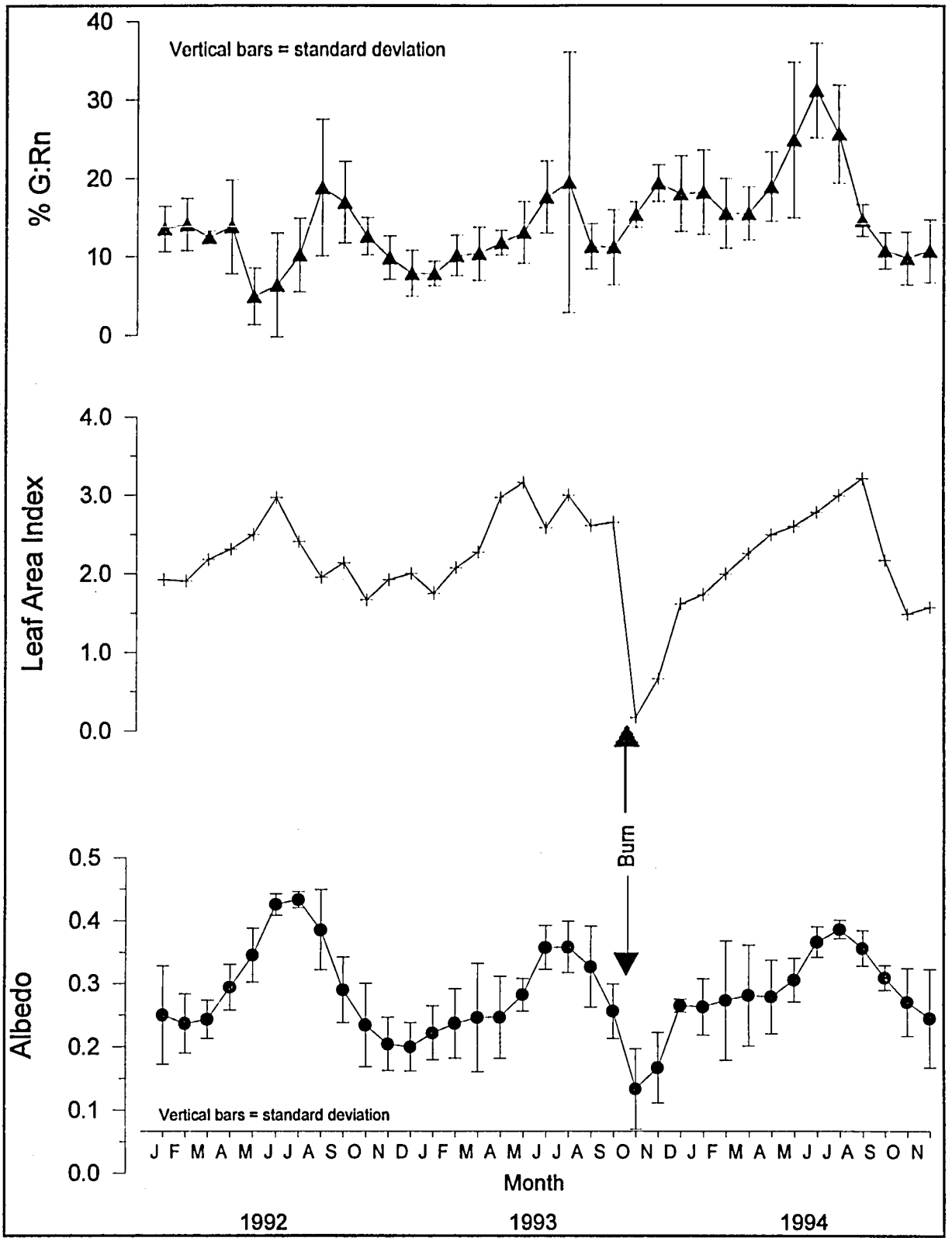

Figure 3.3 Seasonal trends in the monthly means of the albedo, leaf area index (live plus dead material) and percentage of soil heat flux to net radiation for the grassland in catchment VI.

in July. These winter values are high when compared to other vegetation types. For example, Kalma & Badham (1972) found that the albedo for mixed grass was 0.22 while that of crops was 0.18-0.30. The high albedo of 0.42 recorded in catchment VI is equivalent to reflectance off old snow (Rosenberg, Blad & Verma 1983). This may be attributed to the increase in specular radiation brought about by the low sun angles during the winter months. In winter the homogeneous grassland surface behaves more like a mirror than a diffuser and simple reflection results. This is depicted by the parabolic relationship of albedo in catchment VI where the proportion of radiation reflected in winter is greater than in summer (Figure 3.3).

Albedo decreased with the onset of the growing season when there was an increase in plant cover. The lowest reflectance was recorded in October 1993 after the prescribed treatment burn was applied. The low reflectance coefficient at this time is a function of the blackened surface following the burn . The decreased albedo results in higher absorption of solar radiation and an increase in surface heating. The increase in albedo in the 1993/94 growing season corresponded to an increase in canopy cover.

Leaf area or amount of ground covered determines the ratio of direct evaporation from the soil to transpiration from the plants. Brun, Kanemasu & Powers (1972) found that the proportion of water lost as transpiration in soybean was closely correlated to leaf area index. In the grasslands of this study the pattern of the leaf area index closely followed that of albedo (Figure 3.3). Total leaf area index generally increased from 2 to 3 between September and May. This increase corresponded to an increase in the canopy during the growing seasons. The subsequent decrease in leaf area index can be attributed to the drying out of the vegetation following the frosts. After the treatment burn in October 1993 the leaf area index decreased to 0.1 and then increased rapidly to 3.0 as the canopy recovered during the 1994 growing season.

The portion of the incoming net radiation that heats the soil surface is important for determining the amount of available energy for the evaporation process (R_n - G). In most modelling exercises the proportion of G to R_n is assumed to be 10% (i.e. the R_n is reduced by 10%)(Campbel 1992). The monthly averages of the percentage of G:R_n in catchment VI showed a distinct seasonal trend increasing in winter and decreasing during the growing season (Figure 3.3). Although ratios were

very variable ranging from 4% (May 1992) to 30% (June 1994), the average values fell within the 10-15% range.

3.3.2 *Evaporation*

3.3.2.1 The energy balance above the grassland

The Bowen ratio measurements of the evaporation component of the energy balance were made from October 1990 to July 1995. Apart from minor data losses resulting from low battery conditions or broken thermocouples, this represents a continuous data set of approximately 1 800 days. This is the first study of its kind in South Africa which has attempted to use the Bowen ratio technique for long term measurements of evaporation in remote sites.

During summer (e.g. DOY 5, 1992 Figure 3.4) the diurnal trend in the components of the energy balance were characterized by high net incoming radiation (± 800 Wm^{-2} at midday) interspersed with low values of radiation (<300 Wm^{-2}). The low values were caused by the high incidence of clouds at this time of the year. Clear sunny mornings followed by convective thunderstorms in the afternoon are a typical feature of the study area. Most of the radiant energy at this time of the year was partitioned into the latent heat of evaporation (~ 500 Wm^{-2}), with the rest going into sensible heat and soil heat flux (~ 200 Wm^{-2} each). In spite of the high incidence of cloud in summer, evaporation amounted to approximately 3-5 mm per day. The low vapour pressure deficit (0.1-0.5 kPa) in summer indicates that evaporation was driven by high available energy rather than the turbulent transfer component.

By contrast, in winter the vapour pressure deficit was high, ranging from 1.0 kPa in the early morning to 2.0 kPa in the afternoon (Figure 3.5). Under these very dry conditions one would expect evaporation to be high. However, in spite of sunny cloudless days, evaporation in winter was <1 mm per day. This low value can be attributed to low net radiation (± 300 Wm^{-2}) of which only 100 Wm^{-2} was partitioned into the latent heat of evaporation. The remainder of the available energy was partitioned equally into sesible and latent heat flux. Another factor contributing to low evaporation was the seasonal dieback of the vegetation.

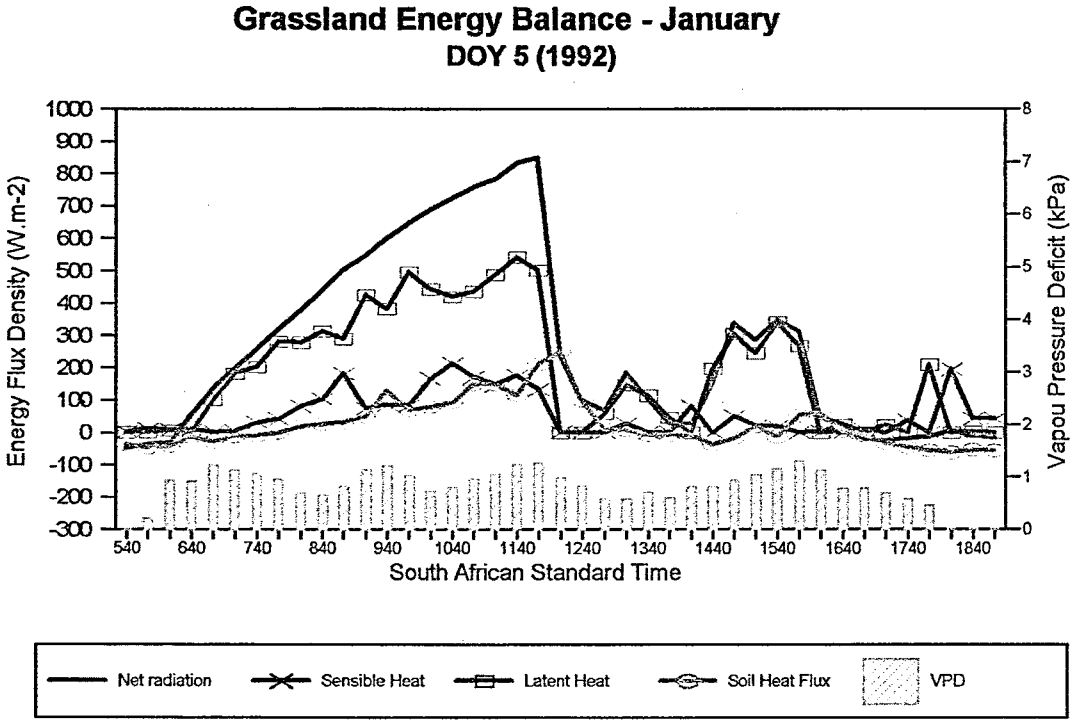

Figure 3.4 The energy balance for the grassland in catchment VI on a typical summers day.

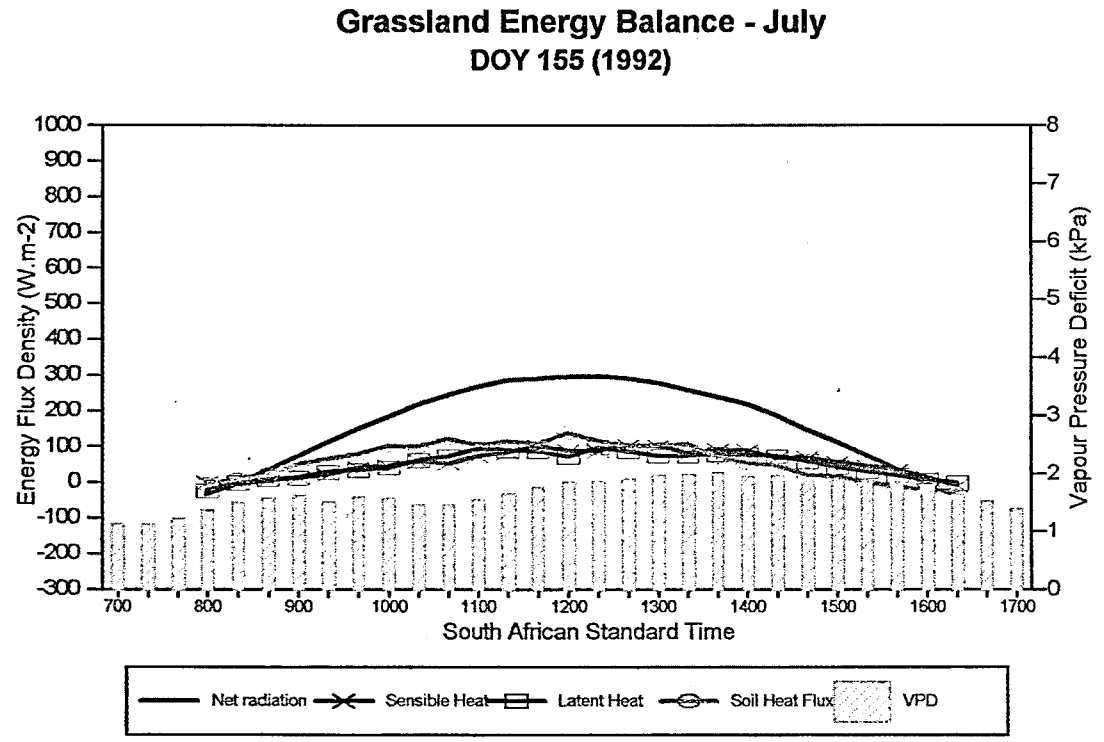

Figure 3.5 The energy balance for the grassland in catchment VI on a typical winters day.

3.3.2.2 Seasonal trends in daily evaporation: 1990/91 - 1993/94

Evaporation from the study site (moderate slope, north aspect) was measured continuously from September 1990 to June 1995. Evaporation ranged between 3-7 mm per day during the wet season and dropped to <1 mm per day during the dry winter months (Figure 3.6).

In the seasonal climate of the Drakensberg, the grassland vegetation exhibits a pattern of growth and dieback which coincides with seasonal variations in evaporation. In the dry season, when temperatures are low and frost is frequent, the above-ground vegetation dies off. The underground parts remain dormant until temperatures rise in spring. Evapotranspiration is low during this dormant season due to the reduction in transpiring leaf surface.

Total daily evaporation for 1990/91, 1991/92, 1992/93 and 1993/94 was 681 mm, 752 mm, 698 mm and 651 mm respectively (Figure 3.6). The average evaporation over the four year study was 695 mm. Thus approximately 54% of the annual rainfall is evaporated back into the atmosphere and is not available for streamflow generation. The low variation in evaporation, irrespective of the rainfall, indicates that soil moisture seldom limits evaporation. This is attributed to the deep soils which buffer the effects of variable rainfall. The close relationship between evaporation and net radiation (Figure 3.5) indicates that evaporation is driven by energy.

3.3.2.3 Evaporation from the riparian zone

Riparian zones play a vital part in the hydrology of catchments. Modelling the water loss from strategic catchments should therefore take into account the effect of the riparian zone on evaporation. In 1993 a second Bowen ratio unit was assembled in the riparian zone to monitor differences in evaporative losses between the control site (north) and the riparian zone. The daily evaporative losses in the riparian zone closely followed losses from the control site (Figure 3.7a). The accumulated differences in evaporation between the sites showed that evaporation in the riparian zone was consistently higher in the summer months (Figure 3.7b; DOY 1-80). The accumulated difference (riparian minus control) was 85 mm over this 80 day period (± 1 mm day $^{-1}$). During winter (DOY 81-211) the accumulated difference was only 15 mm (± 0.5mm day $^{-1}$). The results indicate that daily evaporation from the riparian site (490 mm) was 33%

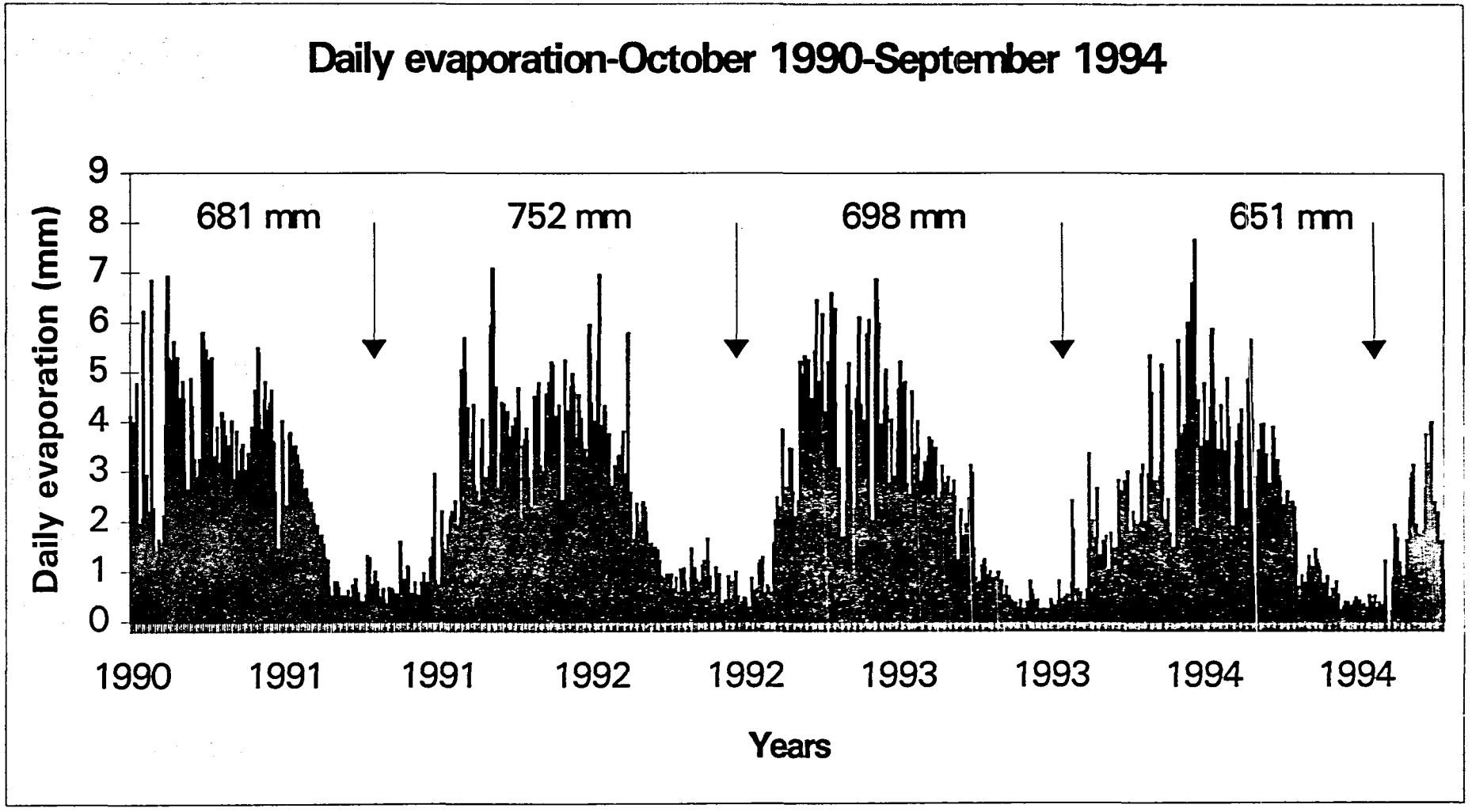

Figure 3.6 Time series trend in daily evaporation measured with the Bowen ratio apparatus from 1990-1994. The arrows indicate the start or end of a hydrological year

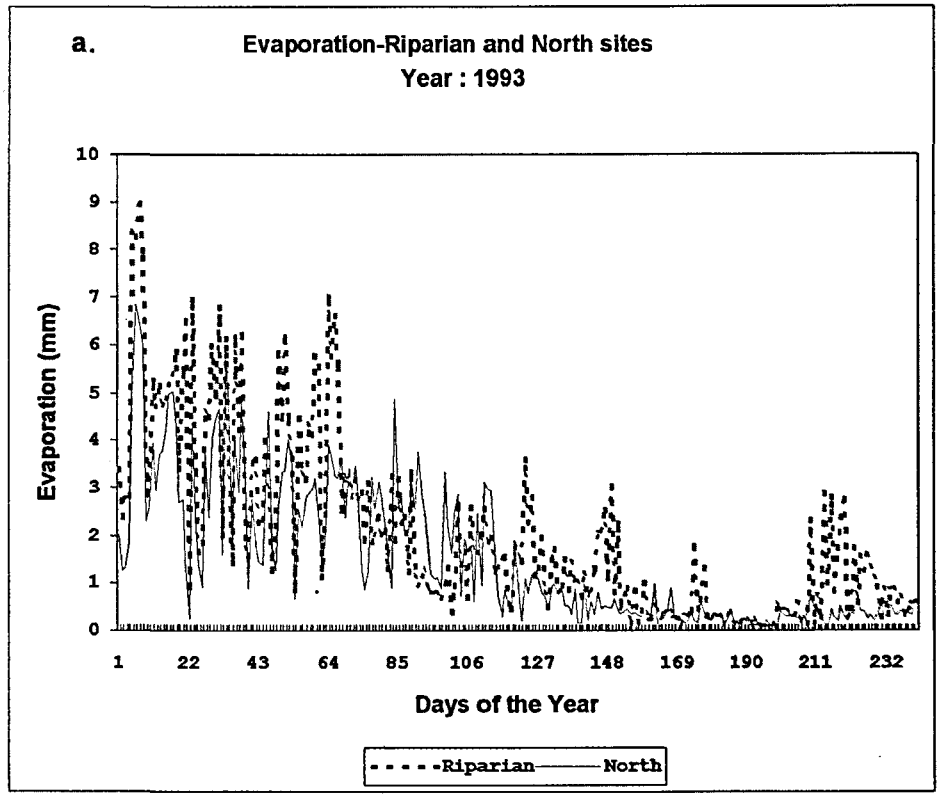

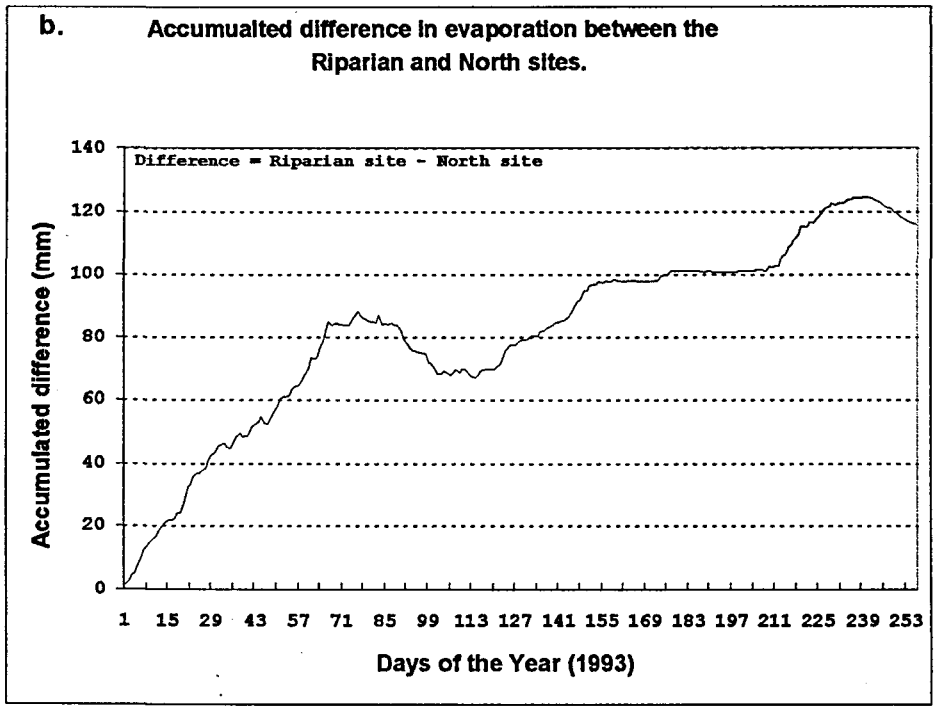

Figure 3.7 a&b. A comparison of daily evaporation (a) and daily accumulated differences (b) on a north and horizontal *Miscanthus capense* riparian site from January to August 1993.

higher than the north facing control site (366 mm). These results are not surprising since higher evaporation rates were expected from the riparian zone which has a higher soil water content and leaf area index.

3.3.2.4 Effect of aspect on evaporation

The Drakensberg catchments are characterized by steep slopes which affect the spatial variation of incoming radiation. Aspect induced differences in radiation may therefore have a significant effect on evaporation.

To examine the effect of aspect on evaporation a third Bowen ratio unit was set up in catchment VI in November 1992. At two weekly intervals the entire apparatus was dismantled and transferred between the east and west aspects of the catchment. This enabled direct comparison between the control site on the north aspect and the east/west aspects. Evaporation from the sites was measured continuously during 1993.

Evaporation from the different aspects showed similar trends, decreasing from a mean of 4 mm in January (DOY 1-30) to < 1.5 mm by the end of April (DOY 120) (Figure 3.8a). The effect of the high incidence of cloud cover and rain in summer is reflected in the daily evaporation having a very jagged pattern, being low on rainy days and high on clear days. Between site differences in evaporation were not readily discernable on a daily basis (Figure 3.8 b). However, comparisons between the two-weekly totals of evaporation indicated that during summer and autumn evaporation was higher from the north aspect than from the east or west aspects (Figure 3.8). The west facing site had a total of 138 mm of evaporation and the east facing site had 145 mm. While direct comparisons between east and west were not possible, the total evaporation for the entire period (DOY 6 to 256) was 10% higher at the north site (312 mm) than at the east/west sites (283 mm). During the winter months of this study (DOY 120-250), the evaporation rates were low (< 0.8 mm) and slope and aspect-induced differences in evaporation were negligible.

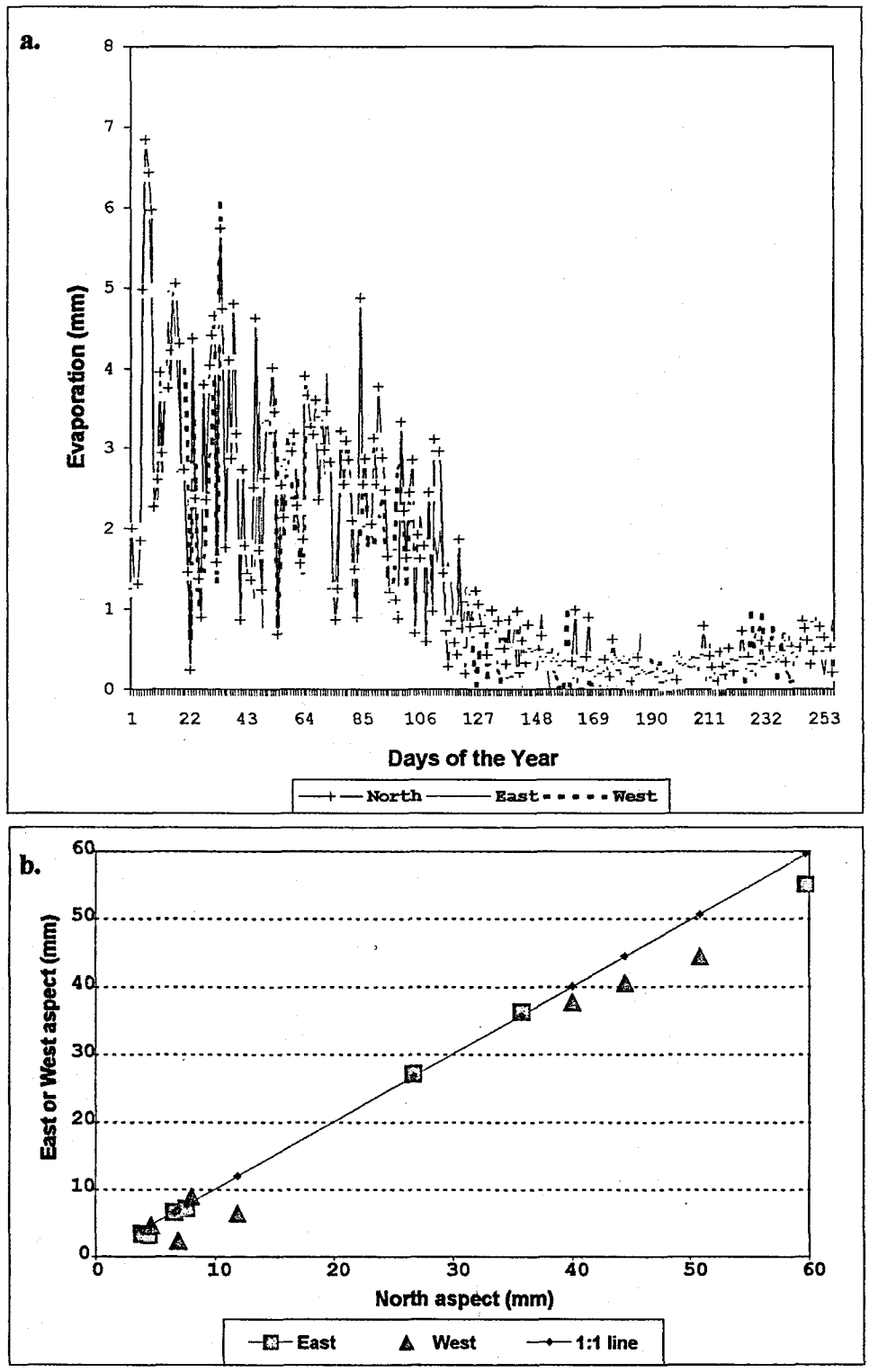

Figure 3.8 a. Daily evaporation from the North, East and West aspect during 1993.
b. Two weekly periods of evaporation from the North, East and West aspects during 1993.

3.3.3 *Verification of grassland evaporation models*

The need for a reliable method of estimating evaporation on a daily or weekly basis using only regularly recorded climatological data has been long sought after by hydrologists and micro-meteorologists. Mathematical modelling and computer simulation are techniques that attempt to conceptualise and integrate the various components of a system into a realistic representation of the system.

Simulation is one of the most widely used techniques in operations research and decision making (Law & Kelton, 1982). As a management tool, models are used to:

1. Make long term predictions
2. Select the best alternative that fits the desired requirements
3. Determine production functions to evaluate the impact of management practices
4. Assess risk to allow the choice of management decisions at different probabilities of occurrence (Wright & Hanks, 1987).

In addition, modelling assists scientists by increasing the understanding of the different aspects of ecosystems and their interrelationships. As a research tool, models can be used to:

1. Help with the generation of hypotheses
2. Provide an analytical mechanism for studying the system of interest
3. Increase the level of understanding of systems
4. Provide direction for further research
5. Allow inferences about the system of interest without destroying or disturbing it.

Water use models of grasslands have been evolving over many years. Their history can be split in two parts. The first models were empirically based. The models used by Rogler and Haas (1947) and Sneva and Hyder (1962) related range herbage production to precipitation and available water. Smoliak (1956) and Johnston *et al.* (1969) included other climatic data, in addition to precipitation and available water, to predict range herbage production. The site specificity of these models limits their general applicability. The later grassland models were

water balance climate models. Aase *et al.* (1973), Hanks (1974), de Jong and MacDonald (1975), Hanson (1976), Rasmussen and Hanks (1978) and Wight and Hanks (1981) developed such models to predict evaporation from natural grasslands while the first comprehensive ecosystem model was developed 14 years ago by Innis, (Innis, 1978). Grassland models have seen little development or adaption to South African conditions and managers are largely bound to models developed for agricultural lands. Research on the water use of commercial trees has received high priority, but cannot be appreciated in land use terms unless compared to the water use of the natural vegetation (e.g. grassland) prior to afforestation. Only then can the effect of altered evapotranspiration with change in land use be simulated.

One of the first methods for predicting evaporation from routinely recorded weather data was derived by Penman (1948):

$$Q_E = \frac{S}{S+\gamma}(R_n - G) + \frac{1}{S+\gamma}\rho c_p (1/r_{av})(e_a^* - e_a), \qquad \text{..... (1)}$$

Where Q_E is the evaporation in energy units; S is the slope of the saturated vapour pressure versus temperature curve; γ is the psychrometric constant; R_n is the net radiation, G is the ground heat flux; e_a is the vapour pressure in the air at the temperature T_a measured at the same point as the vapour pressure; r_{av} is the aerodynamic resistance for latent heat transfer, ρ is the density of air, and C_p is the specific heat of air at constant pressure. This equation combines the energy budget with a mass transfer equation to eliminate the need for measuring humidity and temperature at two levels. However, the resulting estimate is only applicable when the evapotranspiration rate is independent of the moisture content of the soil. Such conditions occur when the soil is wet or when actual evaporation is equivalent to potential evaporation. When there is a lack of soil moisture, plant water stress restricts the evaporation rate. Under these conditions the Penman equation can be applied with measured net radiation to estimate the potential evaporation: an upper bound to the actual rate of evaporation.

The Penman equation was adapted by Monteith (1965) to be applicable under all soil moisture conditions. The Penman-Monteith equation still assumes a one dimensional flux of vapour, but otherwise it is applicable under all conditions. The modification introduced an extra term, the stomatal resistance (r_s), which results from the movement of water vapour from the sub-stomatal

cavities to the surface of the leaf. The Penman-Monteith equation (PM) is expressed as:

$$Q_E = \frac{S}{S+\gamma(1+r_s/r_{av})}(R_n - G) + \frac{1}{S+\gamma(1+s/r_{av})}\rho c_p(1/r_{av})(e_a* - e_a) \quad \ldots\ldots\ldots\ldots\ldots \quad (2)$$

This equation is based on a sound conceptualisation of the physical processes of evaporation from plant canopies, but cannot be applied easily because of the difficulties of estimating the stomatal resistance. A number of studies have shown that the Penman-Monteith form of the combination equation consistently out performs other calculations of evaporation (Black *et al.*, 1970). This equation includes more of the factors that influence canopy water loss than other equations, and is therefore expected to provide better estimates. It has not been used in the past in operational applications because of its additional data requirements and the need to define standard values for the reference crop. However, with the capabilities of microprocessor-based dataloggers to do real time computations, such limitations have been removed, and the more physically sound Penman-Monteith equation has become feasible for operational applications.

Slatyer and McIlroy (1967) defined another method of estimating evaporation termed the "equilibrium" condition. These conditions exist when air moves over a wet canopy with a long fetch, so that it becomes vapour saturated. Under these conditions, they reasoned the only large resistance is r_a, when compared to r_i and r_s reducing the Penman - Monteith equation to:

$$\alpha_{equilibrium} = \frac{\Delta}{\Delta+\gamma} \quad \ldots\ldots\ldots\ldots\ldots\ldots \quad (3)$$

where the term α represents the fraction of evaporation relative to the total available energy flux density ($I_{net} - F_s = L_vF_w + F_h$). Thus, L_vF_w is found by simply subtituting $\alpha_{equilibrium}$ into the energy balance equation and solving for $L_vF_{w\ equilibrium}$:

$$L_vF_{w\,equilibrium} = \frac{\Delta}{\Delta+\gamma} \cdot (I_{net} - F_s) \quad \ldots\ldots\ldots\ldots\ldots\ldots \quad (4)$$

Data collected from the Bowen ratio apparatus were used to test the Penman-Monteith equation and equilibrium equation (Savage, Everson & Metlerkamp 1995) for the grassland vegetation

studied in this project. Comparisons were made for selected periods during summer, autumn and winter. Two criteria were used to assess the success of the model fit. The first was to compare the 20 minute estimates of measured and modelled evaporation. The second criterion was the difference between the measured and modelled cumulative evaporation over the measurement period.

3.3.3.1 Net radiation

A potential problem in the use of the equilibrium concept is that neither net radiation nor soil heat flux are measured routinely at weather stations in South Africa. However, solar radiation is monitored at most sites (Reid 1981). The catchment VI data (net radiation, air temperature, solar radiation and albedo) were used to determine whether routine measurements of solar radiation could be used to predict net radiation. The predictions were made for four day periods selected during summer, autumn and winter.

Estimates of the isothermal net radiation are made from the sum of the net solar radiation and the net isothermal long-wave radiation:

$$R_{ni}=a_s S_t+L_{ni}, \qquad \text{.....(5)}$$

where a_s is the albedo (absorptivity of water for solar radiation), S_t is the incident solar radiation measured by the datalogger, and L_{ni} is the atmospheric radiant emittance minus the water emittance at air temperature. Under clear skies, L_{ni} closely approximated by:

$$L_{nic}= 0.0003\,T_a - 0.107 \ (kWm^{-2}) \qquad \text{.....(6)}$$

where T_a (°C) is the air temperature. In cloudy conditions, L_{ni} increases (approaches zero). Cloudiness was estimated from the ratio of measured to potential solar irradiance: S_t/S_o. A cloudiness function was computed from:

$$f\left(\frac{S_t}{S_o}\right) = \frac{1}{[1+0.034\exp(7.9\ S_t/S_o)]} \qquad \text{.....(7)}$$

The net isothermal long-wave is then calculated as:

$$L_{ni} = f\left(\frac{S_t}{S_o}\right) L_{nic} \qquad \text{..... (8)}$$

This equation requires the computation of S_o, the potential solar radiation of a horizontal surface outside the earth's atmosphere (extra-terrestrial radiation). This is calculated from:

$$S_o = 1.36 \sin \phi \qquad \text{..... (9)}$$

where 1.36 (kW m^{-2}) is the solar constant, and ϕ is the elevation angle of the sun. Sin ϕ is computed from:

$$\sin \phi = \cos d \cos l + \sin d \sin l \cos[15(t - t_0)] \qquad \text{..... (10)}$$

where d is the solar declination angle l is the latitude of the site, t is the datalogger clock time, and t_0 is the time of solar noon. Sin d was estimated from:

$$\sin d = -0.37726 - 0.10564J + 1.2458J^2 + 0.75478J^3 + 0.13627J^4 - 0.00572J^5 \qquad \text{(11)}$$

where J is the day of the year.

The cosine is computed from the trigonometric identity:

$$\cos d = (1 - \sin^2 d)^{1/2} \qquad \text{..... (12)}$$

The time of solar noon was calculated from:

$$t_0 = 12 - L_c - E_t \ (hr) \qquad \text{..... (13)}$$

where L_c is a longitude correction and E_t is the "Equation of Time". The longitude correction was

$$L_c = \frac{(L_s - L)}{15} \qquad \text{..... (14)}$$

calculated from:

L_s is the longitude of the standard meridian and L the longitude of the site.

The equation of time has an additional correction to the time of solar noon that depends on the day of the year. Two equations are used, one for the first half of the year and one for the second. For the first half:

$$Et = -.0.04056 - 0.74503j + 0.08823j^2 + 2.0516j^3 - 1.8111j^4 + 0.42832j^5 \qquad \text{..... (15)}$$

where j = J/100. For the second half (J>180),

$$E_t = -0.05039 - 0.33954j + 0.04084j^2 + 1.8928j^3 - 1.7619j^4 + 0.4224j^5 \qquad \text{..... (16)}$$

where j = (J - 180) / 100.

3.3.3.2 Aerodynamic resistance

Estimates of aerodynamic resistance (r_{av}) and canopy or surface resistance (r_s) are required for solving the Penman-Monteith equation for evaporation. An estimate of the aerodynamic resistance for application to plant canopies can be derived from measurements of wind speed profiles. However, such measurements are time consuming and expensive because of the number of anemometers required. Alternatively, the aerodynamic resistance that occurs between a specific height above the ground and the apparent source or sink for heat can be derived from wind profile theory (Monteith, 1973):

$$r_{av} = \frac{[\ln(z-d)/z_0]^2}{k^2 U(z)}$$

d (the zero plane displacement) is 0.63 x canopy height (m),

z_0 (roughness parameter) is 0.13 x canopy height,

U_z is the mean wind speed at height z, and

k is von Karman's constant (0.4).

3.3.3.3 Stomatal resistance

A number of environmental factors including leaf temperature, light, leaf water potential and vapour pressure deficit affect stomatal resistance. Because the manner in which stomates control transpiration is so complex it is usually measured using steady state porometers. As this is not practical in mixed grass swards, we estimated mean values of the stomatal resistance for summer and winter by using an inverse solution of the Penman-Monteith equation. This was possible because the detailed data sets collected included all the variables in the equation with the exception of stomatal resistance.

The most suitable approach in the calculation of transfer resistances, will be to use the inverse solution of the combination equation, (Calder, 1990):

$$r_a = \frac{\rho C_p (q_s(T) - q)}{\lambda E (\Delta' + C_p/\lambda) - \Delta' H}$$

where:

r_a	=	aerodynamic resistance
ρ	=	density of air
C_p	=	specific heat of air at constant pressure
λ	=	latent heat of vaporization of water
$q_s(T)$	=	saturated specific humidity at temperature T
q	=	specific humidity (dimensionless)
E	=	evaporation rate (mm/hr)
Δ	=	the change of saturation vapour pressure with

		temperature (kPa $°C^{-1}$)
Δ'	=	the change of saturated specific humidity with temperature (kPa $°C^{-1}$)
H	=	available energy flux per unit area.

3.3.3.4 Soil heat flux density

When net radiation is positive the soil heat flux density is usually estimated as a fraction of the net radiation. For complete canopy cover (the condition specified for potential evaporation) the soil heat flux is estimated as 10% of the net incoming radiation.

3.3.3.5 Interception

There is increasing evidence from process studies that evaporation of intercepted rainfall is likely to be a major cause of any observed differences in the water yield of afforested and grassed catchments. Interception loss is extremely difficult to measure for low, multi-stemmed vegetation such as grassland. Grasslands are frequently burnt in the Natal Drakensberg, resulting in negligible litter accumulation. Canopy and litter interception are therefore ignored in these grasslands.

3.4 Results

The relationship between the net radiation measured at the Bowen ratio study site during summer, autumn and winter and the values predicted from this model using standard weather data were very good (Figure 3.9). One of the critical factors in the quantification of net radiation was selection of the correct albedo. The best fit was obtained using an albedo of 0.3, which was very similar to the 0.25 measured at this time (Figure 3.3). In winter the albedo value used (0.45) was very close to the actual value of 0.42. These data show that the net radiation can be modelled very accurately from standard weather station data if the albedo can be adjusted to suit the prevailing seasonal conditions.

Values of the stomatal resistance calculated from the inverse Penman-Monteith equation showed

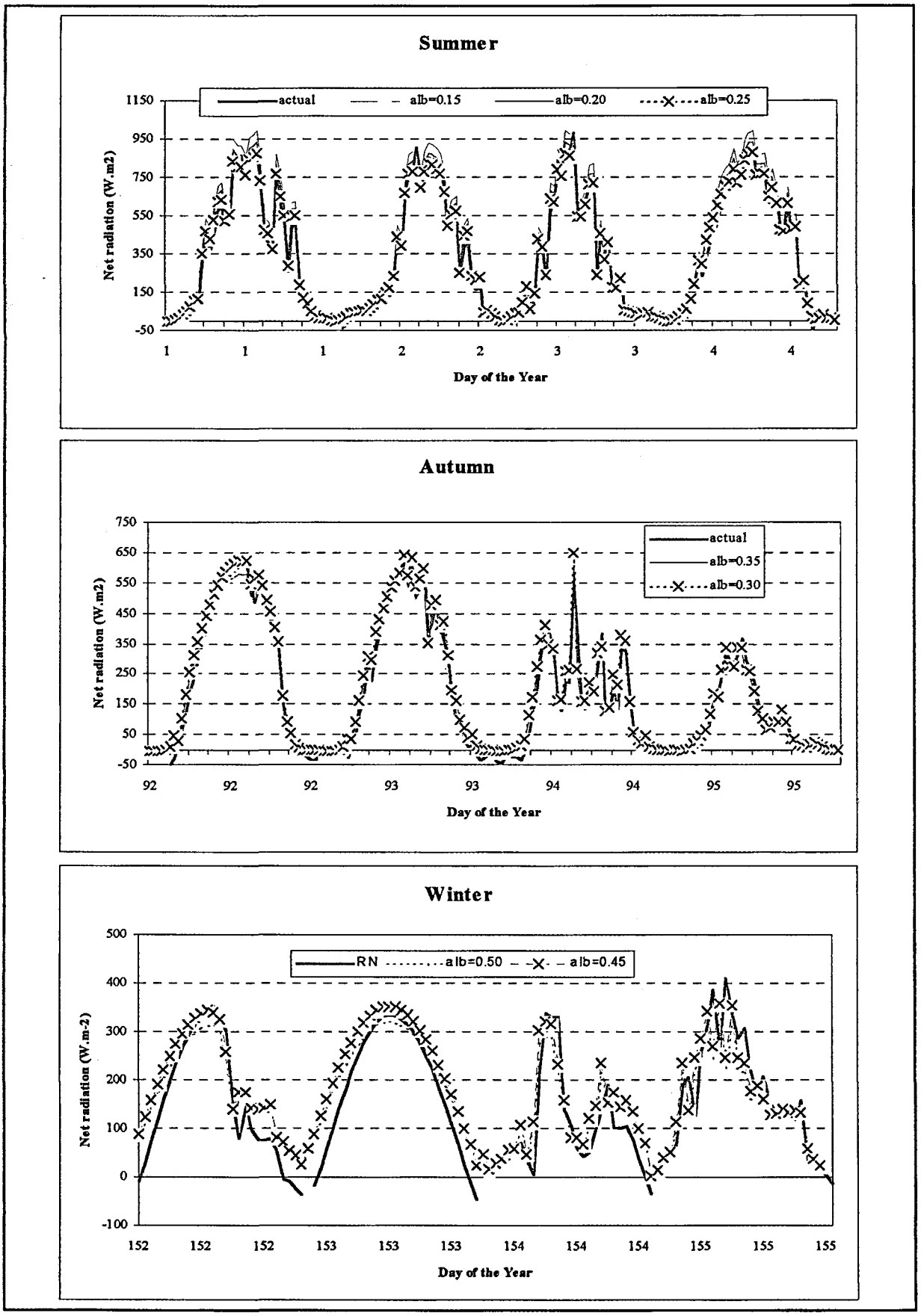

Figure 3.9 Comparisons of modelled and measured net radiation over four day periods in catchment VI for the summer, autumn and winter seasons.

Values of the stomatal resistance calculated from the inverse Penman-Monteith equation showed that the average summer value (February) was approximately 20-100 s m^{-1} (Figure 3.10). This indicates that the grasses were transpiring freely during the day and soil water was not limiting. These values are close to the standard for reference crops (70 s m^{-1}, Smith 1991). By contrast, winter stomatal resistances (August) were 100-500 s m^{-1}, indicating the dormant state of the grasses (Figure 3.10). Stomatal resistance of 50 s m^{-1} (summer), 70 s m^{-1} (autumn) and 200 s m^{-1} (winter) were used for calculating the Penman-Monteith evaporation.

Measurements of evaporation from grassland using the Bowen ratio technique, the Penman-Monteith equation and equilibrium rate during summer, autumn and winter (1993) are shown in Figure 3.11. The diurnal trends in the Penman-Monteith data were smooth in comparison to the Bowen ratio technique. All three sets of data exhibited the same temporal variations which closely followed daily trends of net radiation. The diurnal trends of the Bowen ratio and Penman-Monteith equation showed closest agreement (Figure 3.12). Although the equilibrium evaporation followed a similar pattern, they were always higher, particularly in autumn and winter (DOY 91-181, Figure 3.12). For example, the total evaporation in the winter month of June for the Bowen ratio (9.9 mm) showed little agreement to that of the equilibrium evaporation (47.6 mm, Table 3.1). This over-estimation is attributed to the fact that the equilibrium concept assumes a humid air flow over the canopy. In winter when the canopy is dry, this condition is not met, resulting in poor agreement with actual evaporation. In the six month period from January to June 1993 the Penman-Monteith under-estimated evaporation by 13% while the equilibrium evaporation rate was 55% higher than the Bowen ratio estimates.

Table 3.1 Monthly totals of evaporation estimated using the Bowen ratio, equilibrium equation and Penman-Monteith model.

Month	Jan	Feb	March	April	May	June	Total
Bowen ratio	100.6	85.8	75.7	46.4	20.2	9.9	338.6
Equilibrium equation	139.5	96.2	89.1	85.9	68.2	47.6	526.5
Penman-Monteith	93.2	59.2	50.5	44.5	28.8	16.4	292.7.

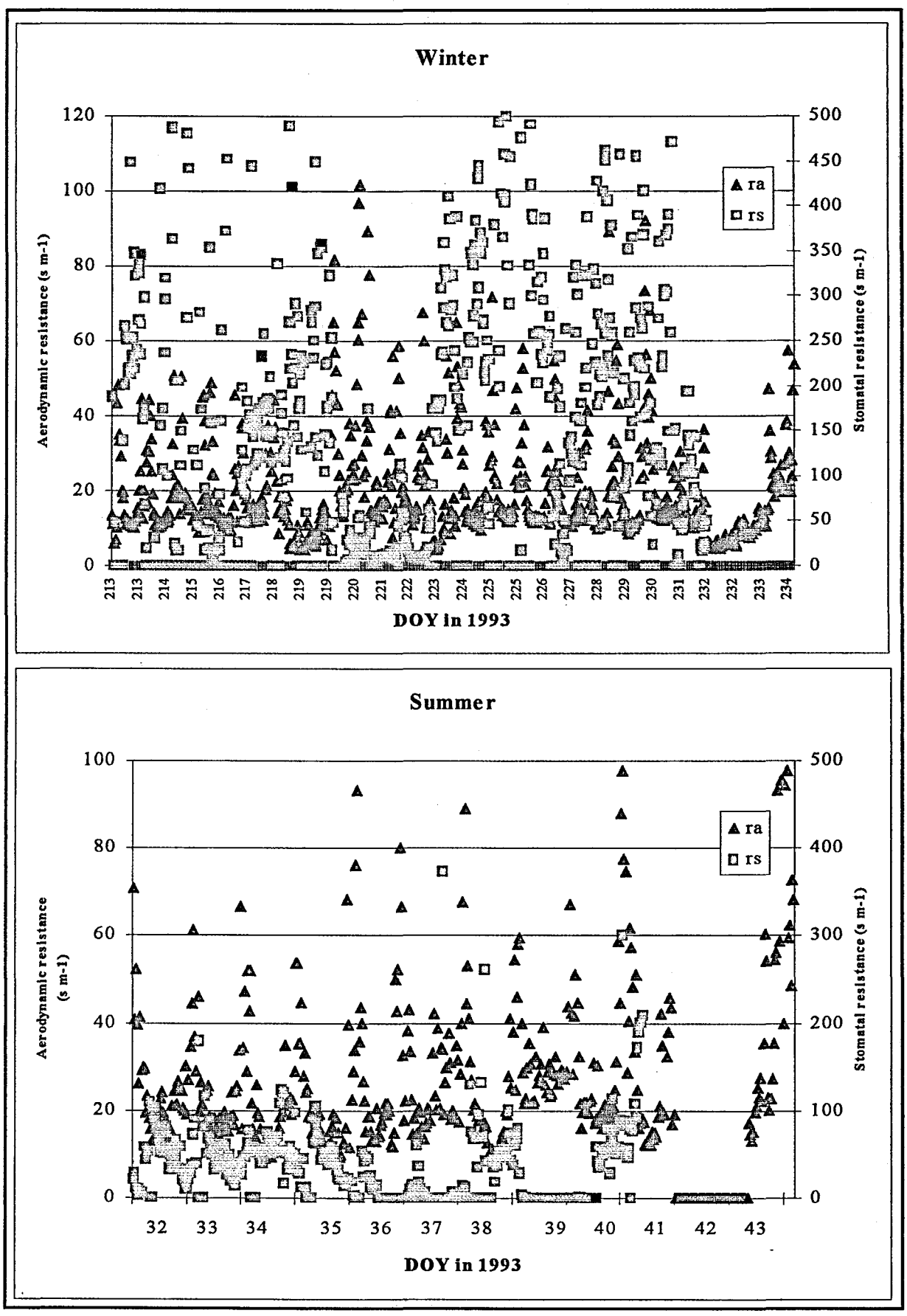

Figure 3.10 Aerodynamic (r_a) and stomatal resistance (rs) for summer and winter.

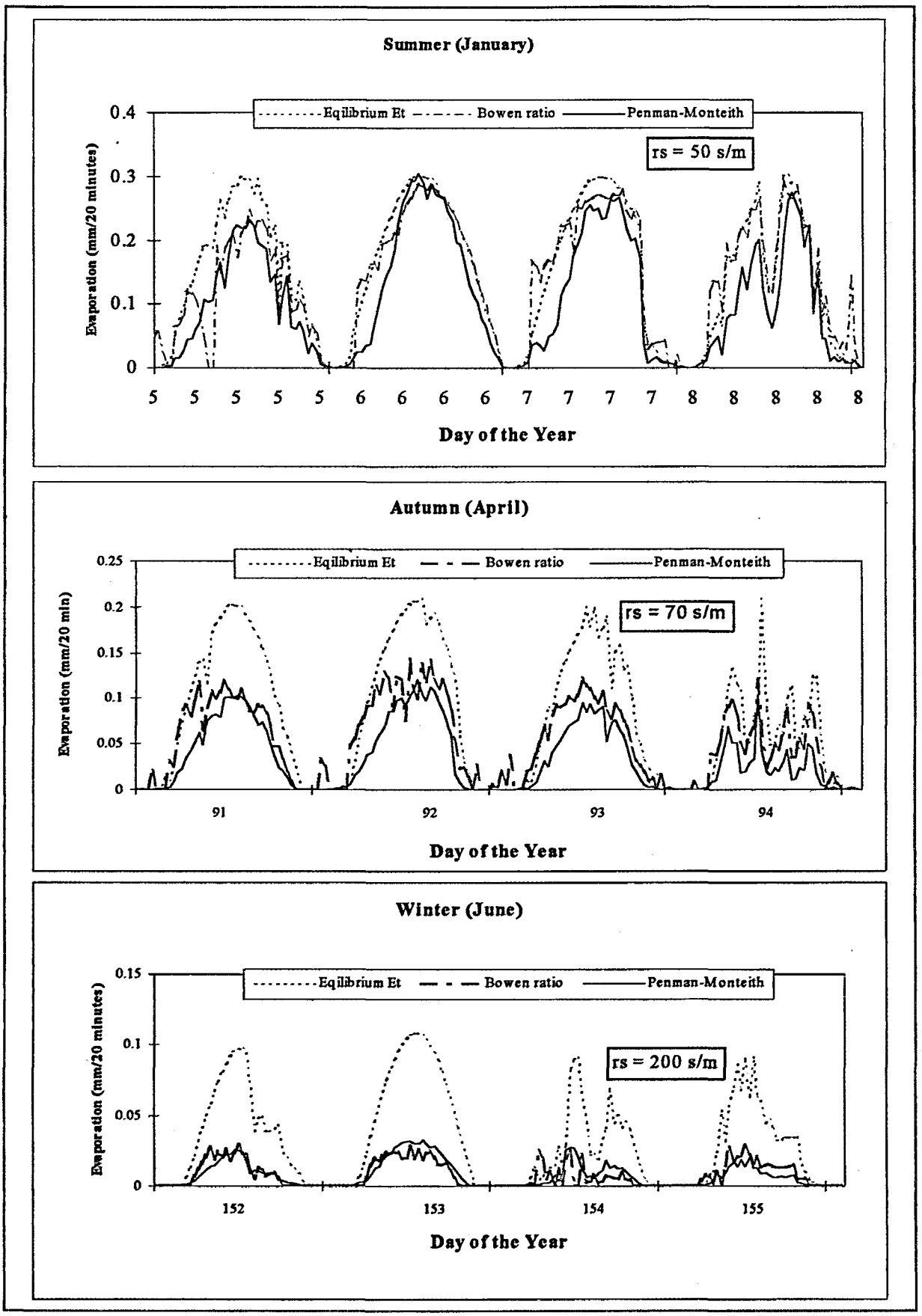

Figure 3.11 Comparisons of actual and modelled radiation for the summer, autumn and winter seasons

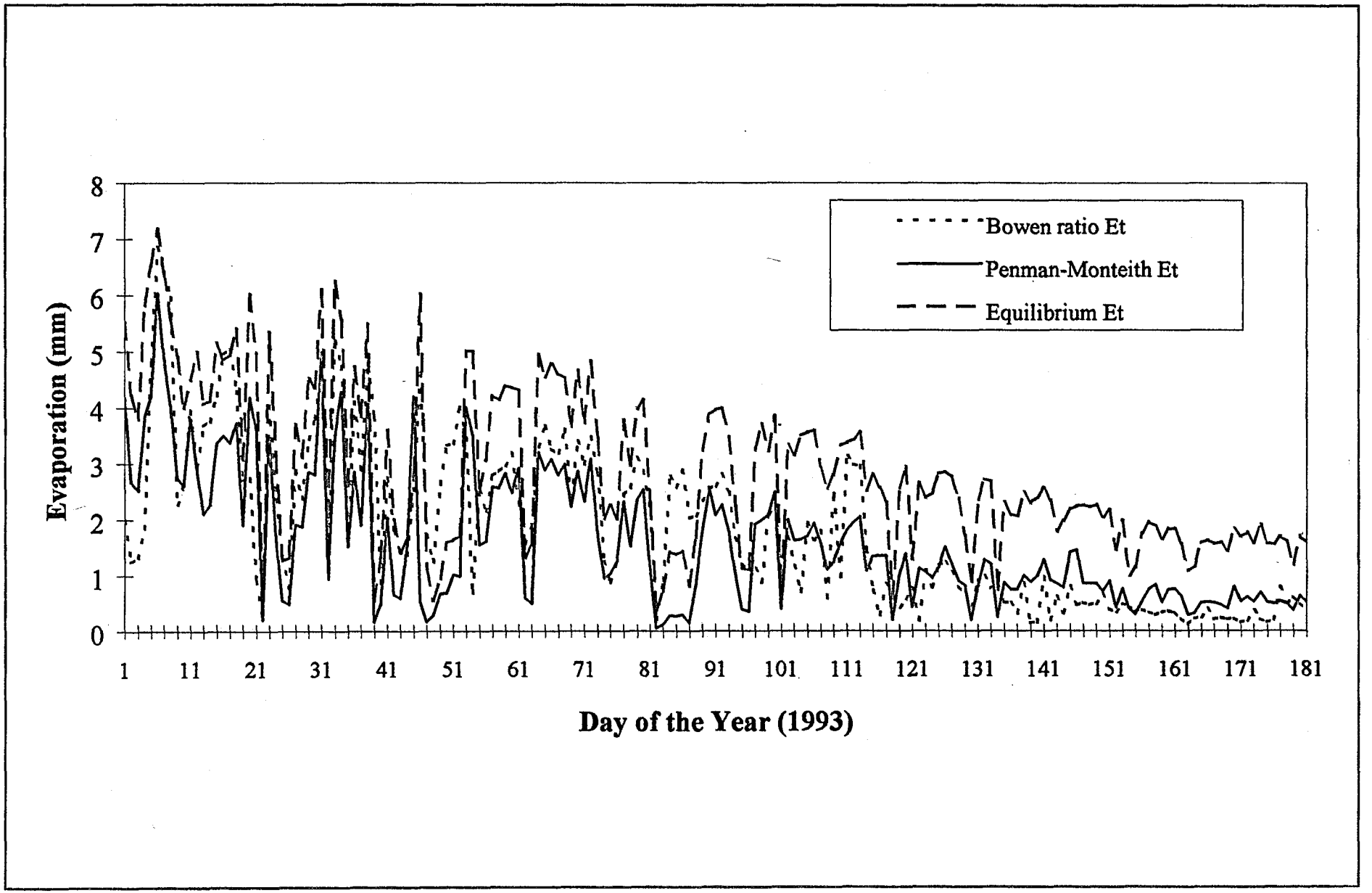

Figure 3.12 Comparison of the Bowen ratio, Equilibrium and Penman-Monteith evaporation rates from January to June 1993.

3.5 Conclusion

The results of this study indicate that the evaporation rate of grassland catchments can be accurately modelled by using the Penman-Monteith combination equation. Although this is an elaborate model and requires detailed climatic data (net radiation, air temperature, vapour pressure and wind speed) its accuracy far outweighs these considerations. Net radiation is the only parameter that is not routinely measured at South African weather stations. It can, however, be easily estimated from solar radiation which is measured at most weather stations.

The results show that the stomatal resistance can be set to 50 s m^{-1} in summer, 70 s m^{-1} in autumn and 200 s m^{-1} in winter for accurate measurements of evaporation. The simpler equilibrium equation, which does not take into account the aerodynamic and stomatal resistances, is unsuitable for estimating evaporation of the grassland sites of this study.

Chapter 4

SOIL WATER

4.1 Introduction

Soil water content is a critical variable in many processes, and its determination is of vital importance in efforts to improve plant growth and water use efficiency. In particular, future studies to analyse or model infiltration, flux and redistribution of water in catchments are dependent on accurate measurements of *in situ* water content.

Soil water content can be expressed as a dimensionless mass or volume ratio. The gravimetric water content is based on the mass ratio:

$$\theta_m = M_w / M_s$$

where θ_m is gravimetric water content, M_w is water mass and M_s is dry soil mass. The volumetric water content, θ is based on the ratio:

$$\theta = V_w / V_s$$

where θ is volumetric water content, V_w is volume of water and V_s is total soil volume. Gravimetric and volumetric soil water content are related to each other as:

$$\theta = r_s \cdot \theta_m$$

where r_s is the dry bulk density of the soil. Soil water contents can be measured by direct methods such as gravimetric, or by indirect ones based on neutron thermalization, gamma ray attenuation or electrical conductivity and capacitance. In this chapter we investigate three techniques for determining the soil water content in catchment VI. The field studies are used to

in catchment VI. The field studies are used to estimate changes in soil water storage and to model the temporal and spatial distribution of soil water on a hillslope.

4.2 A comparison of three soil moisture measurement techniques

Three indirect methods of measuring soil water (neutron probe, capacitance probe and time-domain reflectometry) were examined in the field and compared to the direct gravimetric technique (control).

4.2.1 *Neutron probe*

4.2.1.1 Basic principles and theory

The Neutron probe technique is a nondestructive method for measuring the water content of soil (Reginato & Nakayama 1987). This method is based on the fact that the hydrogen nucleus has the same mass as a neutron. When the two collide there is a transfer of energy which slows down the neutron. This change in energy is measured with a neutron probe.

The neutron probe contains a fast neutron source and a slow neutron detector, a pulse counter, a cable connecting the two, and a transport shield. The shield is fitted to the protruding upper end of an aluminium access tube which is positioned vertically in the soil. The probe is lowered directly into the access tube to successive measurement depths by means of a cable. A depth indicator and moderator which acts as a field standard are incorporated on the shield. The counter unit remains at the surface; this incorporates the electronic controls, the readout display, the battery which powers the system and the circuits which count the pulses from the probe.

The probe contains a radioactive source which emits fast neutrons into the surrounding soil. Collisions with the nuclei of the soil atoms, predominantly those of hydrogen in the soil water, cause the neutrons to scatter, to slow and to lose energy. When they have slowed to a 'thermal' energy level they are absorbed by other nuclear reactions. Thus a 'cloud' of slow neutrons is generated within the soil around the source. The density of this cloud, which is largely a function

of the soil water content, is sampled by a slow neutron detector in the probe. The electrical pulses from the detector are amplified and shaped before passing up the cable to the counter unit where their mean count rate is displayed. The count rate is translated into the soil moisture content (by volume) using an appropriate calibration curve.

4.2.1.2 Methods

Fourteen aluminium access tubes approximately 20 m apart and 2 m deep, were placed along a 300 m transect in catchment VI. The access tubes were installed in March 1990 while moisture contents were still high. During installation gravimetric samples and corresponding count ratios were collected. Count ratios were routinely taken from these sites twice weekly at 0.25 m intervals.

Bulk densities were determined to a depth of 1 m. Soil samples were oven-dried at 105 °C and the percentage soil water content (on a mass basis) determined. A similar procedure was followed at monthly intervals between May and August, except that the soil samples were collected from cores taken approximately 1 m from the access tubes. The samples therefore represented a moisture gradient from saturated (March) to dry (August), the complete range of possible conditions represented in the catchment.

At the end of August there were 5 pairs of readings (gravimetric and corresponding count ratio) for each depth (8) for every tube (14). However, not all tubes were 2 m deep and eventually 353 pairs of readings were used in the calibration of the instrument (Appendix A). The mean bulk density was 0.82 (Table 4.1). Soil water content was converted to volumetric water content from the previously determined values of the soil bulk density.

4.2.2 *Capacitance Probe*

4.2.2.1 Basic principles and theory

The capacitance technique provides rapid *in situ* measurements of the dielectric constant (real and imaginary parts) of soil (Brisco & Pultz, 1992). The volumetric soil water content (θ) is calculated using the empirical relationship to convert the real part of the dielectric constant (ϵ_r)

to θ. This approach is possible because of the large dielectric constant of water at microwave frequencies (60-80 kHz) compared to the dielectric constant of dry soil (2-5 kHz).

The capacitance probe consists of a sensor linked to a hand held frequency reader by a fibre optic cable. The sensor measures the dielectric constant of the soil with a temperature compensated, highly stable, electronic oscillator and the output is displayed by a frequency reader.

Table 4.1 Soil Characteristics at the lysimeter site in catchment VI.

BULK DENSITY :

Soil Depth	Dry Season		Wet Season		Mean
0.20 m	0.660	0.786	0.868	0.886	0.80
0.50 m	0.898	0.899	0.847	0.798	0.86
0.75 m	0.803	0.757	0.662	0.784	0.75
1.00 m	0.863	0.799	0.905	0.844	0.85
				Mean =	0.80

POROSITY:

Soil Depth	Dry Season		Wet Season		Mean
0.20 m	75.10	70.35	67.25	66.55	69.8%
0.50 m	66.09	66.09	68.05	69.89	67.5%
0.75 m	69.70	71.44	75.00	70.41	71.6%
1.00 m	67.42	69.85	65.87	68.16	67.8%
				Mean =	69.2%

SOIL WATER CONTENT:

Mean when saturated: 64% by volume

Maximum when saturated: 70% by volume

4.2.2.2 Methods

A capacitance probe (type IH1, Didcot Instruments Co. Ltd., Oxford, UK) was used to measure volumetric soil moisture content in catchment VI. The calibration procedure is outlined in Appendix B. The installation of the access tubes for the capacitance probe required an exceptionally careful and rigorous technique. When used in shrinking soils difficulties arise due to the development of variable air gaps. Since soil samples from catchment VI have shown shrinkage of 25% the installation of the access tubes was delayed until the winter period (July 1993), when the soil was driest.

A series of extension handles were used to lower the sensor into PVC access tubes. An access tube extension piece was placed on the access tube and a "click-stop" device ensured that the probe could be located precisely at 2 cm depth intervals. The handle is sectional and sections were screwed together to provide sufficient length to permit the probe to be inserted to the full length of the access tube. An electrical field was generated between two annular electrodes within the probe; this penetrated into the surrounding soil and the universal frequency is calculated from the sensor reading. The volumetric soil water content was read directly from the calibration curve.

4.2.3 *Time Domain Reflectometry*

4.2.3.1 Basic principles and theory

Time domain reflectometry (TDR) is a non-destructive technique for simultaneous measurement of soil water content and soil electrical conductivity. The description given here is a summary of the theory and installation procedures described in Appendix C.

The time domain reflectometry technique propagates a balanced waveform which travels down a coaxial cable and waveguide and is influenced by the type of material surrounding the conductors. If the dielectric constant of the material is high, the signal propagates slower. Because the dielectric constant of water is much higher than most materials, a signal within a moist medium propagates slower than the same medium when dry. Thus moisture content can be determined by measuring the propagation time over a fixed length probe embedded in the soil.

4.2.3.2 Methods

The Time Domain Reflectrometry (TDR) equipment was set up in CVI at the end of September 1994. The system developed by Campbell Scientific comprises a Tektronix 1502B cable tester equipped with a SDM 1502 Communications Interface and the PS1502B Power Control Module. The probes used (8) were the PB30B, which is a two rod probe with 0.3 m stainless steel rods. A balun moulded into the cable joined the twin lead cable from the probe to the multiplexer. The TDR requires no prior calibration.

4.2.4 *Gravimetric technique*

4.2.4.1 Basic principles

The traditional method of direct soil water content measurement is the gravimetric technique (Gardner 1987). Soil samples are removed and then weighed prior to and following a drying process. When samples are taken with a soil auger, usually the volume of the sample is not known and only the gravimetric water content can be measured. For conversion of gravimetric water content to volumetric water content an independent measure of soil bulk density is necessary.

4.2.4.2 Methods

Soil samples (±100 g) were collected in plastic bags to prevent evaporation. After weighing, the soil samples were placed in a conventional oven for drying to constant weight. The drying time was at least 24 h at 105 °C.

4.3 Field trial to test different techniques for measuring soil moisture

The field experiment in which the TDR, neutron probe, capacitance probe and gravimetric sampling were compared was carried out in catchment VI from October 1994 to the end of December 1995. The eight TDR probes were inserted horizontally into two profiles, at four depths (i.e. two replicates at each depth). The depths chosen were 0.125 m, 0.375 m, 0.625 m and 0.820 m. Two neutron probe and two capacitance probe access tubes were placed within

0.5 m of the TDR probes. These were sampled weekly. Three gravimetric samples were collected at weekly intervals at the following depths: 0.1- 0.15 m, 0.35-0.40 m, 0.60-0.65 m and 0.80-0.85 m. The gravimetric soil samples were taken at a site approximately 4 m along the contour away from the other techniques because of the destructive nature of the technique. Since the results were similar for all depths, the 0.375 m depth was arbitrarily selected for the comparative study.

4.3.1 *Results*

A typical TDR trace obtained in soils from Cathedral Peak, showing the start and reflection points is shown in Figure 4.1. Very clear wave forms were found in these soils so that soil water content was easily determined. The fractional volumetric water content (θ) from the TDR technique remained constant at 0.41 from DOY 271 to DOY 301. The first significant rain storm (35 mm) resulted in a rapid increase in θ to 0.45 (DOY 304, Figure 4.2). From DOY 305 to DOY 340 only small rain events (<10 mm) occurred and θ declined steadily to 0.41. The effect of rain events >10 mm on θ is evident from the increase between DOY 345 and 365. There was little difference in θ between the two TDR sites .

Comparison of the different techniques showed good agreement between the gravimetric, TDR and neutron probe. Differences in θ were generally less than 0.02 (Table 4.2). The capacitance probe did not agree well with any of the other techniques.

Table 4.2. A comparison of the volumetric water content of the four different soil monitoring techniques.

DOY	Gravimetric	Neutron	Capacitance	TDR
271	-	0.41	0.52	0.41
279	-	0.39	0.54	0.40
286	-	0.39	0.56	0.41
293	0.40	0.40	0.54	0.42
300	0.39	0.39	0.50	0.41
306	0.51	0.50	0.49	0.46
314	0.51	0.51	0.49	0.45
321	0.46	0.44	0.49	0.44
329	0.42	0.44	0.50	0.42
334	0.41	0.40	-	0.42

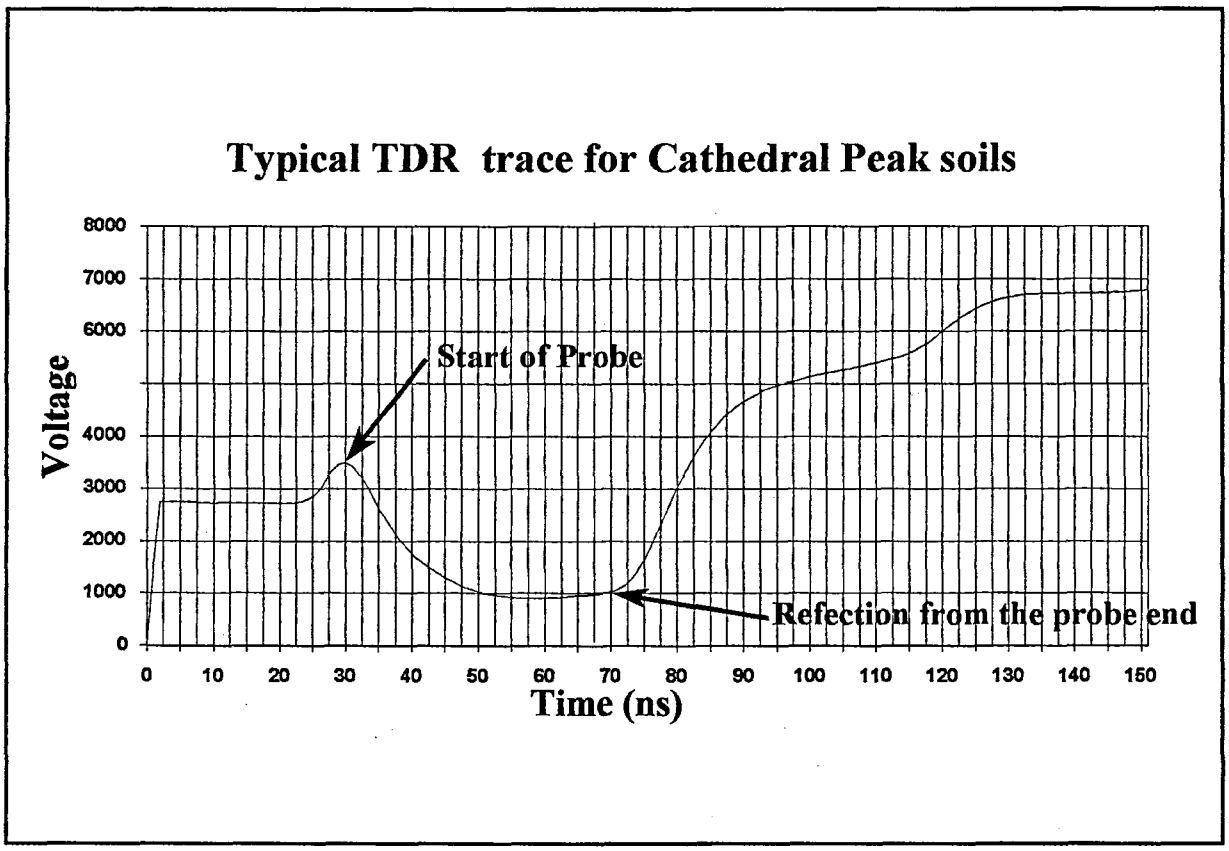

Figure 4.1 A typical wave form obtained with 0.3 m probes for a typical soil at Cathedral Peak.

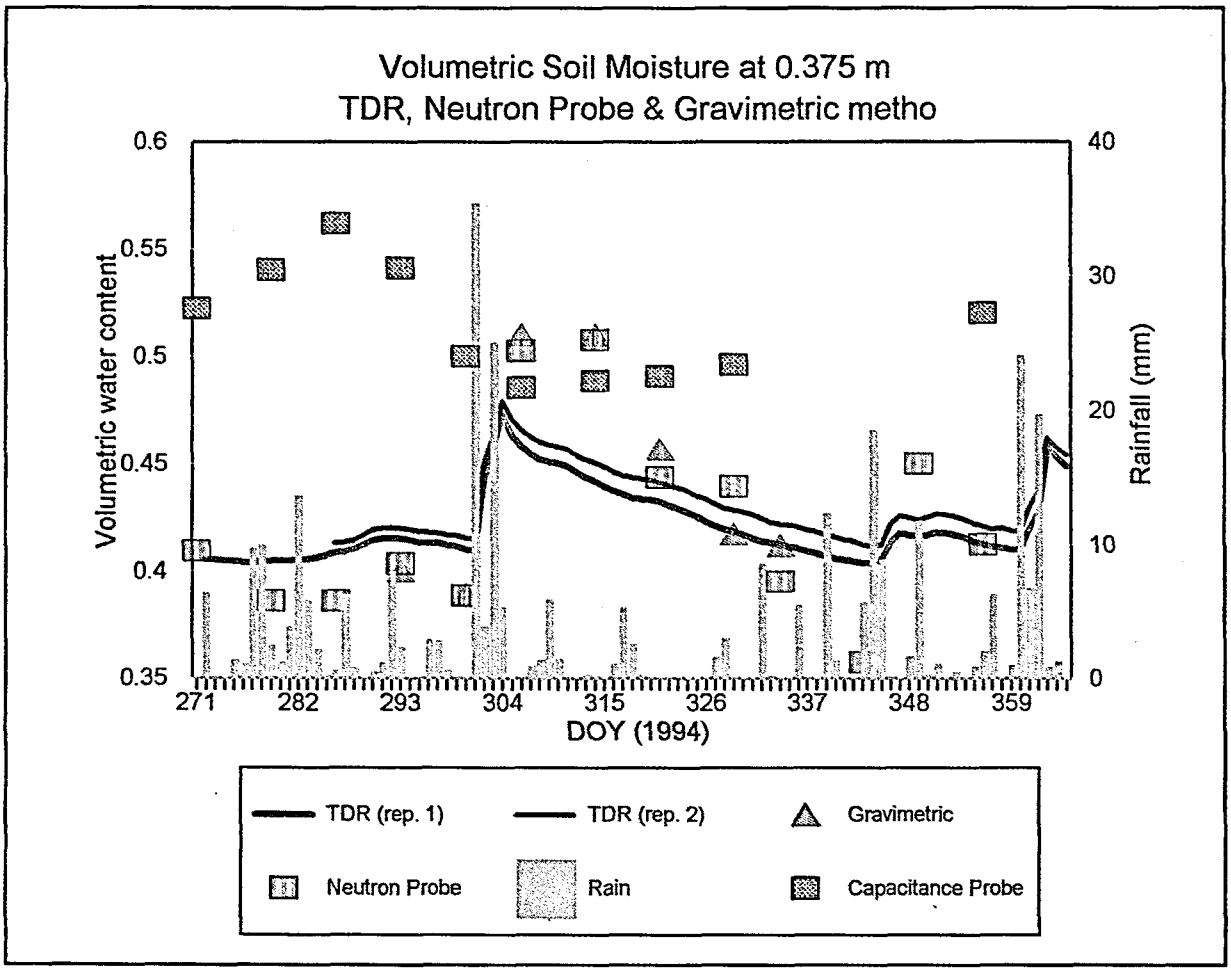

Figure 4.2 A comparison of four different techniques of measuring volumetric water content.

Trends in θ using TDR over the four different depths showed that moisture at 0.125 m fluctuated daily in response to small variations in rain (Figure 4.3). During periods of very low rain (DOY 290-300 & DOY 305-342), evaporation from the soil is high, resulting in marked decreases in θ (Figure 4.3). There was a general trend of the soil being progressively drier with increasing depth. Trends at the three greater depths were very similar. With the exception of the high rain event on DOY 304, little water infiltrated beyond the 0.12 m depth. The real time measurements depicted in Figure 4.3 illustrate the potential of this instrument for measuring *in situ* volumetric water content.

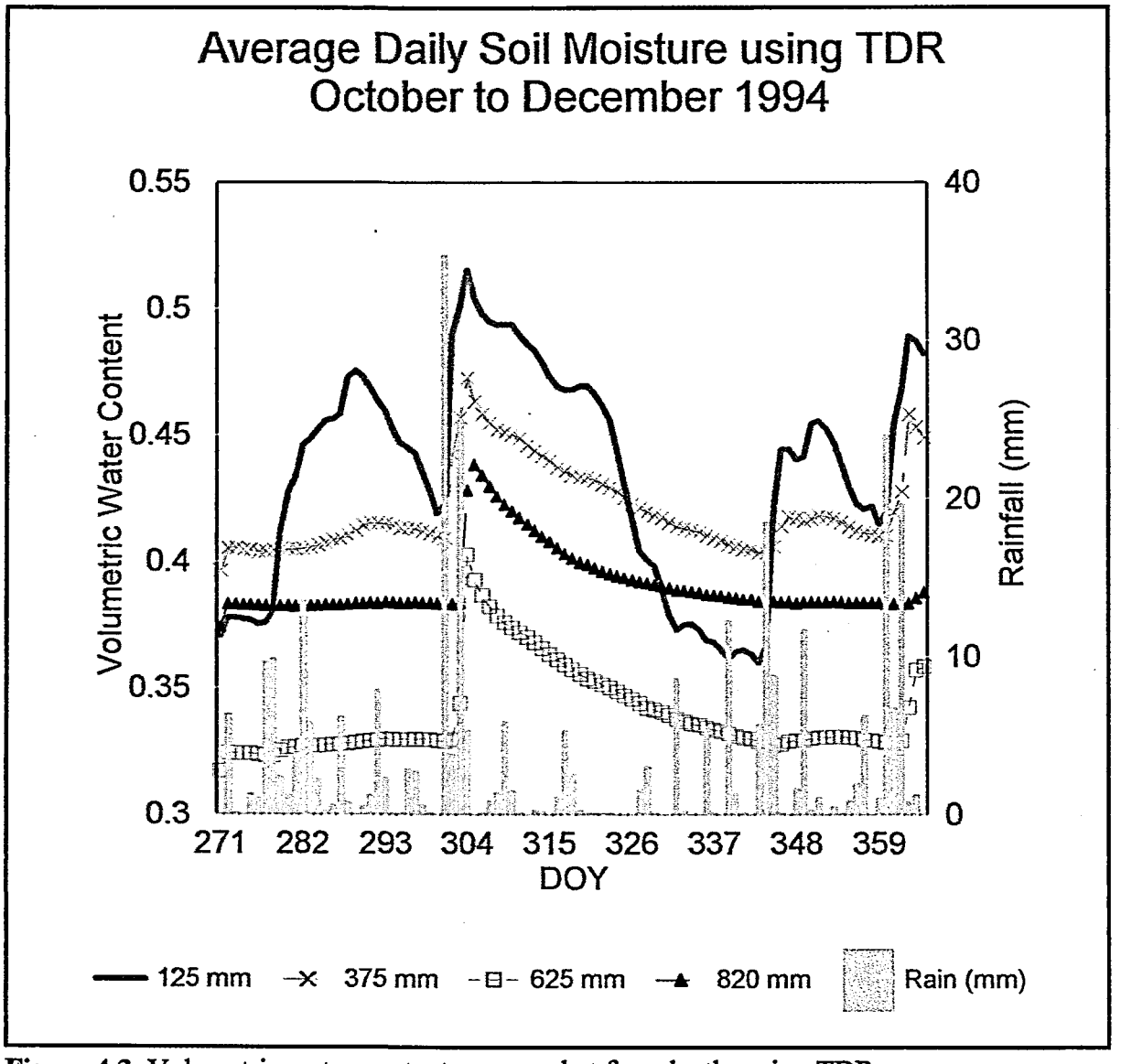

Figure 4.3 Volumetric water content measured at four depths using TDR.

4.3.2 *Discussion and conclusions*

The determination of soil moisture using the capacitance probe was discontinued because of problems with calibration and poor fit of regression lines. The best results were obtained with the neutron probe and TDR techniques which gave accurate estimates of volumetric water content when compared to the other methods. The limitations and advantages of the methods used are outlined below.

The gravimetric technique was the most simple and cheapest method for determining soil moisture. However, the destructive nature of sampling, the time delay for drying of samples and the intensive labour required are drawbacks of the gravimetric method.

The neutron probe technique was a reliable and accurate method for measuring soil water. The neutron probe is best used in situations where non destructive measurements of moisture are required in the same profiles on many occasions. Besides its non-destructive attribute, one of the main advantages of this method is its precision. It is a research tool that is suitable for routine work providing that the field procedures are carefully supervised and the data scrutinised as soon as possible after the readings are taken. The method can produce very good or very bad results, depending on the skill and interest of the field staff.

In spite of the continual improvements in the neutron moderation technique for measuring water content, the fact that it cannot be automated and is labour intensive limits its usefulness. Since the instrument responds to total hydrogen and not just the hydrogen component of the available water in soil, there is a need for calibration for every situation. Incorrect calibration curves may cause bias in this method. Since the neutron method requires a relatively large sampling volume, one of its limitations is the inability to measure close to the soil surface. The radiation hazard is an added disadvantage of this method.

The biggest advantage of the TDR technique over the neutron probe was the ease of automation and the ability to collect hourly or daily soil moisture, as opposed to the weekly samples for the other techniques. This makes the data interpretation much easier. The fact that the TDR can be used without calibration is also a big advantage.

Since the TDR method can give measurements over identical sampling volumes, errors due to spatially variable soil properties are reduced. The recent technical advances of automation and multiplexing for hydrological applications enable TDR to be applied successfully to field conditions.

The capacitance probe has distinct advantages over the neutron probe including portability, lack the radiation hazard and speed of measurement. One of the problems with this technique is that it depends upon specific electrode configurations and detailed calibration. The sensitivity of the probe to small variations in soil properties also created problems in calibration. Since the probe is very sensitive to small variations in soil properties, the presence of gaps, cavities, stones or roots in proximity to the access tube can create anomalous results. The dense root profile and high porosity of the soils in this study may have attributed to the failure of the probe to provide accurate measurements of the moisture content.

4.4 Soil moisture distribution in a hillslope segment

Discharge of excess rainfall from hill slope segments of a catchment into streams is commonly partitioned into three components - surface runoff, shallow subsurface flow and deep groundwater flow. Depending on the soil hydrological properties, each of these components may dominate runoff (Dunne & Black 1970; Freeze 1972; Mosley 1979). One of the conditions for surface or shallow subsurface flow is the presence of a soil layer of low hydraulic conductivity at or just below the soil surface. Surface runoff will also occur below any point on a hill slope where a water table intersects the soil surface. Where the limiting hydraulic conductivity in the soil profile exceeds the rainfall intensity, water will move through an unsaturated zone to the regional water table and then discharge as groundwater flow. An understanding of these physical processes is important for watershed management. A study was therefore initiated in the Cathedral Peak catchment area to monitor infiltration of rainfall events through successive soil layers and determine its redistribution between rainfall events.

The study was conducted on a grassland hill slope in the experimental catchment VI at Cathedral Peak. The soils in catchment VI are generally deep, and are underlain by an impermeable layer of basalt. Recharge rates to the ground water table were estimated for comparisons with measured discharge rates from the gauging weir at the catchment outlet.

4.4.1 *Method*

A 300 m transect for soil water assessment was laid out along a topographic gradient from the upslope region into the margin of the saturated zone. A Troxler neutron moisture meter was used for the determination of soil water content. Fourteen aluminium access tubes were placed along the transect, approximately 20 m apart and to a depth of 2 m. Weekly count ratios were routinely taken from these sites at 0.25 m depth intervals. The calibration procedure is described in Appendix A. Mass water content was converted to volumetric water content from previously determined values of the soil bulk density. From these data the total profile water content was calculated from each of the 14 access tubes.

4.4.1.1 Water content profiles

Weekly soil water contents at various depths, $\theta(z)$, for the months of January to July for an upslope access tube (site 6) are given in Figure 4.4. This time period was selected to illustrate the change in $\theta(z)$ from the wet summer through to the dry winter period. The period from January to March 1991 was characterised by frequent rain events, which are reflected in the water contents, which were generally high (> 43%) over all depths. Both the upper and lowermost regions had water contents of 50%. Low rainfall in April through to July, resulted in a gradual but progressive drying from the soil surface to a depth of 1.2 m. For example the uppermost layer dried from approximately 50% in March to 38% by the end of June. The drying out of the soil was reflected in the tensiometer data for April, where surface matric potentials (ψ), approached -80 kPa (Figure 4.5.). These values were close to the driest values which these instruments can record, before air entry through the ceramic cup causes the instrument to malfunction.

Water content at depths below 1.2 m remained largely unchanged throughout the year, indicating that there is little or no loss of water by evaporation from these deep regions. Previous studies of the root distribution of grasses in this area, showed that even the finest grass roots do not penetrate beyond 1.2 m. It is in this region of permanently saturated soil that most water moves under the influence of gravity to the low slope sites. During the active growth

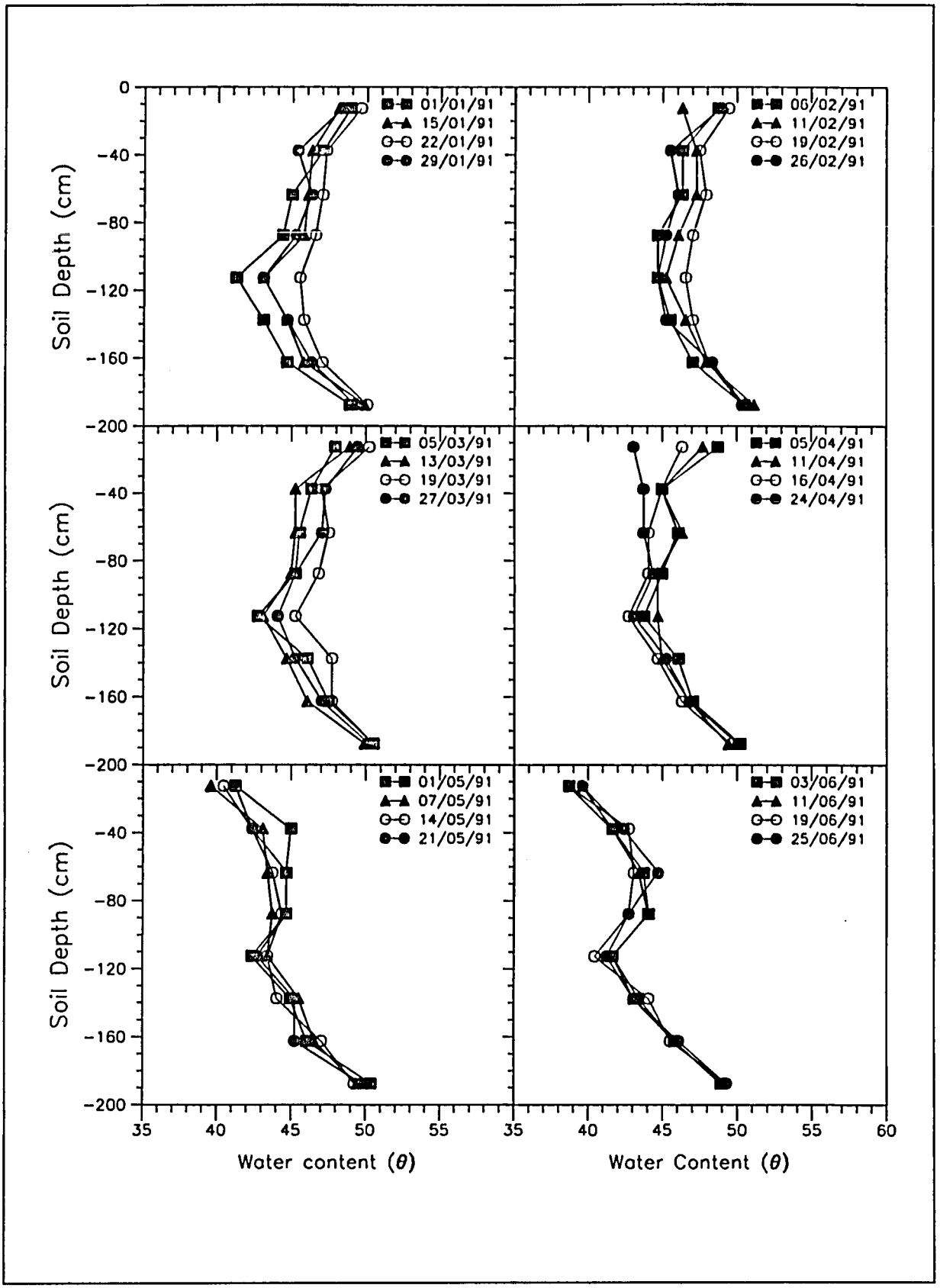

Figure 4.4 Soil water content profiles, $\theta_{(z)}$, for an upslope site in catchment VI, for the six month period, January to June 1991. Weekly profiles are plotted within each month.

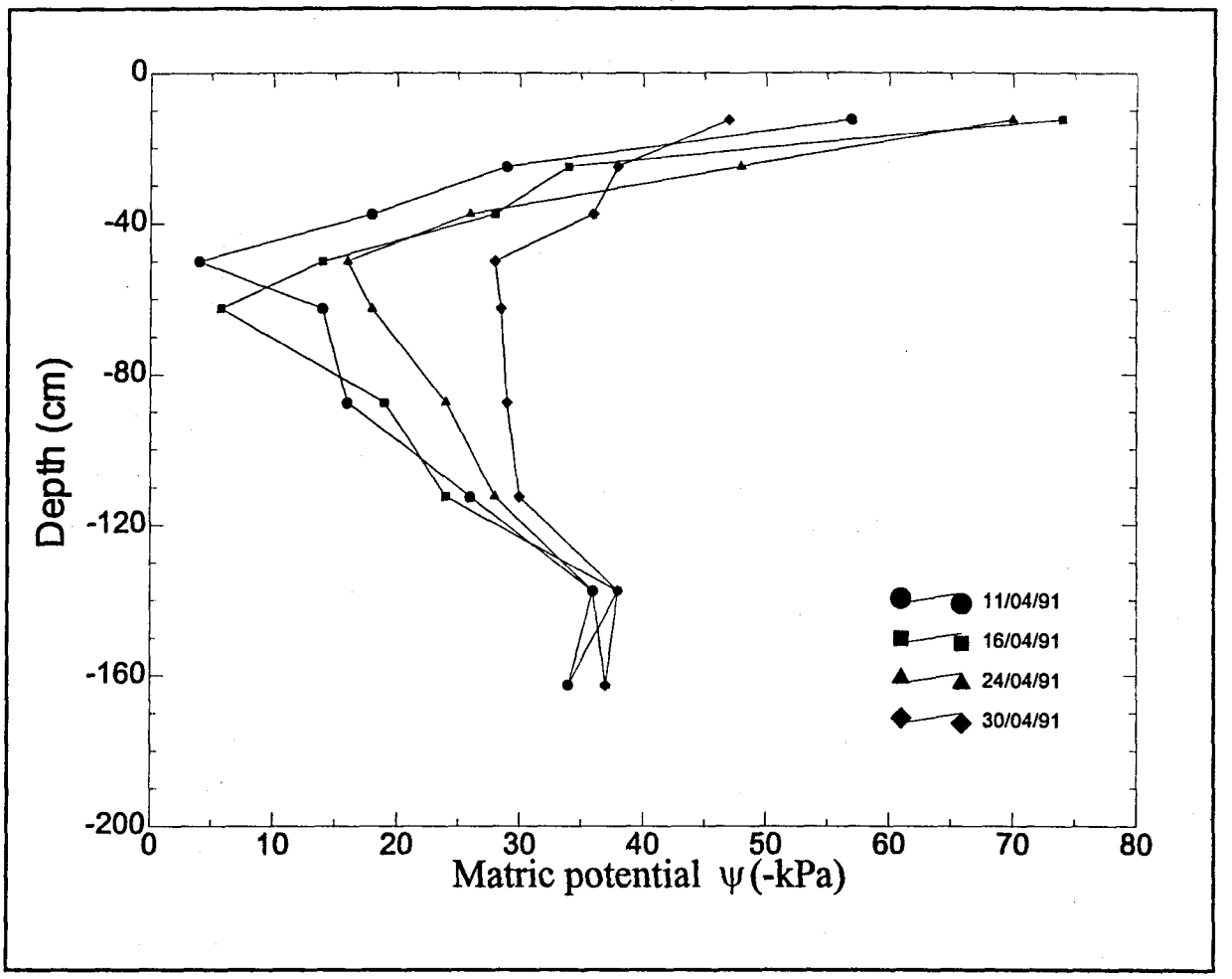

Figure 4.5 Matric potentials, ψ, at various depths for an upslope site in CVI, during April 1991.

season, the decay curve of the soil moisture reservoir can be used to estimate transpiration. Although the soil moisture changes can be measured very precisely, the direction of the movement remains unknown. The installation of adjacent tensiometers is required to determine the direction of vertical soil water movement. From the tensiometer data the area of maximum potential is identified, at which the potential gradient is zero (e.g. the inflection region between 10 and 20 kPa corresponds to a depth of approximately 50 cm in Figure 4.5). Because the potential gradient is zero the soil water flux at this point is also zero. This point defines the position of the 'zero flux plane' at that moment. Above the zero flux plane the potential gradient and hence the soil water flux is upwards, supplying the demands of evaporation. Below the zero flux plane the gradient and flux are downwards, representing drainage to the groundwater. Weekly soil water contents $\theta(z)$ at various depths for the months of January to July for the riparian zone access tube (site 14) are given in Figure 4.6. The more vertical profiles in the

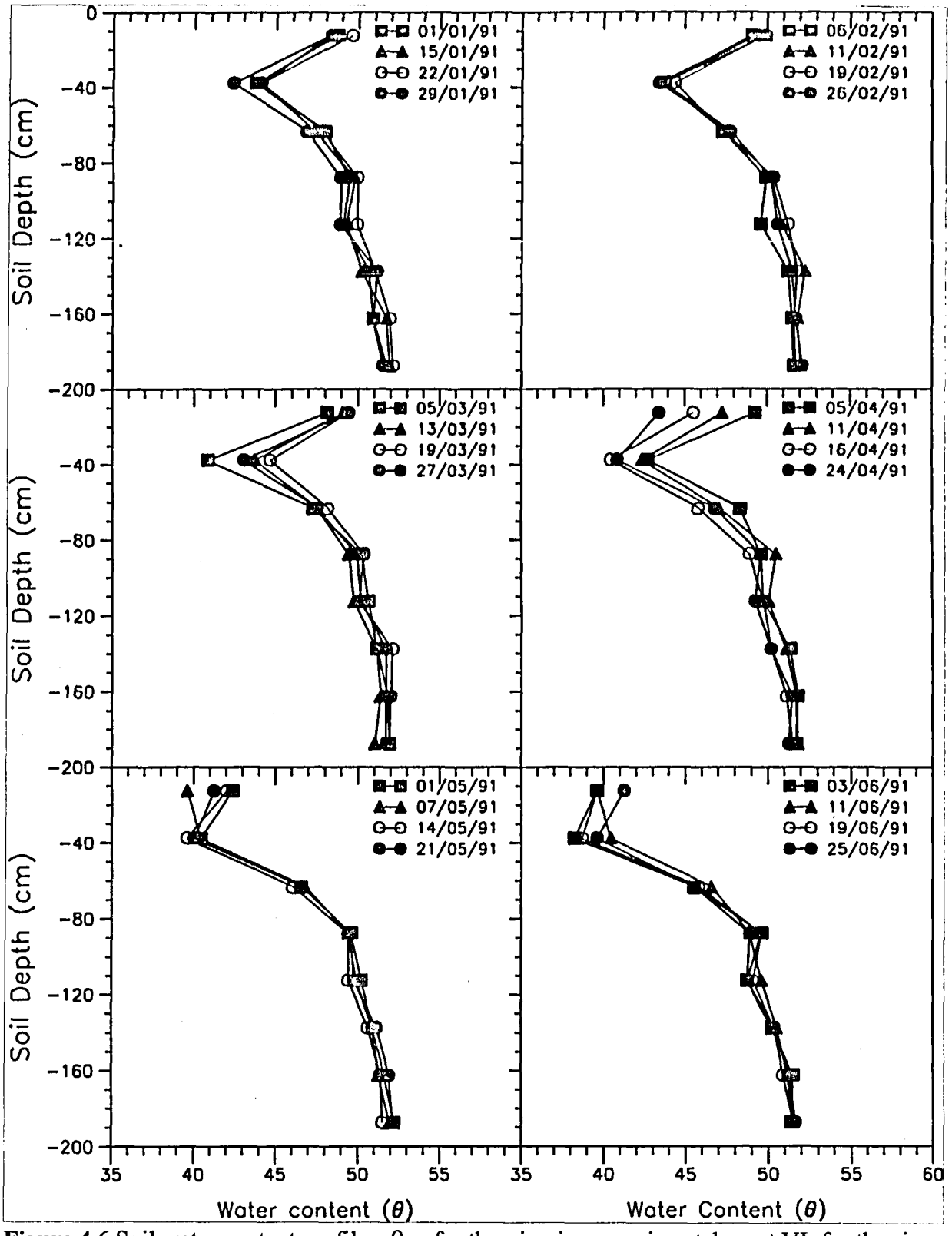

Figure 4.6 Soil water content profiles, $\theta_{(z)}$, for the riparian zone in catchment VI, for the six month period, January to June 1991. Weekly profiles are plotted within each month.

lower regions (from -80 cm downwards) contrasts sharply with those from the upland region. This indicates the presence of a permanent water table. The curves also showed a consistent region of low water content at -40 cm, in the region where the A and B soil horizons interface. The A horizon in this area is characterised by a black, friable soil, high in organic matter. The B horizon is a heavy grey clay. The susceptibility of the A horizon to drying is clearly illustrated in the curves from April to June, where the upper layer dried from approximately 50 to 37%.

Weekly readings of the total profile water content for an upslope site are shown in Figure 4.7. The effect of the summer rains in the recharging of the soil profile (October to February) are evident. Similarly the depletion during the dry winter period (March to August) are illustrated by these data. Total profile water contents for the 2 m sample depth ranged from 850 mm in winter to 965 mm in summer. Comparison of the soil water storage at the beginning and end of each hydrological year showed that changes were small (-11, -45, +7 and -14 mm for 1990/91, 1991/92, 1992/93 and 1993/94 respectively) (Figure 4.7). This confirms the validity of assuming that storage from one hydrological year to the next is negligible. The unusually high water contents of these soils are not easily reconciled with the low bulk densities measured for these soils. This requires further study as it may explain the high water yielding capacity of the soils of these catchments.

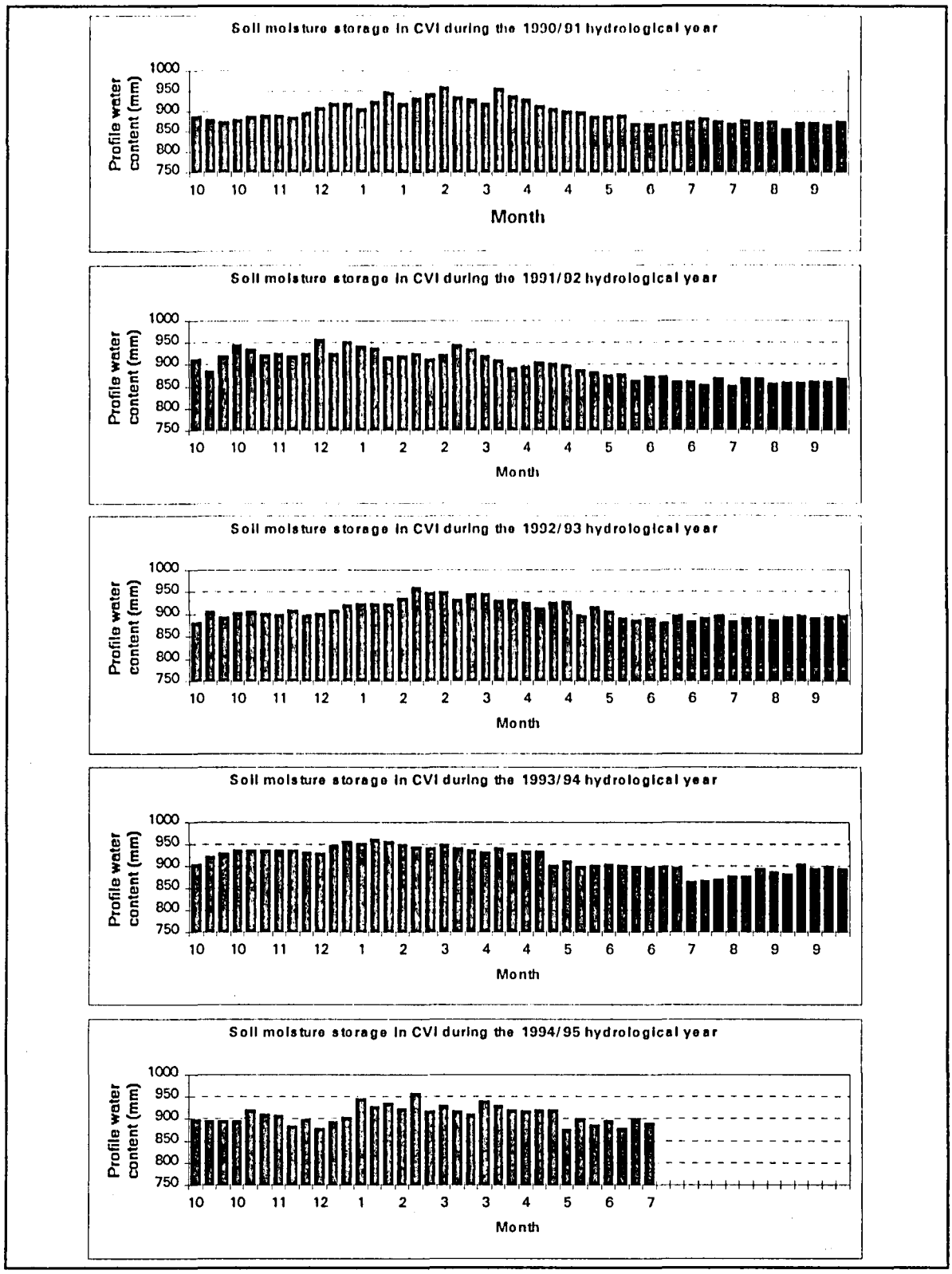

Figure 4.7 Weekly total profile water content in catchment VI (September 1990 to July 1991).

4.5 Soil water content - spatial and temporal variability

A knowledge of the spatial and temporal variations in soil water content at catchment scales is important to the understanding of most hydrologic processes. The distribution of infiltration and subsequent runoff across a catchment is known to be controlled by variations in soil water content. In this study the spatial variation in soil physical properties and spatial and temporal variations in soil water content are investigated using geostatistical methods for a hillslope in CVI. Geostatistical methods are used to determine the spatial structure observed from regionalised variables (i.e. a set of measurements such as water content). Three basic geostatistical methods that are frequently used in spatial analysis are autocorrelation, semivariance and generalized covariance (Loague 1992).

Autocorrelation is the process that expresses the linear correlation between the members of a spatial series and other members of the same series separated by fixed intervals in space. The graphical representation of spatial dependency, ρ (**h**) against lag, h, is an autocorrelogram. This has a maximum value of 1 at $h = 0$ and decreases with increasing lags to -1. If the random variable is strongly dependent on its neighbouring values, then the autocorrelogram will decay slowly. If spatial dependence is weak, the decay will be rapid.

Semivariance expresses the distribution of variance as a function of separation between the spatially dependent components of a random function. Spatial dependency is characterized by λ (**h**) which is plotted against h to give a semivariogram. The semivariogram may reach a limiting value called a sill that is equal to the variance of the data. The distance between the origin and the point at which the sill is reached is called the range. Observations separated by distances greater than the range are not correlated. If measurements are totally without correlation, the semivariogram will exhibit a nugget effect. A primary application of a semivariogram is kriging in which estimates are made of variables at unsampled locations. The regional variable is described by the drift. If the drift is not constant the data may be biased. This problem is overcome using the generalized covariance technique which eliminates the need to estimate the drift.

4.5.1. *Data Analysis*

The aims of the data analysis were:

(i) to develop a model and fitting technique to predict water content at any point in time and space,

(ii) to determine a method for reconciling the driving mechanisms (daily rainfall, and evaporation) with the changing soil water content, modified by local physical properties of the soil.

The preliminary analysis comprised the count ratios taken from the original 14 neutron probe access tubes at 8 depths and for 17 weekly periods from January 6 to May 5, 1992. The positioning of the tubes was along a single 300 m transect at 10 m intervals. Preliminary analysis of neutron probe data indicated that it would be necessary to expand the original network to adequately determine the spatial and temporal distribution of moisture on a representative hillslope. In 1992 the number of access tubes was increased to 31 to gain complete coverage of one side of the streambank. These 31 access tubes were monitored at weekly intervals for 8 depths from October 1992 to the end of February 1995.

4.5.2. *Soil survey*

To improve the spatial information about the soil properties, a survey was carried out to determine the soil particle size distribution in the experiment. Samples were taken from 35 positions at 5 depth increments, on one side of the streambank. The sampling depths were 0-200 mm, 200-400 mm, 600-800 mm, 800-1000 mm and 1800-2000 mm. The samples were analyzed for clay, silt and sand fractions by the Cedara soil physics laboratory. These analyses were completed in January 1993.

4.5.3. *Data organization and programming*

The neutron water count records were organized into data files suitable for access by statistical

4.5 Soil water content - spatial and temporal variability

A knowledge of the spatial and temporal variations in soil water content at catchment scales is important to the understanding of most hydrologic processes. The distribution of infiltration and subsequent runoff across a catchment is known to be controlled by variations in soil water content. In this study the spatial variation in soil physical properties and spatial and temporal variations in soil water content are investigated using geostatistical methods for a hillslope in CVI. Geostatistical methods are used to determine the spatial structure observed from regionalised variables (i.e. a set of measurements such as water content). Three basic geostatistical methods that are frequently used in spatial analysis are autocorrelation, semivariance and generalized covariance (Loague 1992).

Autocorrelation is the process that expresses the linear correlation between the members of a spatial series and other members of the same series separated by fixed intervals in space. The graphical representation of spatial dependency, ρ (**h**) against lag, h, is an autocorrelogram. This has a maximum value of 1 at $h = 0$ and decreases with increasing lags to -1. If the random variable is strongly dependent on its neighbouring values, then the autocorrelogram will decay slowly. If spatial dependence is weak, the decay will be rapid.

Semivariance expresses the distribution of variance as a function of separation between the spatially dependent components of a random function. Spatial dependency is characterized by λ (**h**) which is plotted against h to give a semivariogram. The semivariogram may reach a limiting value called a sill that is equal to the variance of the data. The distance between the origin and the point at which the sill is reached is called the range. Observations separated by distances greater than the range are not correlated. If measurements are totally without correlation, the semivariogram will exhibit a nugget effect. A primary application of a semivariogram is kriging in which estimates are made of variables at unsampled locations. The regional variable is described by the drift. If the drift is not constant the data may be biased. This problem is overcome using the generalized covariance technique which eliminates the need to estimate the drift.

4.5.1. *Data Analysis*

The aims of the data analysis were:

(i) to develop a model and fitting technique to predict water content at any point in time and space,

(ii) to determine a method for reconciling the driving mechanisms (daily rainfall, and evaporation) with the changing soil water content, modified by local physical properties of the soil.

The preliminary analysis comprised the count ratios taken from the original 14 neutron probe access tubes at 8 depths and for 17 weekly periods from January 6 to May 5, 1992. The positioning of the tubes was along a single 300 m transect at 10 m intervals. Preliminary analysis of neutron probe data indicated that it would be necessary to expand the original network to adequately determine the spatial and temporal distribution of moisture on a representative hillslope. In 1992 the number of access tubes was increased to 31 to gain complete coverage of one side of the streambank. These 31 access tubes were monitored at weekly intervals for 8 depths from October 1992 to the end of February 1995.

4.5.2. *Soil survey*

To improve the spatial information about the soil properties, a survey was carried out to determine the soil particle size distribution in the experiment. Samples were taken from 35 positions at 5 depth increments, on one side of the streambank. The sampling depths were 0-200 mm, 200-400 mm, 600-800 mm, 800-1000 mm and 1800-2000 mm. The samples were analyzed for clay, silt and sand fractions by the Cedara soil physics laboratory. These analyses were completed in January 1993.

4.5.3. *Data organization and programming*

The neutron water count records were organized into data files suitable for access by statistical

packages. The soil analysis data from 32 sampling positions and rainfall precipitation records were also arranged into suitable files. A common co-ordinate system for all the site locations was established. On this system, the y-axis represents a line from zero at the lower part of the hillslope (the riparian zone) and runs 220 meters to a position about 50 m above the Bowen ratio site. The axial extent of this line (the x-axis) is 100 m and encompasses the entire neutron probe network. The altitude (z co-ordinate) corresponded with the 1900 m contour interval which passed through the origin of the grid. The altitudinal gradient from the bottom (y=0) to the top was 52.82 m. The CSIR Bowen ratio site was located on the co-ordinates x=91.25;y=171.25 and z=29.5.

Analysis of the data required setting up GEOEAS data files containing running neutron probe count ratio means and soil physical properties for spatial variogram analysis. A software package (GSLIB) was used to check for correctness. This package comprises a series of Fortran subroutines designed for kriging. This method allows for an objective assessment of placing grids and offers insights into the data that would not otherwise be available. Some problems were encountered in the compilation due to the non-standard code but these were overcome. Verification was carried out by running data through the package SOILKRIG (Clarke & Dane 1991) and GSLIB and comparing results. This resulted in the generation of an executable program for universal kriging in 3 dimensions, allowing for external drift. This was thoroughly verified against SOILKRIG and found to be much faster in execution time.

The second major task was to establish a suitable interface whereby the gridded output from GSLIB could be imported into SURFER for graphical presentation. This enabled graphs to be plotted of kriged predictions in horizontal or vertical slices and slices over time. A major disappointment was the lack of success in getting the GSLIB version of CO-KRIGING to work, and in spite of thorough searches through contacts overseas the only CO-KRIGING programme available is that of SOILKRIG.

The SOILKRIG program AX was used for the estimation by cross-validation of variogram model parameters. This was based on running means of water count data at 9 selected dates in the year, at all 8 depths. Once a model had been chosen for a particular data set, cross-validated residuals were used to check for outlying data points. A number of data values were removed from the data

banks after this checking. Verified data sets together with the appropriate parameter sets were then available for kriging.

The next stage of analysis involved running these 3-dimensional data sets through the GSLIB universal kriging program to produce 3-D grids of predicted values. These in turn were graphically portrayed by horizontal or vertical slices printed as contour graphs by SURFER. Trends over time during 1993 were kriged for 9 different sites chosen to lie in a plane which allows for easier interpretation. This enables specific points to be examined.

4.5.4. *Results*

4.5.4.1 The temporal-spatial model

The soil water content values can be visualized in a 4-dimensional space. The first 3 dimensions are the latitude, longitude and depth below the soil surface of a given point and the 4th dimension is time. Instruments in the Cathedral Peak catchment area recorded count ratios (which may be directly converted to water content by means of a quadratic calibration equation) at 31 sites and 8 depths per site at weekly intervals during 1993 and 1994.

4.5.4.2 Parameter fitting

The technique chosen for model fitting and prediction was kriging, (Journel and Huijbregts 1978, Cressie 1991). The first stage of fitting a 4-dimensional model by kriging was the selection of 8 different dates during 1993 to cover the seasonal changes through summer and winter. At each date a 3-dimensional model was fitted to the data. More specifically, the measure of soil water content chosen for analysis was the cumulative mean count ratio at any time averaged over 5 successive records. Parameter estimation was done by cross-validation (Clarke & Dane 1991). Figure 4.8 illustrates the goodness of fit for changing values of the variance parameters (the range, nugget and vertical anisotropic ratio). Technically, a stationary model was fitted in the horizontal plane and quadratic drift in the vertical plane.

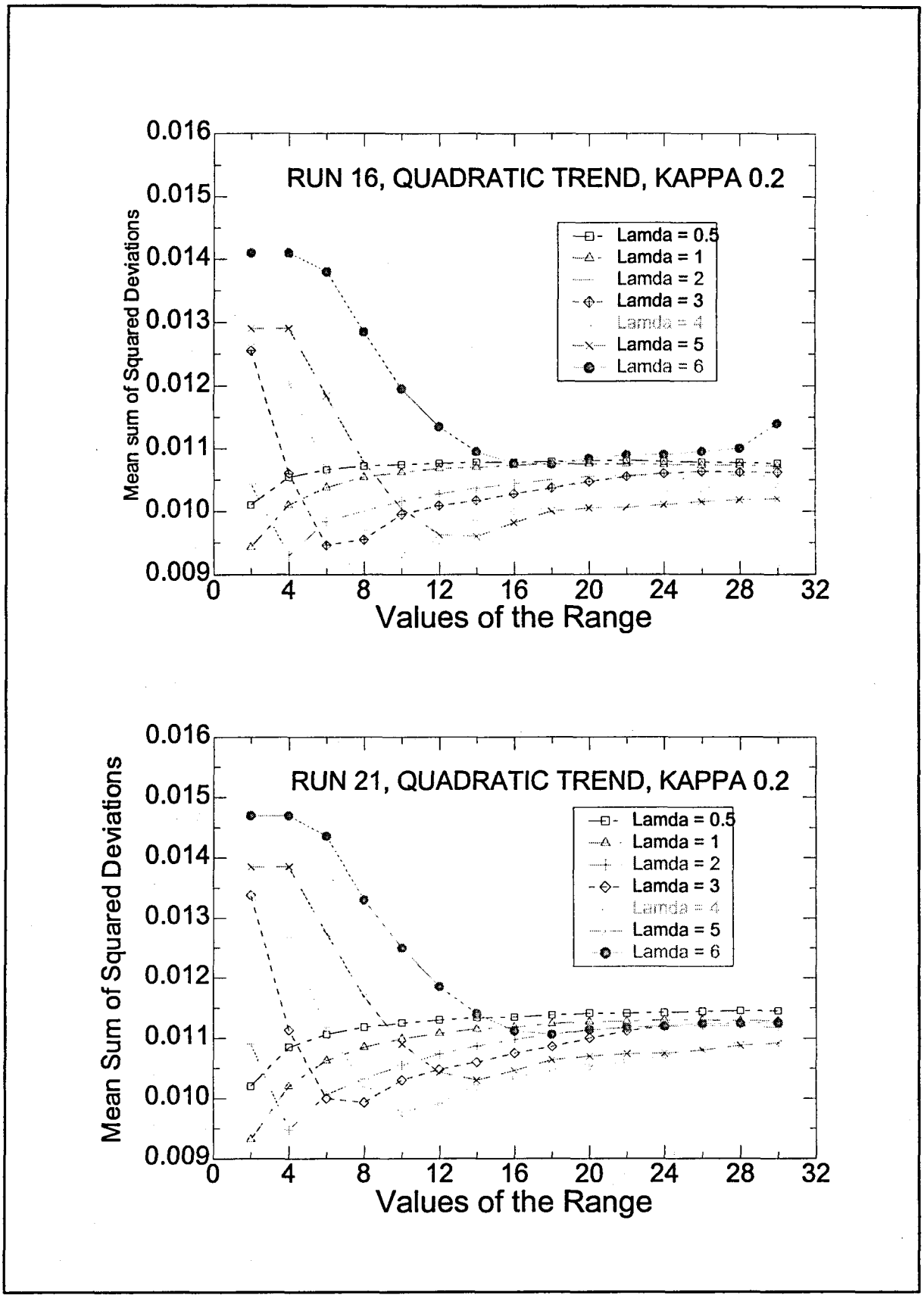

Figure 4.8 Examples of the cross validation of three dimensional spatial water content models for kappa = 0.2 for two dates. Run 16 = March 18 and run 21 = April 20.

4.5.4.3 Graphical displays of soil physical properties.

Estimates of soil physical properties (% clay, sand and silt) were made at four depths (0-0.25 m, 0.25-0.50 m, 1.00-1.25 m, 1.50-1.75 m) and at 33 sites. Three-dimensional models were fitted to these records by cross-validation. Graphs of the horizontal plane at the four depths for the three soil properties (Figures 4.9-4.11) show that the percentages of sand and silt were similar both horizontally and vertically. There was generally little horizontal variation within depths. For example, the percentage sand only varied by 4% in the 0-0.25 m region (Figure 4.9). However the amount of sand and silt increased progressively with increasing depth. The fraction of sand increased from a minimum of 18% at depth 1 to a maximum of 42% at depth 7. The silt fraction increased from 19 to 40% from depths 1 to 7. The clay fraction of the other hand showed an inverse relationship with the sand and silt being very high (60%) in the A horizon (depth1) and decreasing to 15% in the undifferentiated parent material at the greatest depth (Figure 4.11). The high percentage of sand and silt in the deeper zones should result in higher infiltration rates than in the A horizon which has a high clay content.

4.5.4.4 Graphical displays of volumetric water content in space.

Graphical illustrations of 3-dimensional water content predictions at 6 chosen dates (summer to winter) were plotted at 4 depths (Figure 4.12 a -d). These horizontal slices indicate changing water content with depth over time. A vertical slice (Figure 4.13) was positioned to run down the steepest slope of the catchment between sampling points for optimal precision. This particular line down the slope forms the basis of further analysis and we refer to it as the "hillside transect".

On March 18 the hillside transect was uniformly wet and there was little horizontal or vertical variability in the data (Figure 4.12 a- d). At the surface, θ varied between 46 and 49% while the soil was slightly drier at depth 0.25-50 m, an indication of a recent rain event which had not percolated to deeper levels. At depths below 1.0 m the water content was consistently high ($\pm$ 46 %) throughout the year, indicating that regular monitoring is not necessary at these depths.

Greatest variability in soil water was recorded near the surface. Lowest water content was recorded at the surface on the ridge top (July 6 :co-ordinate x=1;y=185, Figure 4.13). Both the

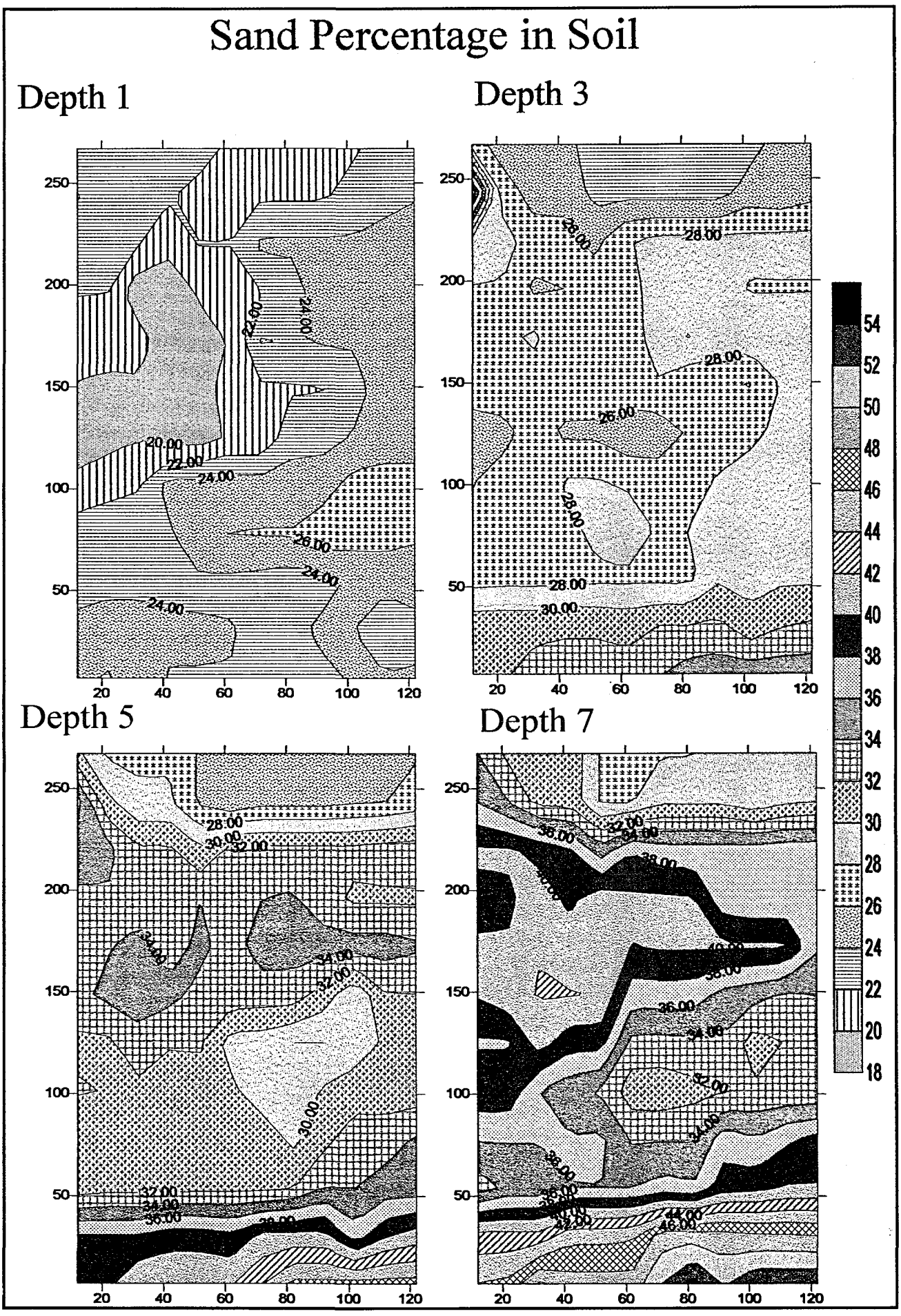

Figure 4.9 Spatial distribution of the percentage sand with increasing depth.

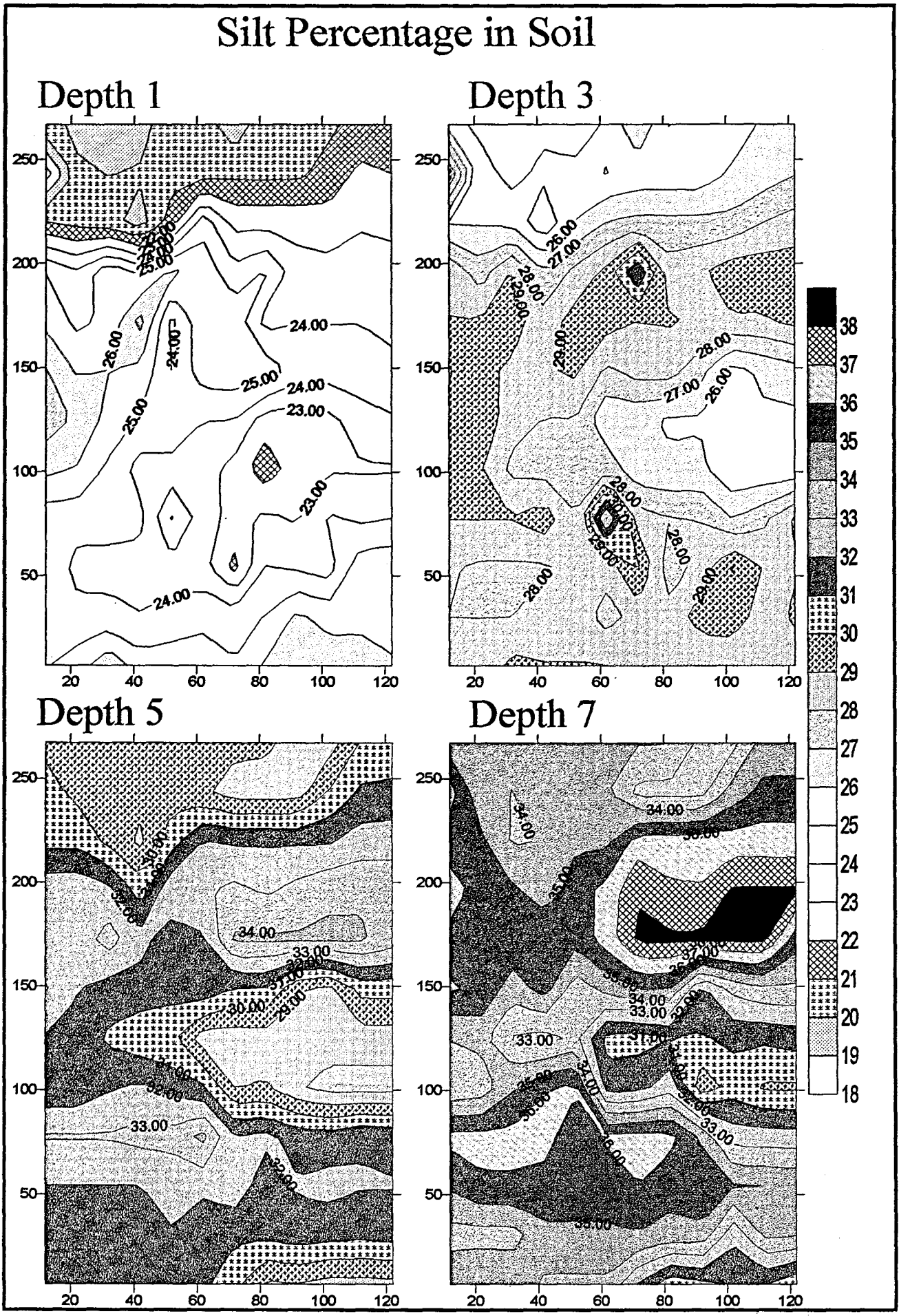

Figure 4.10 Spatial distribution of the percentage silt with increasing depth.

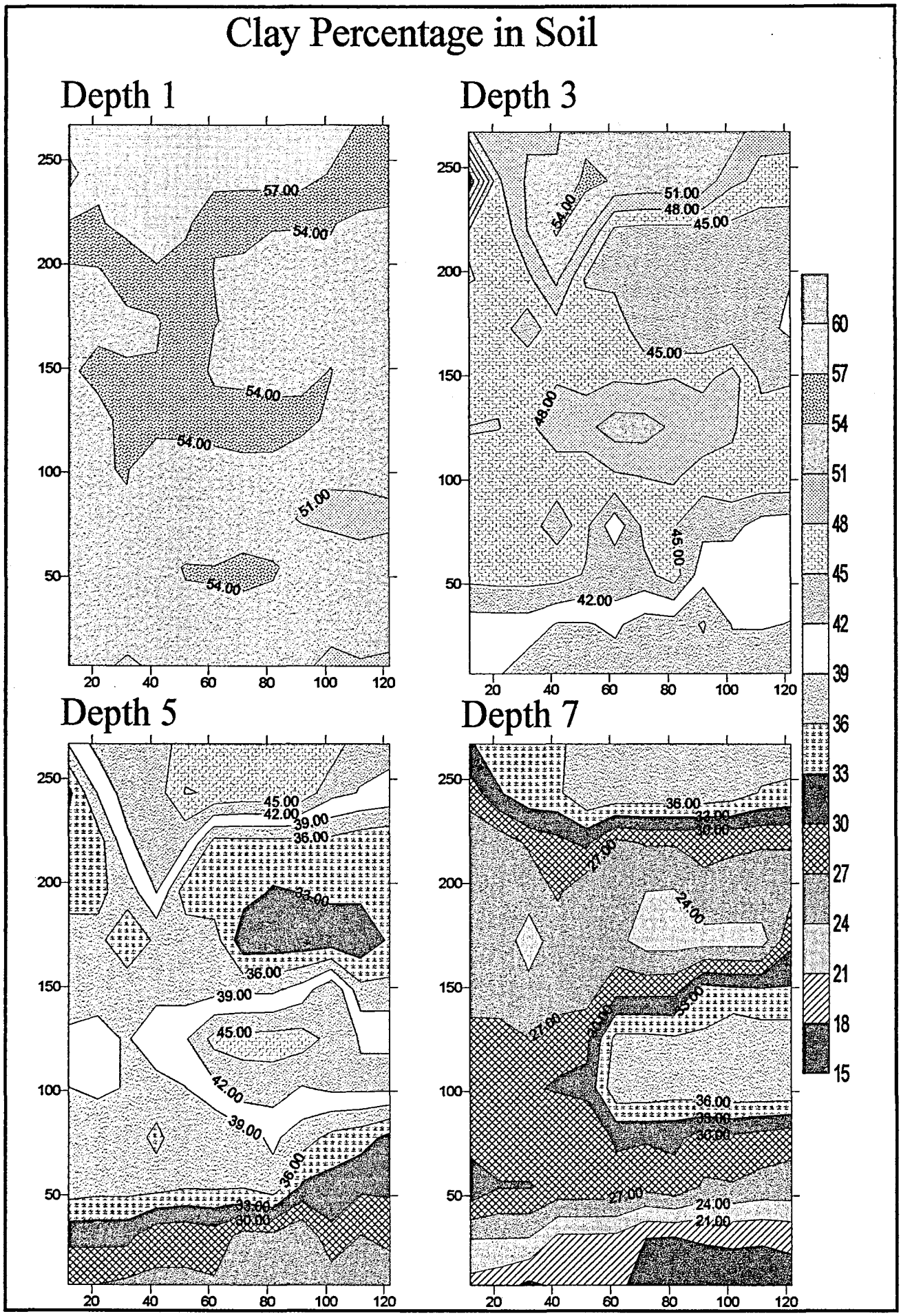

Figure 4.11 Spatial distribution of the percentage clay with increasing depth.

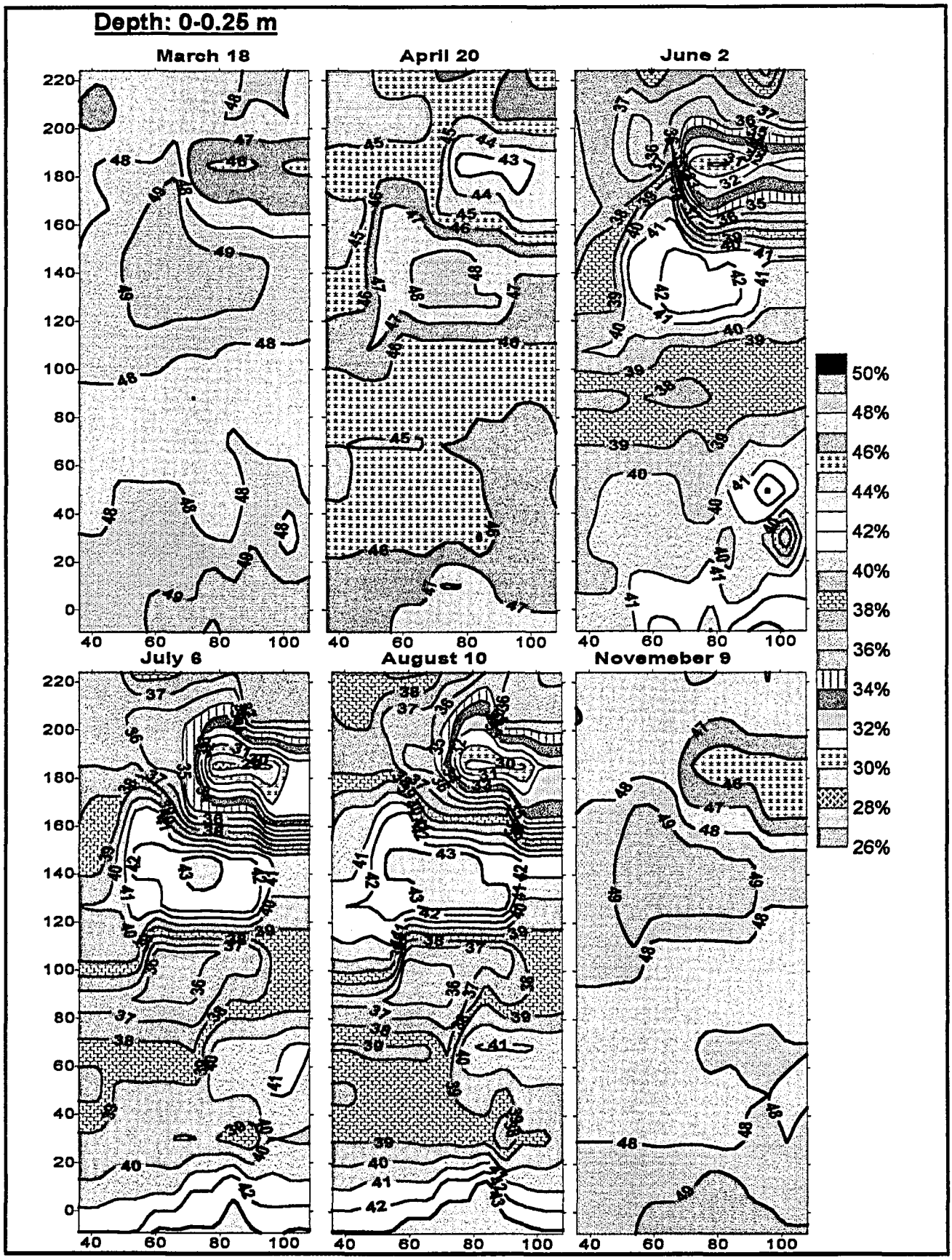

Figure 4.12 a. Seasonal trends in predicted volumetric water content on a hillslope in catchment VI. March to November 1993. Depth 0-0.25 m.

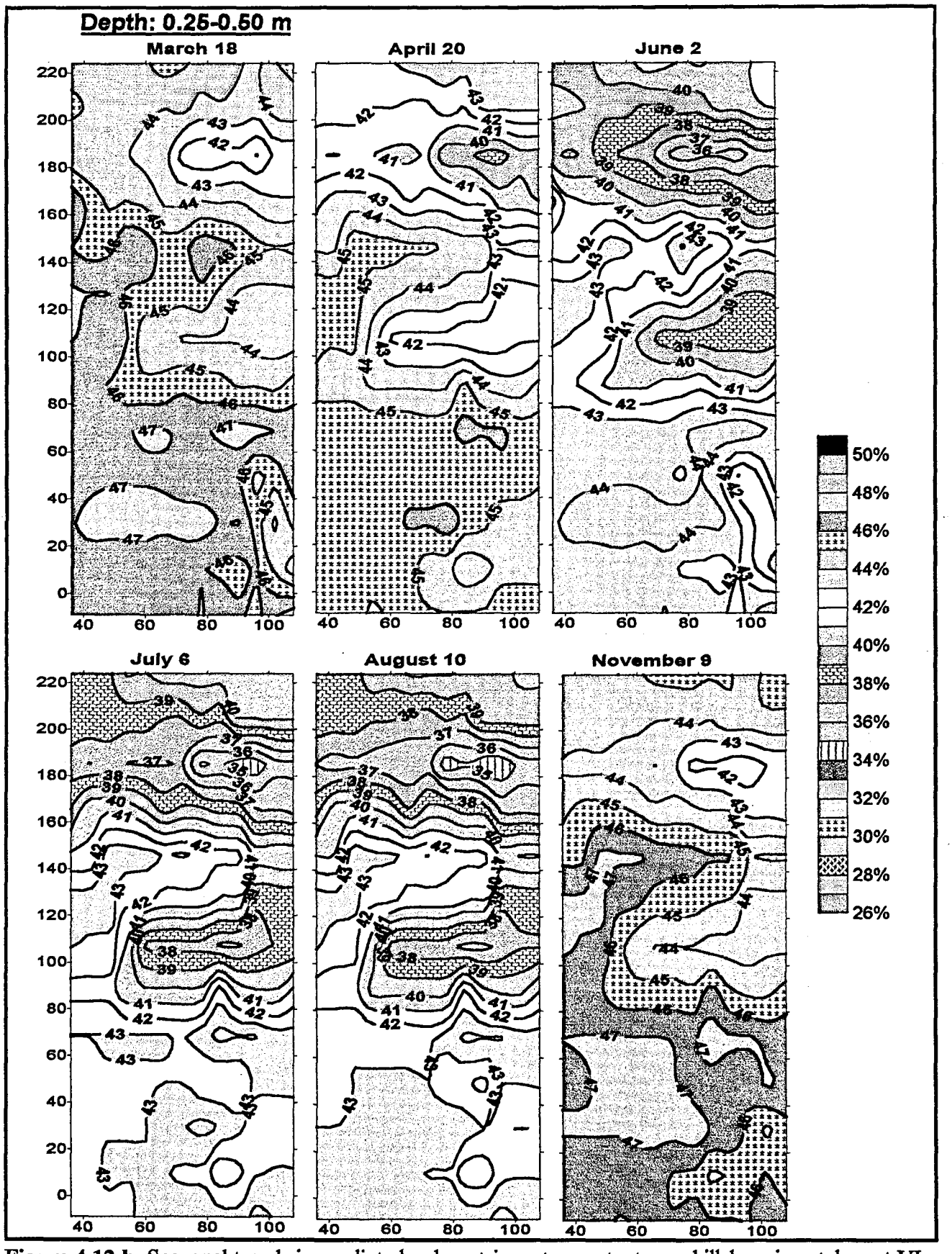

Figure 4.12 b. Seasonal trends in predicted volumetric water content on a hillslope in catchment VI. March to November 1993. Depth 0.25 - 0.50 m.

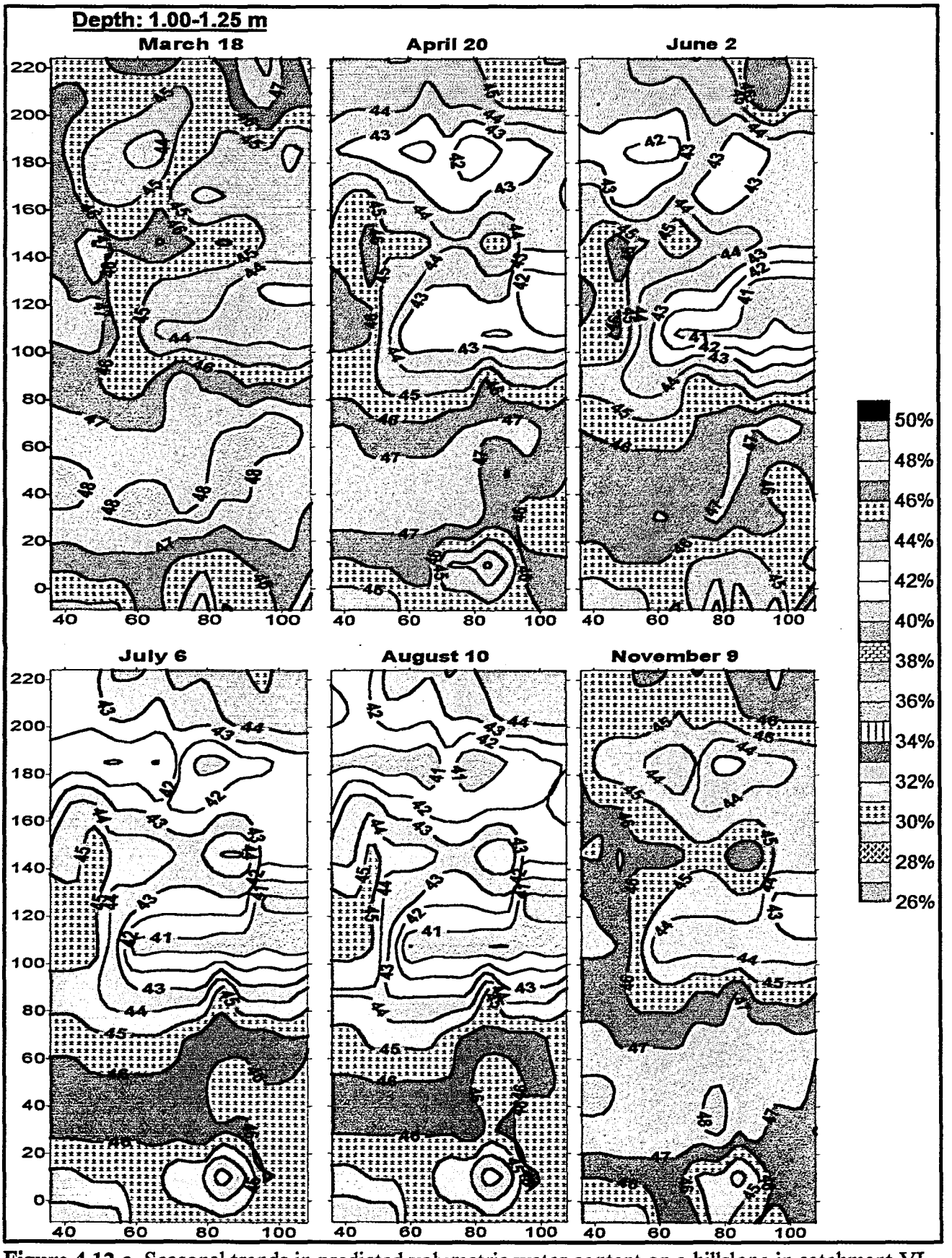

Figure 4.12 c. Seasonal trends in predicted volumetric water content on a hillslope in catchment VI. March to November 1993. Depth 1.00 - 1.25 m.

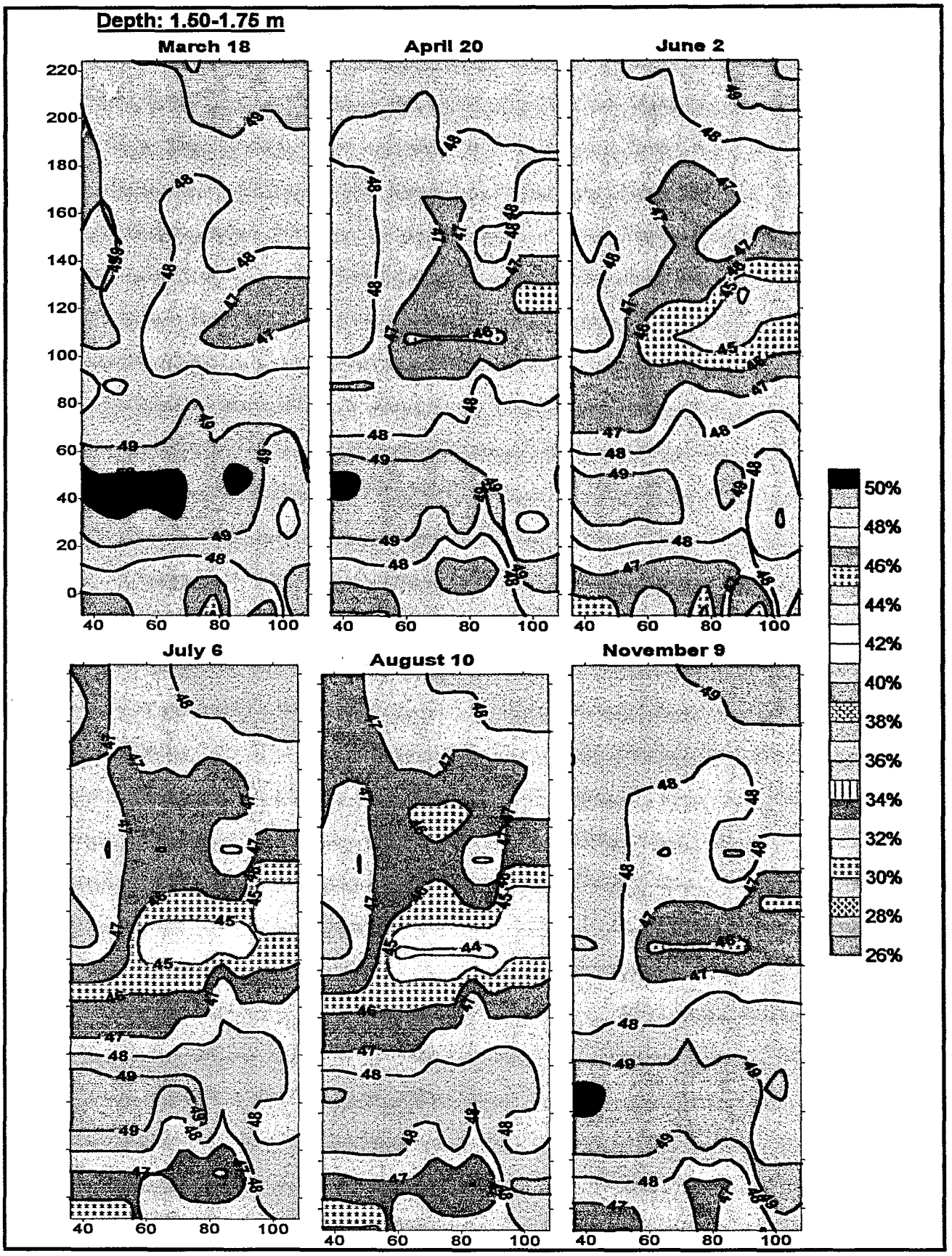

Figure 4.12 d. Seasonal trends in predicted volumetric water content on a hillslope in catchment VI. March to November 1993. Depth 1.50 - 1.75 m.

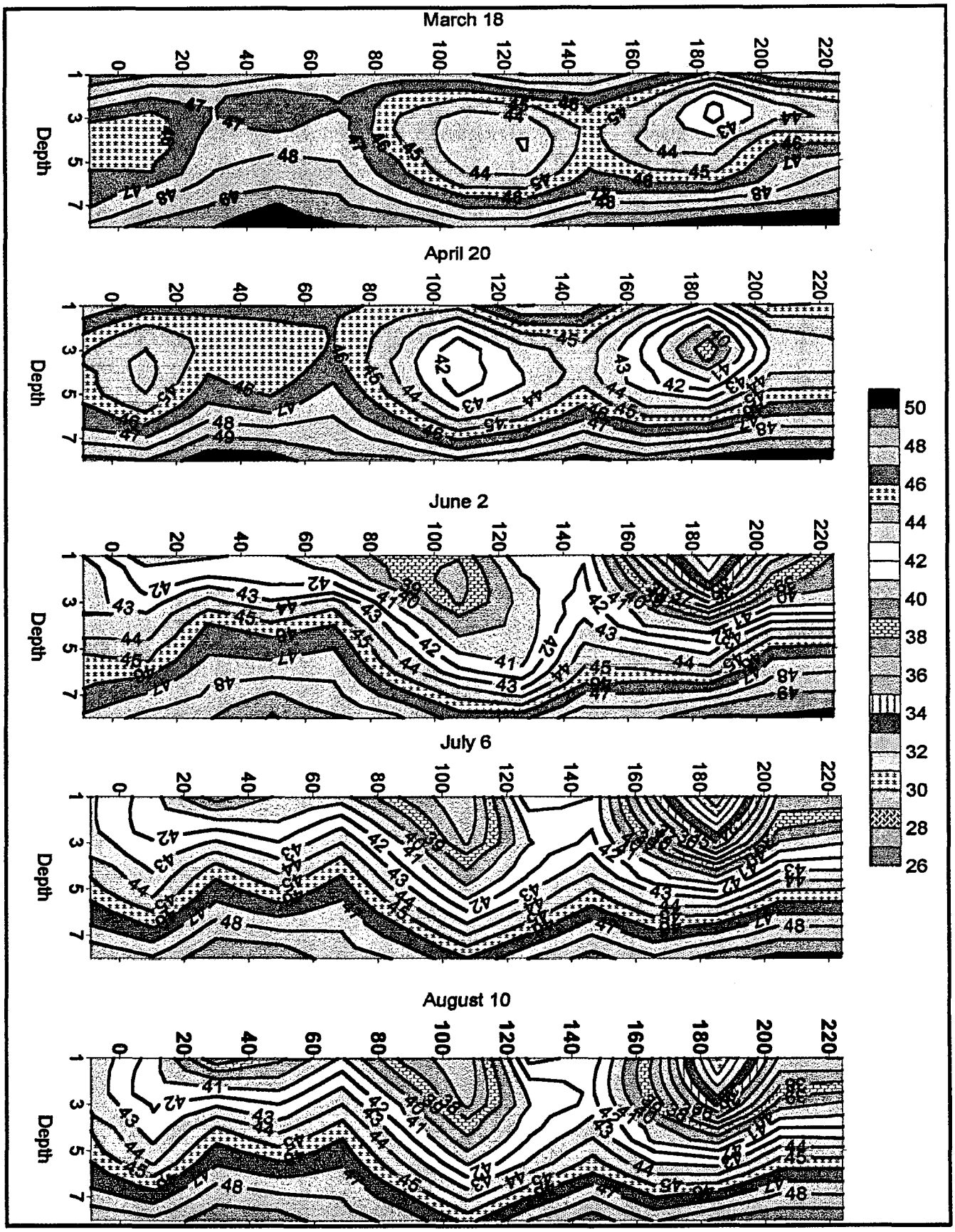

Figure 4.13 Vertical slices down the "hillside" transect showing predicted volumetric water content over time.

horizontal and vertical graphs indicate that in the dry period the sites at the top of the catchment dry out more quickly than those lower down. This is seen by the lighter zones of soil water content towards the top of the catchment (Figure 4.12 a & Figure 4.13).

The graphical profiles demonstrate the complex distribution of soil moisture with changing seasons and position on the hillslope transect. For example, in March the drier zones are confined to "pockets" between depth 3 (0.5 m) and depth 5 (1.0 m). The upper and lower zones are equally wet as is illustrated by the common contour of 47. As the soils dry out during the dry season (April - July) the "pockets" coalesce and form a uniform dry surface layer by August.

4.5.4.5 Time series analyses and graphs

Time series analysis on the 1993 data was carried out by choosing 8 sites which lay along the hillside transect. Using average variance parameter values obtained from the earlier chosen 8 dates, predictions were made at 11 depths at each site for each week of 1993. These predictions were then smoothed by kriging in the time domain to illustrate the seasonal trends in soil water content (Figure 4.14). Parameter values for the time series smoothing were found by variogram analysis.

4.5.5 *Summary of spatial analysis*

Modelling soil water in four dimensions gave a visualization of soil moisture in the hillslope which was not possible in two dimensions. The models show the complex distribution of volumetric soil water within the hillslope and illustrate the difficulties of selecting representative sites in point sampling surveys. The ability to predict soil moisture on a hillslope in time and space provides a powerful tool for landscape management.

4.6 Soil water in the saturated riparian zone

Storm runoff leaving a catchment is generated either by subsurface runoff alone or in combination with surface runoff produced from saturated zones. Research on modelling runoff in catchments has largely focused on lateral flows within mineral soils. However, in catchments with extensive saturated areas, it is likely that significant overland flow will be produced. Models of runoff production need to evaluate the runoff produced from these zones of surface-saturated soil. The present study examines the dynamics of a saturated zone in a small catchment.

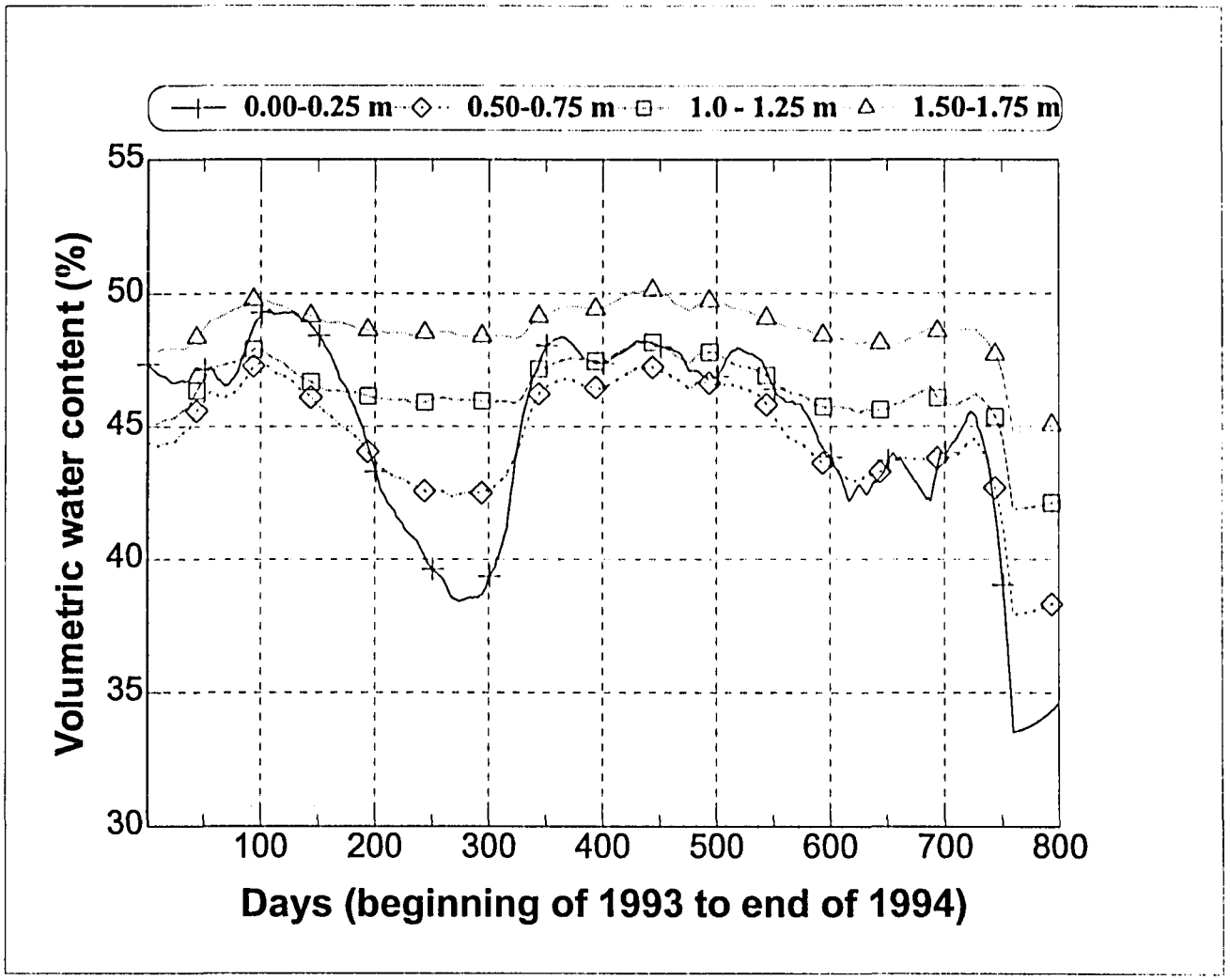

Figure 4.14 Volumetric water content (%) predicted over time at the point y=184 on the "hillslope" transect.

4.6.1 *Method*

To locate the permanent water table ten test wells were installed on three transects radiating from the saturated zone. The water level in these test wells was monitored with a water-level sensor using a capacitance to frequency converter. The sensor consists of a PTFE-insulated wire mounted inside a stainless steel tube. Water forms one plate of the capacitor and the wire the other, while the PTFE insulation is the dielectric. The plate area and therefore the capacitance change linearly with water level. A Keller series 169 depth transducer was used for operation with the Campbell 21X. These transducers provide repeatable, precision depth measurements under field conditions. The sensors utilise a silicon pressure cell that has been fitted into a stainless steel housing with an integral, compliant stainless steel barrier diaphragm. Programs were written for its use with the Campbell 21X data logger.

The Keller probe was used to verify data collected with the capacitance type sensors. The results showed excellent agreement in the trends between the different sensor types. However, when responding to a sudden rainstorm, the capacitance sensor could be out by a 50 mm error. This error was neither consistent nor predictable and is probably a result of temperature induced drift in the sensor electronics. Because of suspected errors in the capacitance sensors, weekly checks of the actual water level against the instrument recording were instituted in early 1992. Any corrections necessary could therefore be made.

An additional 8 test wells were monitored with a depth sensor at weekly intervals. All the test wells were surveyed on to a 2 by 2 metre grid of the saturated zone. A spatial analysis of these data should be possible but was not attempted due to time constraints.

4.6.2 *Results and discussion*

Monitoring the water levels at the ten instrumented test wells and eight manual test wells was carried out throughout the reporting period. Data for 1993 and 1994 are presented in Figure 4.15. Recharge rates of the ground water table for 1994 are shown at 4 positions in the landscape: upslope, margin of the riparian zone, 5 m into riparian zone and 1.5 m from the stream. A comparison of rainfall and water level indicates that the response of the water table to rainfall was immediate at all sites. The trends were similar to those measured in 1993, where there was a distinct depth difference between sites with distance from the stream. The riparian zone water table was close to the soil surface (between 0 and 200 mm depth) in contrast to the upland site where it was approximately 800 mm below the surface of the soil. The upland site responded far more slowly to rainfall inputs, resulting in a smoother curve than the sites in the riparian zone. The margin of the riparian zone showed the most extreme fluctuations, varying between 300 and 780 mm below the surface. The water table fluctuations showed similar trends to the streamflow curve. In spite of there being no significant rainfall (< 15 mm) between early May 1993 (DOY 121) and the end of August (DOY 240), there was evidence of some recharge from upslope areas in the catchment during this very dry period. This is seen by contrasting the upslope and margin sites for this period, where the upslope site declined slowly while at the margin the water table increased slightly.

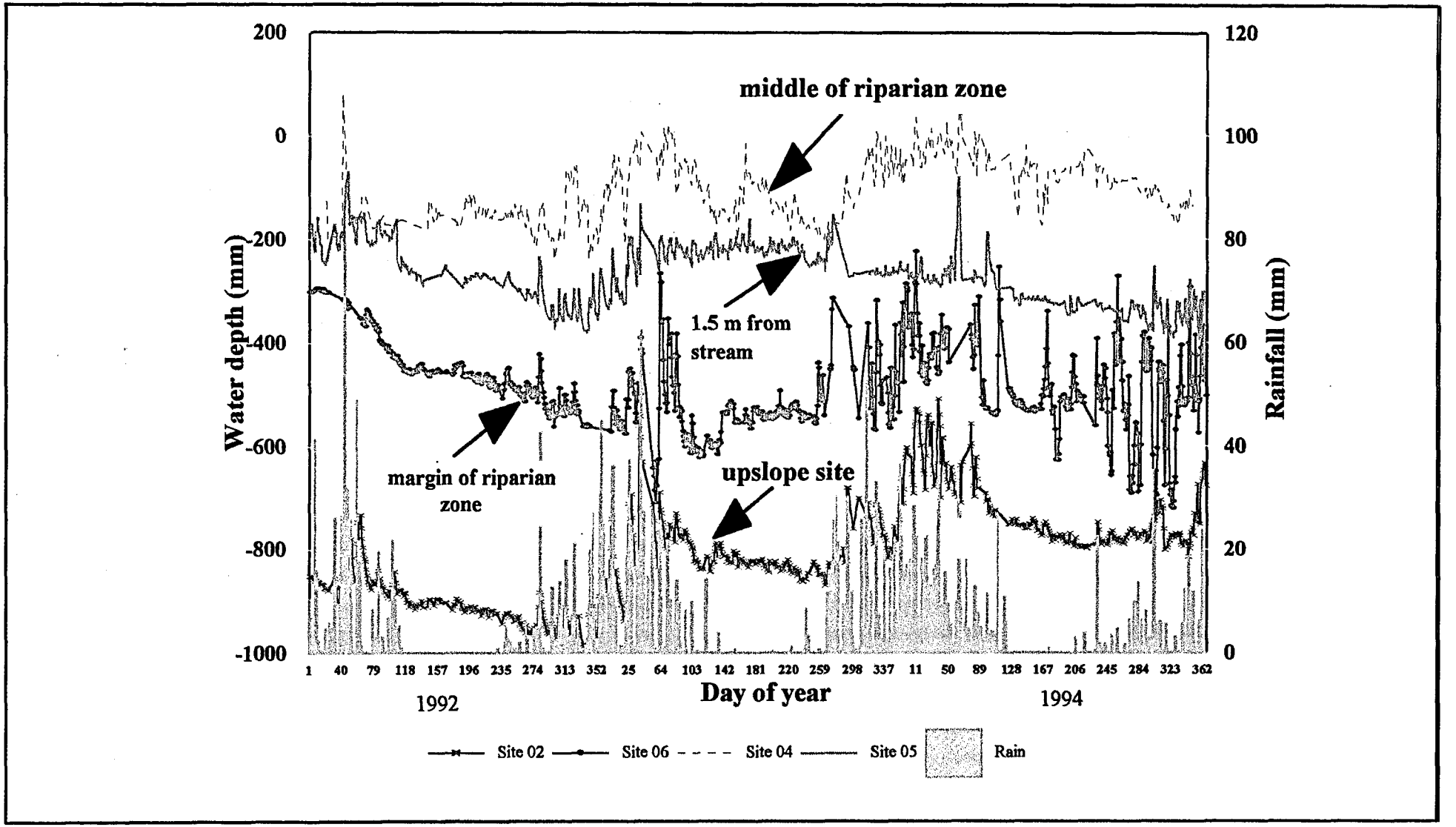

Figure 4.15 Rainfall (mm) and water levels at four test wells in catchment VI from 1992 to 1994

4.7 Ground water monitoring

4.7.1 Method

Six 50 mm diameter test wells were drilled to 0.5 metres below bedrock with a small diamond drilling rig operated by drillers from the Department of Water Affairs. The sites were located within the existing neutron probe network. The depth of the wells varied between 22 m deep, high in the catchment to, 5 m deep near the riparian zone. The soils in catchment VI were therefore much deeper than expected. The drill holes were lined with perforated 50 mm irrigation piping. The water table was monitored for the entire hydrological year 1994/95. The instrument used was a pressure transducer type sensor and Campbell CR21X logger. The water levels were verified manually each week with a modified leaf wetness sensor.

4.7.2 *Results and discussion*

An interesting feature of this study was the depth of the overlying soil material. For example, the total depth from the soil surface to the bedrock in the borehole at site 01 was 22 m. This was surprising since this site was situated on the ridge at the top of the hillslope transect. At the shallowest site the depth to the bedrock was 5.0 m, while at the intermediate site it was 10.5 m.

The manually measured water table depths showed good agreement with the pressure transducer sensors (Figure 4.16a-c). The water table reached its lowest point (-6 820 mm) in January 1995. Very good rains in January and February 1995 resulted in the water table rising to -5 600 mm on DOY 120. This indicates that during the dry season 450 mm of water was lost by subsurface flow.

The water table at the intermediate site D-02 (situated 20 m above the road and between the stream and Bowen ratio site) varied between 5 600 mm below the surface in summer to 6 450 mm in winter (Figure 4.16a). Therefore there was approximately 4 000 mm of water above the bedrock after the long dry spell in the second half of 1994. The increase in the water table from DOY 40 to DOY 120 was due to the heavy rains which fell in January. The response time of the intermediate borehole (10.5 m) was approximately one month. The deepest borehole, D 01 (22 m), had the slowest response time (3 months) (Figure 4.16b). The increase in the water table over the 3 month period was 1 600 mm and translates into a recharge rate of about 15 mm day^{-1}. It therefore takes about 2 months for the water to infiltrate

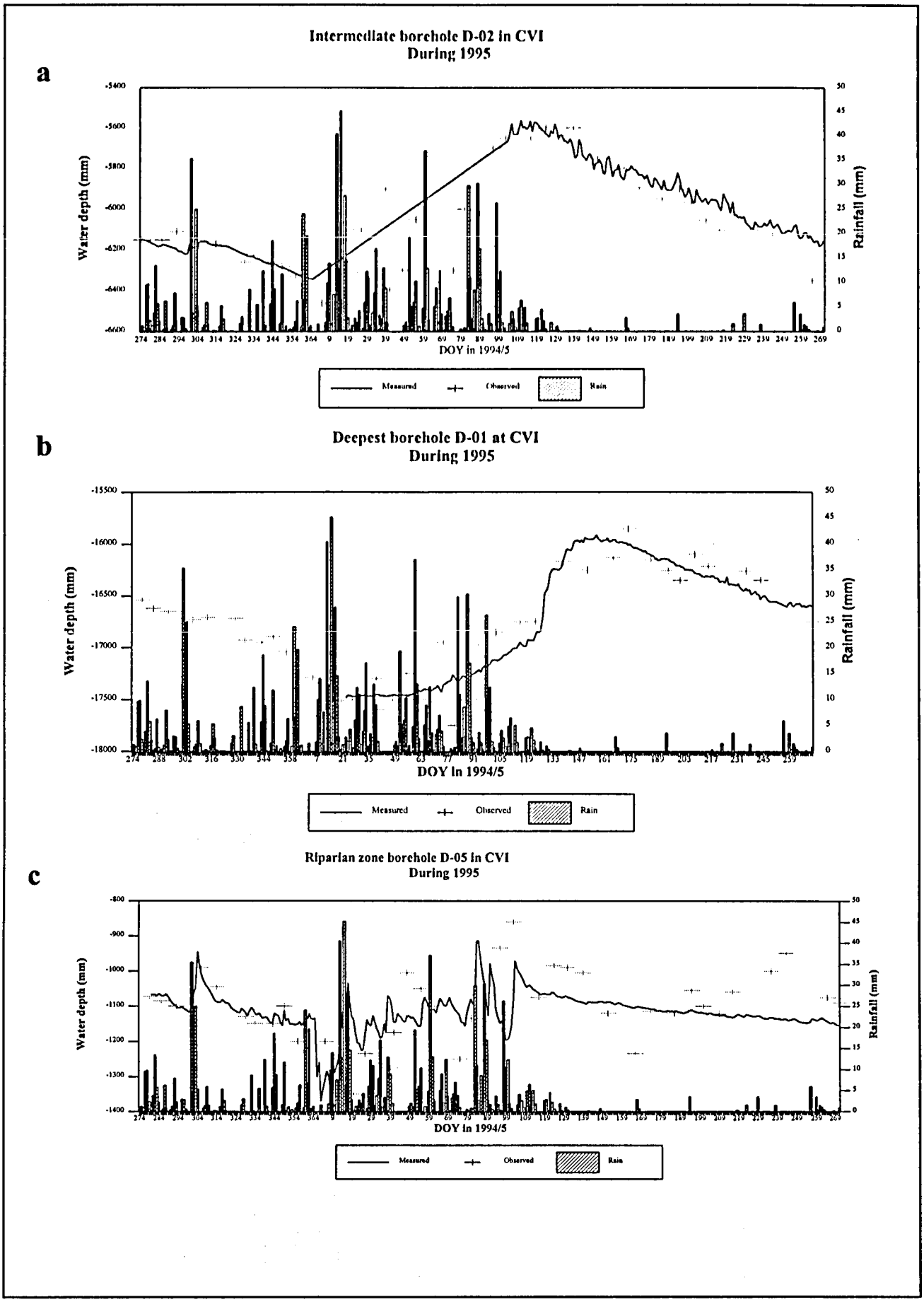

Figure 4.16 The relationship between rainfall and depth to the water table at three sites in catchment VI for the 1994/95 hydrological year.

to the water table at these depths. These observations are consistent with the TDR data, where no increases in θ were measured below 0.125 m.

The total amount of water lost at the various sites showed an interesting trend, with the highest and deepest borehole in the catchment decreasing by 700 mm, the intermediate hillslope sites decreasing by 250 mm and those near the riparian zone decreasing by only 40-90 mm (Figure 4.16a-c). These data suggest that the most important runoff generation process in catchment VI is the underground movement of infiltrated rain (subsurface flow). At all the borehole sites there was no difference in storage water between the beginning and end of the hydrological year. Therefore groundwater recharge controls the vertical distribution of the storage water.

4.8 Conclusion

Soil moisture changes in the grassland catchment of this study varied significantly with season. The annual cycle of soil moisture approximated a sine wave with a maximum in February and a minimum in July. In the dry season there was a gradient of increasing moisture content downslope from the ridge. This indicates that the stream was fed by moisture moving slowly downslope under conditions of unsaturated flow. The lower part of the slope therefore produced runoff early in the storm period while infiltration was still occurring on the upper section of the hillslope transect. The saturated area of the riparian zone increased or decreased in size depending on rainfall amount and antecedent wetness of the soil. This zone therefore produced quick release of water during storms.

Subsurface stormflow was a major component of total stormflow from these grassland catchments. Part of the baseflow from the catchment originated from the deep coarse-textured soils. During the dry winter period baseflow was sustained by the slow drainage of the unsaturated soil at the upper part of the hillslope. The high water levels in the saturated zone were maintained by subsurface flow from the upslope parts of the catchment.

The results of this study indicate that unsaturated subsurface flow of water in the soil is an important component of the hydrology of these catchments. Therefore lumped type models are unlikely to accurately determine the complex moisture conditions found on the hillslope of this study. Models that account for the spatial distribution of soil moisture within a catchment are likely to be the most accurate.

Chapter 5

CATCHMENT WATER BALANCE

5.1 Introduction

Calculating the water use of the grassland vegetation can be made by monitoring the difference between the annual precipitation and measured streamflow (Bosch 1979). Paired catchment studies have also been used to determine the water use of different vegetation types (Bosch 1982). While these studies enable broad estimates of water loss, they do not account for losses by interception and evaporation from the soil.

Water balance is a deterministic relation between the water balance components which are random variables in time and space, with usually unknown probability distributions. The independent input variable is rainfall, which is transformed in the hydrological system into the dependent output variables evaporation, streamflow and change in soil storage.

The atmospheric and land surface systems are dynamically coupled through the physical processes of energy and water supply, transformation (latent and sensible heat), and transport (streamflow) at a land-atmosphere interface (Dyck 1983). In order to develop physically based water balance models which reflect the dynamic interchange of energy at the atmospheric-soil-vegetation interface, both the underlying physical determinism, and the uncertainty in the elements of the water balance dealing with their probability distributions must be included.

The present study aims to develop an understanding of the water balance of a catchment, in order to develop or improve existing hydrologic models. To allow mathematical prediction of the various hydrological variables some simplifications are necessary. The most practical method is the use of the deterministic approach of applying the macroscopic version of the continuity equation. The various continuous water movement processes of the hydrological cycle are lumped over finite time intervals and areas and related by the water balance equation. The volumetric water balance per unit area may be expressed as:

$$P - E_a - SS = Q$$

P = precipitation; E_a= actual evaporation; SS = soil storage; and Q = streamflow (Eagleson,

1978). All terms except P depend upon soil moisture level and distribution which is generally not measured, the problem being overcome by assuming the system to be stationary in the mean. If the integration interval is a full year and expected values are substituted, the change of storage is negligible and the average annual water balance equation is as follows:

$$\overline{P} - \overline{E_a} = \overline{Q} \quad mm\,year^{-1}$$

All components of the water balance equation were measured in catchment VI from 1990/91 to 1994/95. The validity of the data collected could be checked by balancing the equation. Between 1980 and 1989 actual evaporation (E_a) was calculated in the traditional way using the annual water balance equation. This assumes that deep losses of water are negligible and that the soil water content is identical at the beginning and at the end of the hydrological year (1 October and 30 September respectively). With respect to the first assumption, catchment VI is underlain by an impervious layer of basalt, and there is no evidence of faulting, and no deep water losses occur. The second assumption is tested as part of the present study.

5.2 Methods

Evaporation was monitored using the Bowen ratio technique described in detail in section 3.2.1. Soil water storage was monitored using the neutron probe technique described in section 4.2.1.

5.2.1 *Rainfall*

Precipitation was recorded continuously with three tipping bucket raingauges located within the catchment. Areal catchment rainfall was estimated using the Thiessen polygon method.The gauging network was expanded in 1992 to include six tipping bucket raingauges (five 0.2 mm resolution gauges at 1.2 m height and one 0.1 mm resolution ground surface raingauge) for the continuous monitoring of rainfall within the catchment.

5.2.2 *Streamflow*

Streamflow was monitored continuously in catchment VI for the duration of the project. A 457.2 mm, 90-degree V-notch weir was used with a Belfort streamflow recorder which had been recently modified with an MCS 250-01 streamflow encoder. The calibration of the weir was verified by the Department of Water Affairs and Forestry in 1994.

5.3 Results and discussion

5.3.1 *Rainfall*

The variable annual precipitation during the study period provided an ideal opportunity for contrasting the water balance of wet, dry and average hydrological years. Daily precipitation in the five year study period showed the characteristic pattern found in the summer rainfall regions, with the summer months being wet and the winters very dry (Figure 5.1). There was a high frequency of dry days during the period April through September. During 1992 no rainfall was recorded in the months of May, June and July, whilst <3.9 mm fell during this period in 1993 and 1994. During the dry period, the grassland is dormant and evaporation is minimal. However, dry periods during the growing season can be expected to have a significant influence on plant water stress. For example, November 1994 was an exceptionally dry month which received only 33.6 mm rainfall when compared to the long term average of 190 mm.

5.3.2 *Streamflow*

The effect of the contrasting rain years on the stream discharge is clearly illustrated in Figure 5.2. Total streamflow for the study period corresponded closely to annual rainfall. The effect of the good rains in 1993/94 were reflected in the high annual streamflow (863 mm). By contrast, the low discharge in 1994/95 (342 mm) reflected the effect of the unusually dry year.

In every year of the study there was a steady decrease in streamflow from April to the end of September which corresponded with the dry winter period. The advent of the spring rains in October had little impact on streamflow in the catchment. The increase in streamflow was only apparent in January/February when the soil moisture storage was recharged.

The annual runoff during the driest year (1994/95) was 342 mm which represented 34% of the annual precipitation. The effect of this dry year was a continuous low discharge which is depicted by the 'flat' graph with few peaks (Figure 5.2). Streamflow seldom exceeded 2.0 mm day^{-1} throughout the year. In spite of some rains from October onwards (Figure 5.1), the catchment was unable to recharge, and the runoff remained low. The annual runoff during the wet year (863 mm) was 59% of the annual precipitation. Seasonal discharge from the stream reached a peak in February and gradually receded by the end of September.

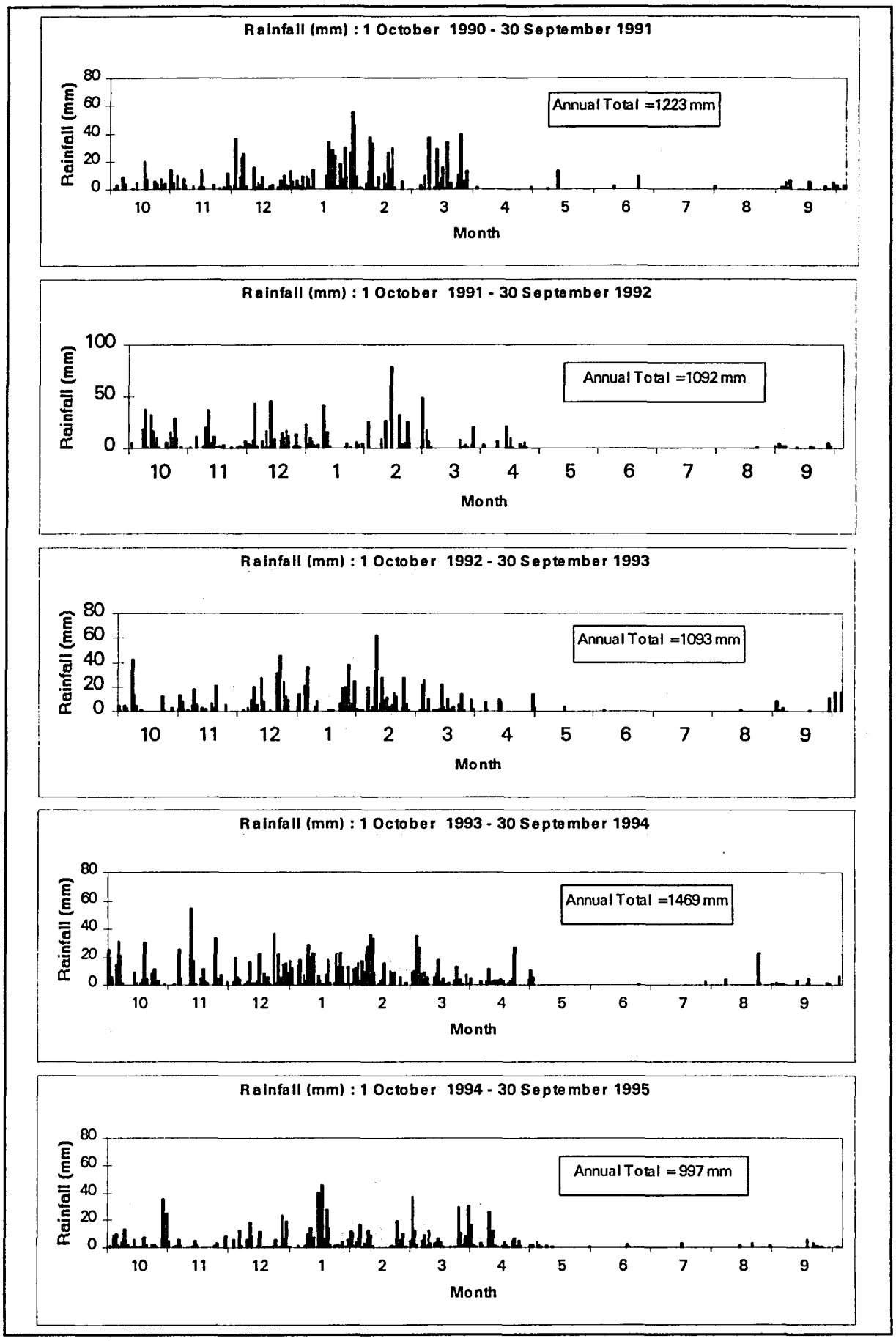

Figure 5.1 . Daily rainfall for the period September 1990 to September 1995.

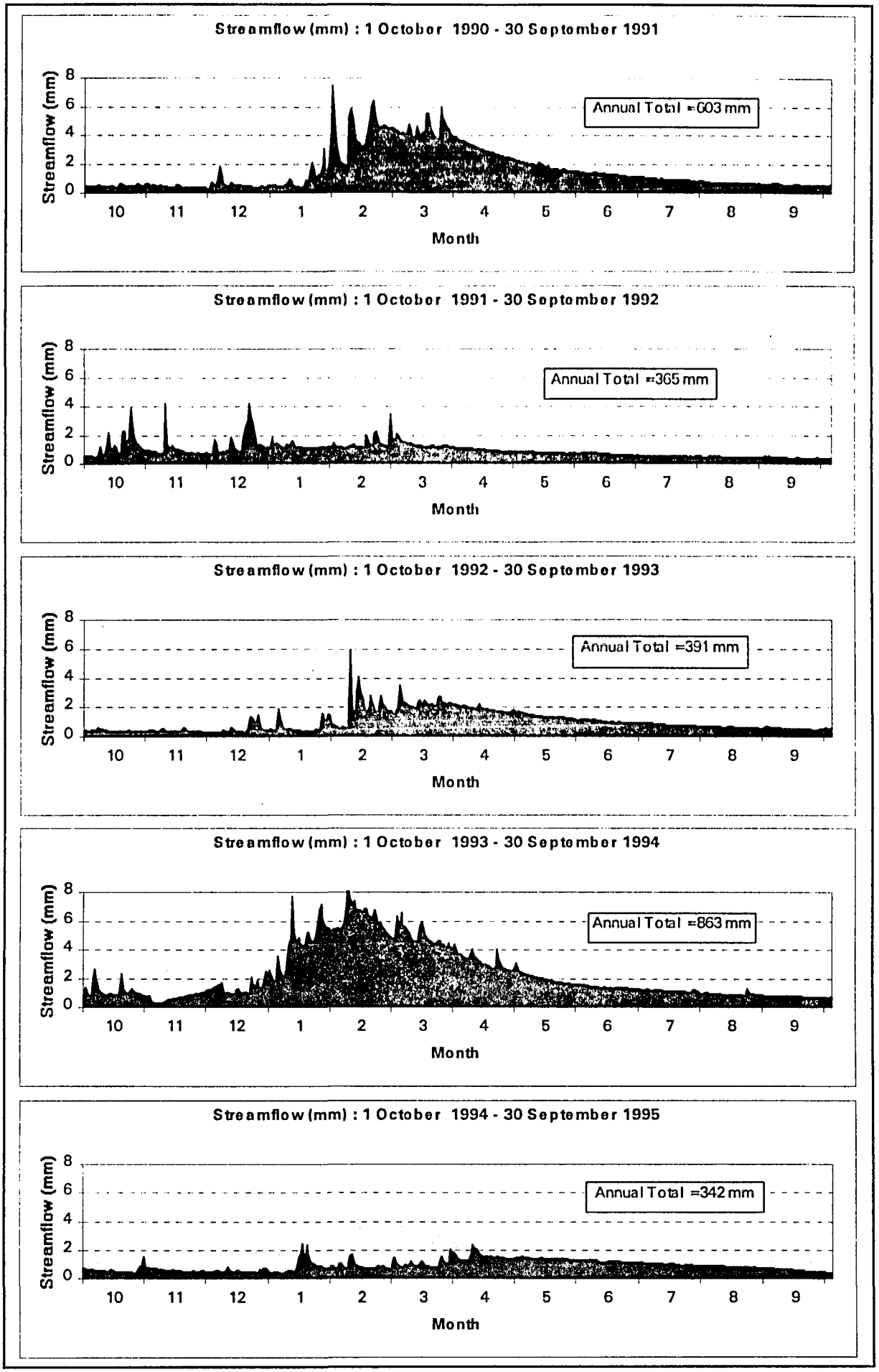

Figure 5.2 . Daily streamflow for the period September 1990 to September 1995.

5.3.3 *Evaporation*

The annual evaporation totals for the four year study period (1990/91 - 1993/94) were 681, 725, 698 & 651mm respectively (Figure 5.3). Although the rainfall varied by 377 mm, there was only 100 mm difference in evaporation (E_a). The low variation in evaporation measured over the four year study period suggests that at this site evaporation is not limited by soil moisture, even in low rainfall years.

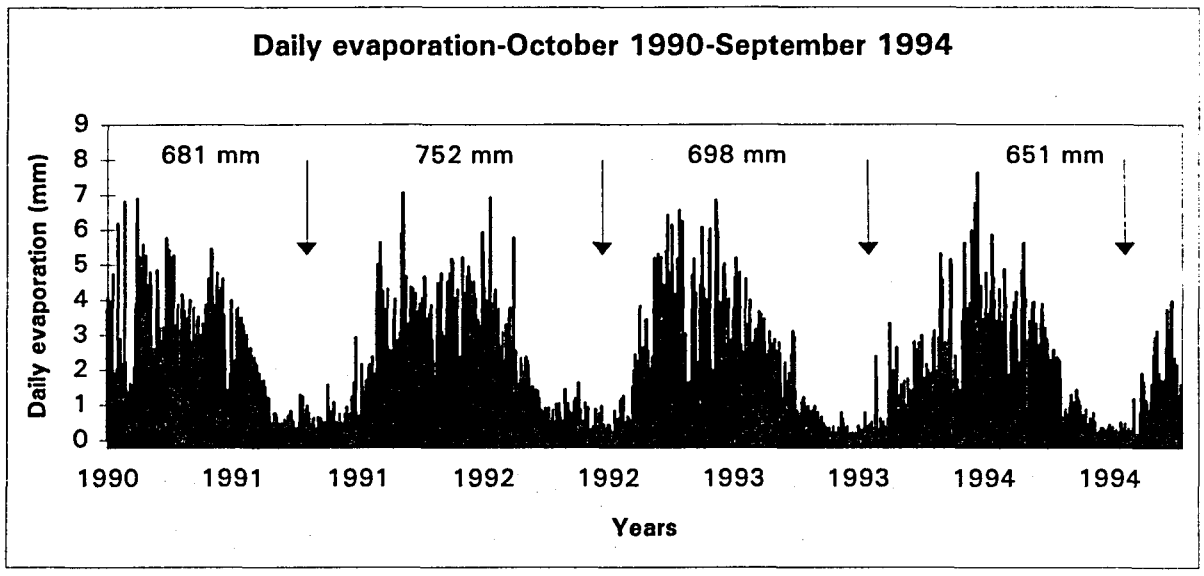

Figure 5.3 . Time series trend in the daily evaporation measured in CVI from 1990 to 1994. Arrows indicate the start and end of hydrological years.

Soil moisture storage in the upper 2.0 m of the profile for the study years (Figure 4.7) indicated that in summer, rainfall recharged the soil profile, while during the dry winter period it was depleted. Total profile water contents ranged from 850 to 960 mm for the 2000 mm sample depth. The maximum value of 960 mm of equivalent water is representative of the catchment in a fully charged stated, while the 850 mm minimum is likely to be closest to the lowest value ever recorded for this catchment (due to the extreme drought conditions). Differences in soil water storage at the beginning and end of the four year period were small (-11, -45, +7 and -14 mm), the only noticeable effect being the inability of the catchment to recharge at the end of 1991/92. At this time there was approximately 45 mm less water in the profile than in the previous year.

These results indicate that differences in soil water storage in average and wet years are not likely to effect water balance computations of E_a by more than 2%. However, the summer drought in 1991/92 would result in a 12% error.

Measured values of P, E_a and SS and the actual runoff measured at the weir (Q_a) were substituted in the water balance equation to solve for Q (Table 5.1). The differences between the measured runoff and that calculated using the water balance equation were small (0.003 to 4.1% of the mean annual rainfall). The agreement of these results confirms the validity of the data collected in this study.

Table 5.2 shows the annual values for P, Q, E_T and E_a for 11 hydrological years at Cathedral Peak's catchment VI. On average 43% of annual precipitation becomes streamflow and the remaining 57% evaporates. The response ratios (Rr in Table 5.2) are similar to others reported in wetter and colder climates of the world. For example in New Hampshire (USA), Likens *et al.* (1977) calculated a response ratios of 0. 61 for the Hubbard Brook catchments, while in Greece, Nakos & Vouzaras (1988), estimated a response ratio of 0.51. In the drier and more arid areas response ratios between 0.07 and 0.25 are common (Lewis 1968, Burch *et al.* 1987 and Pinõl *et al* (1991).

Table 5.1 Components of the water balance equation measured in catchment VI (1990/91 to 1993/94). P = precipitation; E_a= actual evaporation; SS = soil storage; Q = streamflow calculated using the water balance equation; and Q_a = actual streamflow.

Year	P	-	E_a	-	SS	=	Q	Q_a	Difference	% of P
1990/91	1223	-	681	-	(-11)	=	553	603	-50 mm	4.100
1991/92	1092	-	752	-	(-45)	=	385	366	+19 mm	1.700
1992/93	1093	-	698	-	(+07)	=	388	391	-03 mm	0.274
1993/94	1469	-	651	-	(-14)	=	822	863	-41 mm	2.790

Table 5.2 Annual water balance (mm) for Catchment VI for 11 years. Data is for each hydrological year (October to September).

Year	Rain (*P*)	Actual evaporation (E_a)	Run-off (*Q*)	*Potential* (E_T)	Response ratio (Rr)
80	1221	552	668	1503	0.55
81	1067	601	465	1612	0.44
82	909	614	294	1521	0.32
83	1228	493	735	1734	0.60
84	1025	614	411	1578	0.40
85	1306	818	487	-	0.37
86	1578	892	686	1437	0.43
87	1524	779	745	1550	0.49
89	1008	714	293	-	0.29
91	1484	594	736	-	0.49
92	858	655	314	-	0.37
Mean	1200	666	530	1562	0.43

Annual variability of Q and E_a for catchment VI are high. Streamflow (*Q*) ranged from 293 to 745 mm, while E_a ranged from 493 to 892 mm Table 5.2). Figures 5.4 a & b show the relation between annual values of Q, E_a and P in catchment VI. The results of the regression analysis showed that there was a significant positive correlation between streamflow and rain (r = 0.87: p = < 0.001) while there was a poor correlation (r = 0.45: p = NS) between evaporation and rain. This situation can be contrasted to drier climates, where E_a increases with P while there is no significant correlation between Q and P (Pinõl *et al.* 1991). This difference in behaviour can be explained by the relative magnitude of precipitation and potential evapotranspiration (E_T). When precipitation is much greater than E_T, the evaporative demand can be totally satisfied and the remaining water becomes streamflow. In contrast, when rainfall is lower than E_T, then the water supply in the wetter years is still not enough to satisfy all the transpiration and potential evaporation. As a result, streamflow is more dependent on the rainfall distribution in time than on the annual volume. The E_T estimated for Cathedral Peak using A-pan data, shows that rainfall

seldom exceeds E_T, although the magnitude of this difference is not large (Table 5.2). Thus catchment VI is intermediate between the two climatic extremes, but tending towards the situation found in the wetter and colder climates. The slope for linear regression of streamflow on precipitation for CVI was 0.65, indicating that runoff is largely dependent on precipitation. The slope for evaporation versus rainfall on the other hand was only 0.21, indicating that evaporation is largely independent of the annual rainfall.

5.4 Conclusions

The data show that the partition of the main hydrological fluxes into streamflow and evaporation is dependent on the wetness of the hydrological year. In average to wet years the hydrological flux is equally split between evaporation and runoff, while in drier years evaporation becomes

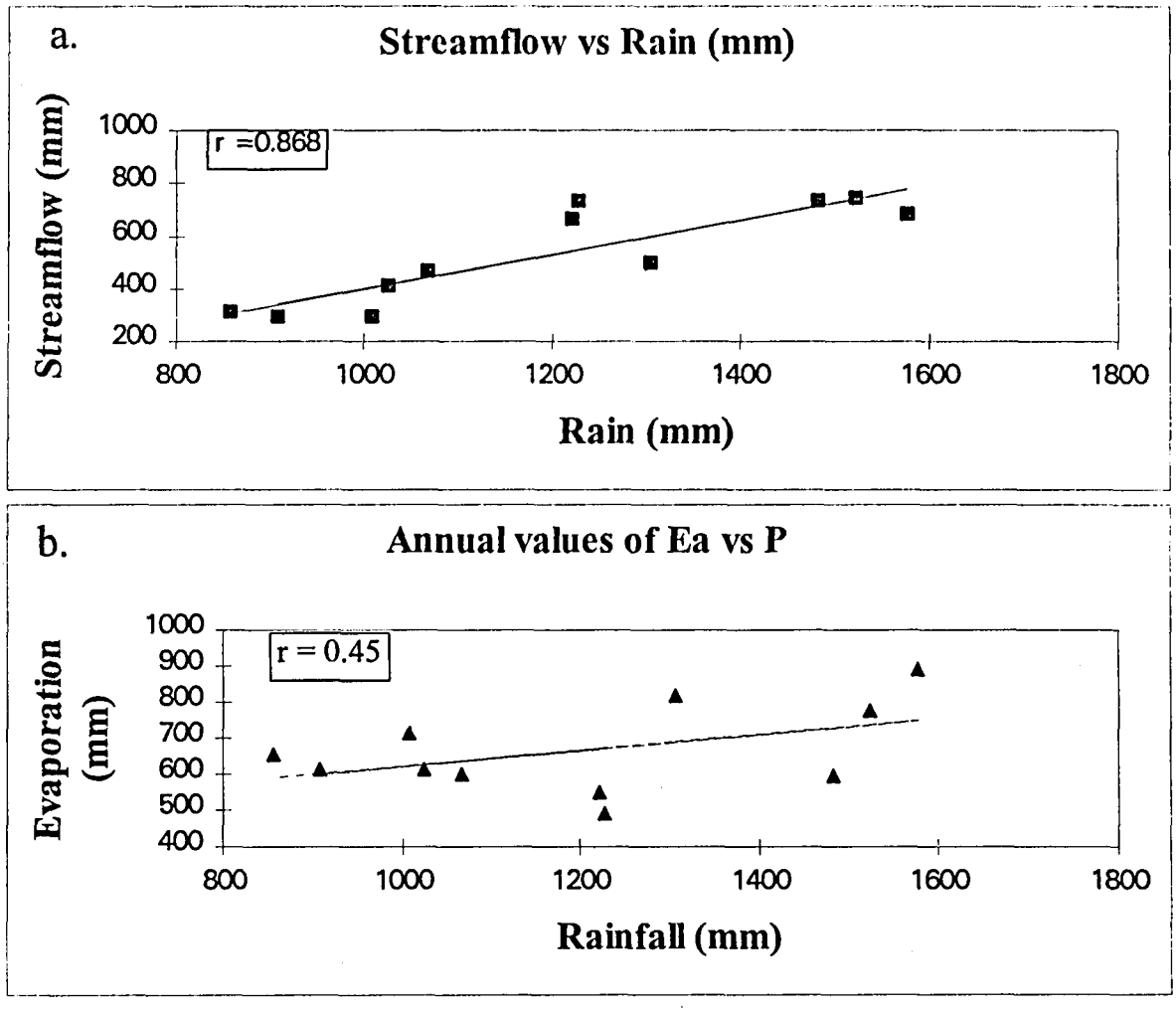

Figure 5.4 a & b. Annual values of Q vs P (Figure 5.4 a) and P vs E_a (Figure 5.4 b) for Catchment VI for an 11 year period. The lines of best fit are described by the equations $Q = 0.65P - 251$ and $E_T = 0.21P + 402.2$.

the dominating component of the water balance. Streamflow was largely dependent on rainfall, and good predictions of streamflow from precipitation and potential evaporation were possible. Evaporation was not closely linked to rainfall, and as a result poor relationships were found. The difficulty of predicting evaporation from rainfall and A-pan data in this climate were highlighted by the *p vs e* relationship and the linear regression of P *vs* E_a data. If realistic models are to be developed, to account for changes in evaporation due to changes in canopy type and climate, they will have to based on more data intensive micrometeorological solutions such as the Penman - Monteith equation.

Chapter 6

MODEL TESTING

6.1 Introduction

For environmental impact studies or decision models, one needs to know where within a catchment, runoff or soil moisture is produced or accumulated. For this, 'distributed' hydrological models are required, which explicitly and cost effectively accommodate the second and third dimensions of catchments (Kruger, 1984). The O'Loughlin model attempts to overcome the problem of determining hydrological flux at a point by simulating homogenous soil profiles mathematically with a complex series of differential equations. This model has the potential to provide solutions to the complex problem of planting commercial trees within or near riparian zones.

The O'Loughlin model is not expected to have the flexibility of ACRU for addressing diverse agricultural and hydrologically related problems. Conversely, there is little chance for ACRU being able to compare with the O'loughlin model for its ability to simulate lateral soil water movement. The two models should therefore be complementary in the planning of catchments in an integrated manner. Until the available models are tested, there will be a reluctance by decision makers and managers to fully utilise the potential of these models. Conversely, use of the models without proper verification could lead to gross errors in water resource planning. The aim of this part of the study was to test the TOPOG and ACRU models on data sets developed for catchment VI.

6.2 Saturated zone modelling (TOPOG)

The TOPOG series of models comprises a terrain analysis based hydrological modelling package that can simulate water movement in complex three dimensional landscapes. The models simulate spatial water movement downslope through the soil, while adjusting water budgets through simulation of evaporation, soil water storage and discharge as streamflow. Evaporation simulations are modified by radiation budgets on differing slopes and aspects, vapour pressure deficits and vegetation types, based on measurement and model estimation. Soil water movement is modelled as a function of soil physical characteristics such as saturated hydraulic conductivity and volumetric soil moisture capacity. TOPOG uses a finite difference solution of

the Richards equation. TOPOG has been applied to data from South African catchments in the eastern Transvaal and Natal Drakensberg (CVI data), using measured rainfall, temperature, humidity, shortwave radiation and streamflow data for comparative purposes. The model builds a numerical representation of a catchment from digitized contours or spot heights, and automatically delineates catchment boundaries by constructing a flow net for the catchment. The flow net is merged with the contour representation to give a simulated catchment consisting of multiple elements. The lateral transfer of water through each element is controlled by soil profile models, themselves represented spatially by digital representations of soil types. Hydrological inputs and outputs are similarly represented and constrained by spatial variations of vegetation. Calculations of the water balance take place in each element, which in turn are modified by simulations of lateral and vertical soil moisture redistributions from above and below each element.

The model is based on a daily time-step, so certain assumptions are made pertaining to rainfall intensity and interception by the vegetation. All overland flow is assumed to reach the channel unless re-infiltrated.

A second, important capability of the model is that of plant growth simulations. TOPOG_IRM does this by modelling carbon assimilation by the vegetation through the Integrated Rate Methodology (IRM), which uses the concepts of multifactor saturation rate kinetics. Plant growth in the model is assumed to be a function of light, water and nutrients only, all of which are controlled by climatic data, and soils information. TOPOG_IRM is therefore well suited to investigations of landscape response to changes in the physical or biological character of the catchment, thus combining the interactions of water yield and plant growth vigour. TOPOG_IRM shows promise, not only for saturated zone modelling, but also site yield simulations in afforested areas.

The software package comprising the TOPOG series, TOPOG_IRM and TOPOG_YIELD (TOPOG_IRM has the same capabilities as TOPOG_YIELD but has the added advantage of the hydro-ecological model), is accompanied by interactive graphics packages for easy manipulation of the model. TOPOG_IRM will only run on computer systems such as SUN workstations or machines of similar or larger capabilities. These systems are available at Jonkershoek where the software is currently being installed.

The package is licensed to the CSIR and there is only one copy, as per contract that the CSIR has with the Division of Water Resources, CSIRO, Australia.

The implementation of the model on local computer systems has not been satisfactory. The model is still in the development phase and there are a number of problems. The data requirements of the model, especially climatic, are complex. This is a result of the way in which the model was designed and built without due regard to the general availability of data such as direct and diffuse radiation and vapour pressure deficit. To overcome this problem the model relies greatly on the output of models such as Steve Running's MTCLIM. At present, output of the model shows high degrees of accuracy where observed data is available. O'Loughlin was rather uncertain as to the capabilities of his model in grassland areas, such as those in Cathedral Peak.

6.2.1 *Conclusion*

Preliminary simulations using TOPOG did not fit observed data well. The results indicated that this could be rectified by debugging the program. However, computational problems prevented the successful running of the TOPOG model. The CSIR is investigating the feasibility of bringing in Australian experts to help with implementation of the system.

6.3 ACRU

In South Africa the hydrological model ACRU (Agricultural Catchments Research Unit) is probably the most suitable vehicle within which to model the comparative water balance of natural grassland and forested catchments. ACRU, together with the GIS system ARC/INFO, is therefore considered as an external framework for the grassland water balance model.

The ACRU model was developed within the Department of Agricultural Engineering, University of Natal to provide a simple decision making tool for agrohydrological problems (Schulze 1995).The model has been used extensively in South Africa for varied applications including water resource assessments (Schulze, Schafer & Lynch 1990), land use management (Kienze & Schulze 1992, Tarboton & Shulze 1993) and irrigation supply (Dent 1988). The recent development of the PC version of ACRU will make the model available to a wide number of users. Validation of the model against observed data is essential if it is to be used with confidence. As there is a scarcity of long term high quality data sets from South African research

catchments (Schulze 1986), the model has largely been verified from data sets from other countries. The present in-depth study of all the hydrological processes in catchment VI provides a continuous five-year data set against which the ACRU model can be validated with South African data.

6.3.1 *General structure of the ACRU model for water budgeting*

Details of the structure of the ACRU model are given by Schulze (1994) and are summarized here. ACRU is a physical conceptual model that conceives a one-dimensional system in which the important processes are included in discrete time units. The model represents the ability of the soil to store and transmit water, while vegetation water use is simulated using hydrological variables. ACRU is a multi-purpose model which has options for outputting runoff, seasonal vegetation yields and water supply analysis. Since the model uses daily time steps, it makes optimal use of daily climatic data. ACRU can operate as a point model, a lumped small catchments model or as a distributed model for large catchments. In the catchment VI study the lumped model was selected to generate a water budget for the catchment.

The aim of the model is to partition the distribution of soil moisture and simulate evaporation. Rainfall not removed as interception or stormflow first enters and resides in the A-horizon. When that is filled the remaining precipitation percolates into the B-horizon. Should the B-horizon attain saturation, vertical drainage into the groundwater store takes place, from which baseflow is generated. Evaporation takes place from previously intercepted water as well as simultaneously from the topsoil horizon (soil water evaporation) and from all horizons in the root zone (plant transpiration). The roots absorb water in proportion to the root mass density of the respective horizons. Evaporative demand on the plant is estimated according to atmospheric demand (through a reference potential evaporation) and the plant's stage of growth.

The generation of stormflow in ACRU is based on the assumption that after initial abstractions (through interception, depression storage and infiltration before runoff commences) the runoff is a function of the magnitude of the rainfall and the soil water deficit from a critical response depth of the soil. The soil water deficit antecedent to a rainfall event is simulated by ACRU's multi-layer soil water budgeting routines on a daily basis. The critical response depth depends on the dominant runoff-producing mechanism. Depths are generally shallow in arid areas characterized by eutrophic (poorly leached and drained) soils and high intensity storms which

produce mostly surface runoff. By contrast, interflow and "push-through" runoff mechanisms dominate high rainfall areas with dystrophic (highly leached, well drained) soils and depths are generally deeper. Not all stormflow generated by a rainfall event is the same day response at the catchment outlet; stormflow is therefore split into quickflow (i.e. same day response) and delayed stormflow, with the "lag" dependent on soil properties, catchment size, slope and drainage density.

6.3.2 *Assessment of the streamflow model*

Initial runs of the model appeared to be under-estimating streamflow (Q) by at least 25%. In order to improve simulations the rainfall was adjusted upwards by 6% to account for under-estimates of rainfall in mountainous terrain.

Nine months of dummy data were appended to the beginning of the composite data file to allow the model to adjust the initial soil water storage terms. It was necessary to add 15 mm of rainfall for 6 days to the dummy data in September to adjust the base flow to that of the observed data. All the other variables were considered feasible for the soils and vegetation of the study area.

6.3.3 *Data organisation*

A composite daily input data file was created from the 5 years of 20 minute meteorological and ancillary data collected in catchment VI between October 1990 and September 1995. The following variables were included:

1. Station ID
2. Year
3. Month
4. Day
5. Observed rainfall (mean of 5 rain gauges situated within the catchment)
6. Maximum temperature
7. Minimum temperature
8. A pan (Little Berg weather station)
9. Observed streamflow
10. Observed soil water content in A horizon
11. Observed soil water content in B horizon
12. Leaf area index (dimensionless)
13. Incoming radiation flux density in MJ m^{-2} day^{-1}
14. Relative humidity in %
15. Wind run in km day^{-1}

A separate file containing observed E_t from 1/10/90 - 30/9/94 was organized for comparison with ACRU. The input information file (Appendix D) was organized in consultation with Prof. Schulze and Mr Pike, as the project team had little prior experience in running the ACRU model. The PC-DOS version of the model was used in all simulations. An excellent user and text manual have been published by the Department of Agricultural Engineering (WRC report No. TT 70/95). The reader is referred to these for specific details of the model.

6.3.4 *Results*

The time series graph of actual and modelled streamflow and the comparative statistics are shown in Figure 6.1 and Table 6.1 respectively. There was good agreement between the actual and modelled trends (coefficient of agreement = 0.87; correlation coefficient = 0.80). In general, ACRU under-estimated streamflow by 15%. This resulted in a 358 mm under-estimation over the five year simulation. The model performed better in the average rainfall and dry years of 1991/92, 1992/93 and 1994/95. The biggest deviation was in the very wet year of 1993/94 when ACRU was clearly under-estimating the catchment runoff.

The accurate estimation of daily E_r (reference evaporation) is a critical factor in the successful application of ACRU (Schulze 1995). In this study monthly means of A-pan data were selected from the input menu to calculate the reference evaporation. Estimates of ACRU E_r over a representative period (1/10/90 - 30/9/93) closely followed actual daily evaporation (E_t) estimated using the Bowen ratio technique. For the period 1/10/90 - 30/9/94 the total E_r and E_t was 2 664 mm and 2 796 mm respectively. This is a good agreement considering the generally accepted poor performance of the A-pan when compared to the highly technical Bowen ratio technique.

A preliminary analysis of the unsaturated flow from the B horizon to the groundwater zone (PERC) and saturated drainage (SUR2) showed that ACRU was unable to account for the predominance of subsurface flow found in catchment VI.

6.3.5 *Conclusion*

The initial simulation undertaken with the ACRU model indicates that hydrological processes in catchment VI can be modelled successfully. Refinements may be necessary to reduce the 15% under-estimation of streamflow. Since the data sets are in place and the PC version is running successfully, further exploration of the potential options of the model is recommended.

Table 6.1 Comparative monthly statistics : Actual versus observed streamflow for CVI (5 yrs data).

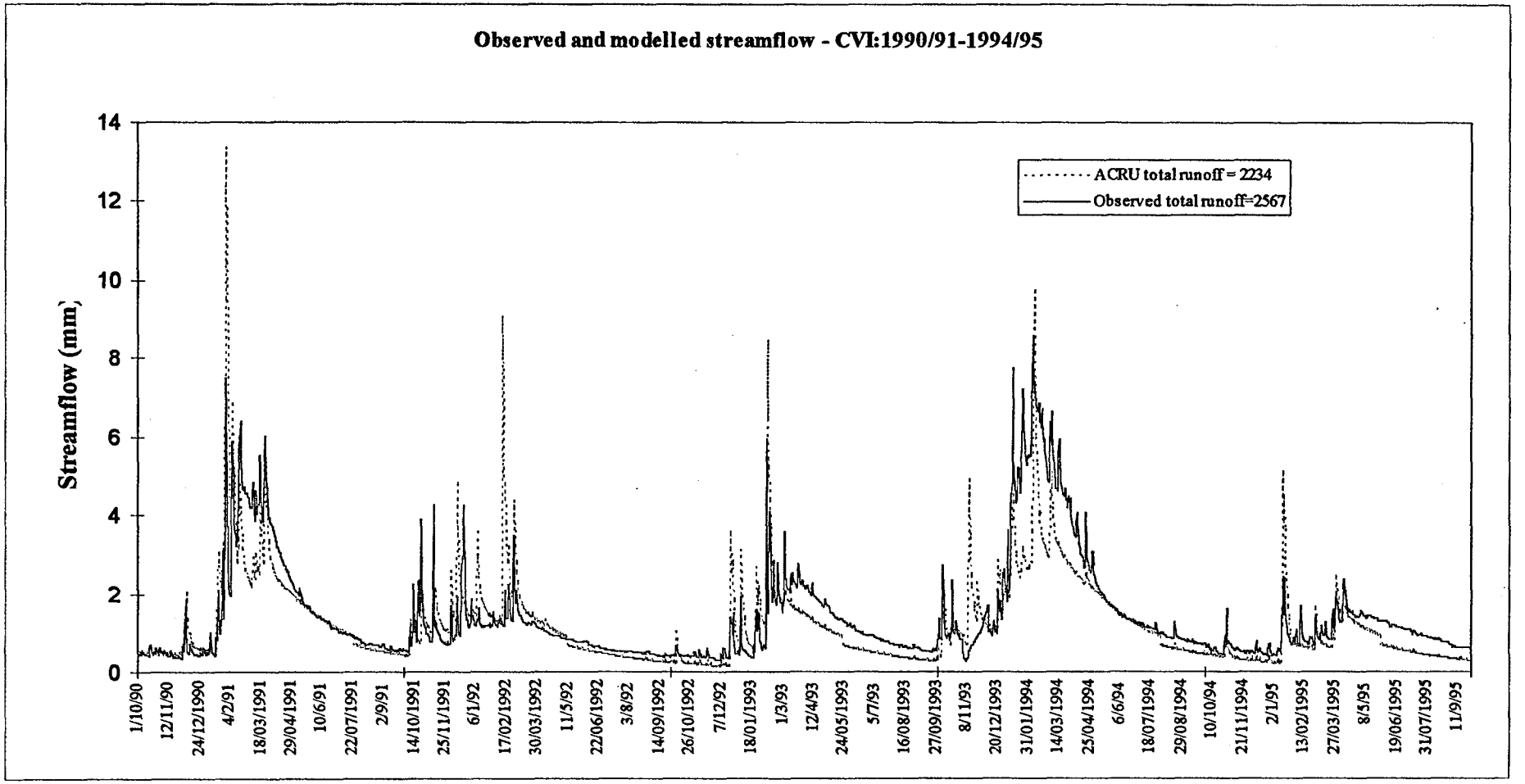

Figure 6.1 Observed and ACRU modelled streamflow for catchment VI at Cathedral Peak for the period January 1990 to September 1995.

Table 6.1 Comparative monthly statistics : Actual versus observed streamflow for CVI (5 yrs data).

Observed variable = STRMFL
Simulated variable = CELRUN

Sample size	=	1744.0

CONSERVATION STATISTICS

Sum of observed values	=	2496.62
Sum of simulated values	=	2138.24
Mean of observed values	=	1.43
Mean of simulated values	=	1.22
% difference between means	=	14.35
t Statistic for comparing means	=	4.87
Variance of observed values	=	1.71
Variance of simulated values	=	1.37
% difference between variances	=	19.71
Standard deviation of observed values	=	1.31
Standard deviation of simulated values	=	1.17
% difference between standard deviations	=	10.39
Standard error of observed means	=	0.03
Standard error of simulated means	=	2.0
% difference between standard errors	=	10.39
Coeff. of variation of observed values (%)	=	91.50
Coeff. of variation of simulated values (%)	=	95.73
% difference between coeffs. of variation	=	-4.62
Skewness coefficient of observed values	=	2.28
Skewness coefficient of simulated values	=	3.07
% difference between skewness coefficients	=	-34.75
Kurtosis coefficient of observed values	=	5.26
Kurtosis coefficient of simulated values	=	16.54
% difference between kurtosis coefficients	=	-214.57
t Statistic for correlation testing	=	55.61

REGRESSION STATISTICS

Correlation coefficient (Pearson's r)	=	0.80
Slope of the regression line	=	0.71
Y intercept of the regression lin	=	.20
Coefficient of determination (SSR/SST)	=	0.64
Coefficient of efficiency	=	0.50
Coefficient of agreement	=	0.87

6.4 General conclusions

The data collected in this study were used to test two hydrological models, TOPOG (a distributed model) and ACRU (a one dimensional model).The study has shown that the practical difficulties of computational analysis using TOPOG will limit the implementation of this model. The ACRU model generally predicted streamflow well except in wet years. The model was successfully validated against the catchment VI data set. One of the current limitations of ACRU is its inability to account for subsurface soil water flow in a catchment. It is recommended that the development of the ACRU model should continue to take this into account.

References

Aase, J.K., Wight, J.R., Siddoway, F.H., 1973. Estimating soil water content on Native rangeland. *Agric. Meteorol.* **12**: 185-191.

Anon, 1996. Sustainable forest development in South Africa. The Policy of the Government of National Unity. White paper. Ministry of Water Affairs and Forestry, Pretoria, South Africa.

Bainbridge, W.R., 1987. Management of mountain catchment grassland with special reference to the Natal Drakensberg. In: Gadow von K (ed) Forestry Handbook. Southern African Inst For, Pretoria.

Black, T.A., Tanner C.B. & Gardner, W.R. 1970. Evapotranspiration fronm a snap bean crop. *Agron. J.* **62**: 66-69.

Bosch, J.M. 1979. Treatment effects on annual and dry period streamflow at Cathedral Peak. *S. Afr. For. J.* **108**: 29-38.

Bosch, J.M. 1992. Streamflow response to catchment management in South Africa. *Proceedings, Hydrological research Basins and Their Use in water Resources Planning*. Landeshydrologie, Berne, Switzerland. 279-289.

Brisco, B. & Pultz, T.J. 1992. Soil moisture measurement using portable dielectric probes and time domain reflectrometry. *Water Resources Research.* **28**:1339-1346.

Brun, L.J., Kanemasu E.T. & Powers W.L., 1972. Evapotranspiration from soybean. and sorghum fields. *Agron. J.* **65**:326-328.

Burch, G.J., Bath, R.K., Moore, I.D. and O'Loughlin, E.M. 1987. Comparative hydrological behaviour of forested and cleared catchments in Southeastern Australia. *J.Hydrol.* **90**, 19-42.

Calder, I.R., 1990. *Evaporation in the Uplands*. John Wiley and Sons, Chichester, UK.

Campbell, G.S., 1992. On-line measurement of potential evapotranspiration with the Campbell Scientific automated weather station. Application note, Campbell Scientific, Inc., Logan, Utah.

Clarke, G.P.Y. & Dane, J.H., 1991. A simplified theory of point kriging and its extension to co-kriging and sampling optimization. Bulletin 609, Alabama Agricultural Experiment Station, Auburn University.

Cressie, N.A.C., 1991. *Statistics for spatial data.* Wiley, New York,

Dent, M.C. 1988. Estiamting crop water requirements for irrigation planning in southern Africa. *Agricultural Engineering in South Africa*, **20**: 7-19.

de Jong, E. & MacDonald, K.B., 1975. The soil moisture regime under native grassland. *Geodorma* **14**:207-221.

Dunne, T. & Black, R.D., 1970. Partial area contributions to storm runoff production in a small New England watershed. *Water Res. Res.* **6**: 1296-1311.

Dyck, S. 1983. Overview on the present status of the concepts of water balance models. In New Approaches in Water Balance Computations (Proceedings of the Hamburg Workshop, August 1983). IAHS Publ. no. 148, pp 3-19.

Dyer, R.A., 1963. Preface to: An account of the plant ecology of the Cathedral Peak area of the Natal Drakensberg. Ed. D.J.B. Killick. *Bot. Surv. S. Afr. Mem.* No. **34**. Govt. Printer, Pretoria.

Eagleson, P.S. 1970. *Dynamic Hydrology*. Mc Graw-Hill Book Co.: New York.

Everson, C.S. & Tainton, N.M., 1984. The effect of thirty years of burning on the Highland Sourveld of Natal. *J. Grassl. Soc. Sth. Afr.* **1**(3): 15-20.

Everson, T.M., van Wilgen, B.W., & Everson, C.S., 1988. Adaptation of a model for rating fire danger in the Natal Drakensberg. *S.A. J. Sci.* **84**:44-49.

Freeze, R.A., 1972. Role of subsurface flow in generating surface runoff. I. Base flow contributions to channel flow. *Water Resour. Res.* **8**, 609-623.

Fuchs, M. & Tanner, C.B., 1970. Error analysis of Bowen ratios measured by differential psychrometer. *Agric. Meteorol.* **7**: 329-334.

Fuchs, M., 1973. The estimation of evapotranspiration. *Arid Zone Irrigation* (B. Yaron, E. Danfors, & Y. Vaadia, eds.) Springer-Verlag, New York, pp241-247.

Gardner, W.R., 1987. Water content: an overview. Procedings of the international conference on Measurement of Soil and Plant Water status. Vol. I.

Granger, J.E. & Schulze, R.E., 1977. Incoming solar radiation patterns and vegetation response: examples from the Natal Drakensberg. *Vegetatio* 35:47-54.

Hanks, R.J., 1974. Model for predicting plant water yield as influenced by water use. *Agron. J.* **66:** 660-665.

Hanson, C.L. 1976. Model for predicting evapotranspiration from native rangelands in the northern Great Plains. *Trans. Am. Soc. Agric. Eng.* **19**:471-477.

Hewlett, J.D. & Hibbert, A.R., 1967. Factors affecting the response of small watersheds to precipitation in humid areas. In: Forest Hydrology, edited by W.E. Sopper & H.W. Lull, pp 275-290, Pergamon, New York.

Innis, G.S. (ed), 1978. *Grassland Simulation Model.* Ecological studies 26. Springer, New York, 298pp.

Johnston, A.S., Smoliak, S., Smith, A.D. & Lutwick, L.E., 1969. Seaonal precipitation, evaporation, soil moisture, and yields of fertilized range vegetation. *Can. J. Plant Sci.*

49:123-128.

Journel, A.G., and Huijbregts, Ch.J., 1978. Mining and Geostatistics, Academic, San Diego, CA., 600pp.

Kalma, J.D. & Badham, R., 1972. The radiation balance of a tropical pasture. I. The reflection of short wave radiation. *Agric. Meteorol.* **23**:217-229.

Kienzle, S.W. & Schulze, R.E., 1992. A simulation model to assess the effects of afforestation on groundwater resources in deep sandy soils. *Water SA*, **18**: 265-272.

Kruger, F.J., 1984. Report on a visit to Australia to attend the Fourth International Conference on Mediterranean-type ecosystems, and related activities. Department of Forestry Communication, A./ 2/6/3/2/54.

Lewis, D.C. 1968. Annual hydrologic response to watershed conversion from oak woodland to annual grassland. *Wat. Resour. Res.* **4**, 59-72.

Law, A.M. & Kelton, W.D., 1982. *Simulation modeling and analysis*. McGraw-Hill, New York, 400pp.

Likens, G.E., Bornmann, F.H., Pierce, R.S., Eaton, J.S. and Johnson, N.M. 1977. *Biogeochemistry of a forested ecosystem.* Springer Verlag, New York, USA.

Loague, K., 1992. Soil water content at R-5. Spatial and temporal variability. *J. Hydrol.*, 139:233-251.

Monteith, J.L. 1973. *Principles of environmental Physics*. Contemporary Biology Series. Edward Arnold, London. 241 pp.

Monteith, J.L. 1965. Evaporation and environment. Symposium of the Society for Experimental Biology 19: 205-234.

Mosley, M.P., 1979. Streamflow generation in a forested watershed, New Zealand. *Water Res. Res.* **15**: 795-806.

Nakos, G and Vouzaras, A. 1988. Budgets of selected cations and anions in two forested experimental watersheds in central Greece. *For. Ecol. Manag.* **24**, 85-95.

Penman, H.L. 1948. Natural evaporation from the open water, bare soil and grass. *Proc. R. Soc. London, Ser. A.*, **193**: 120-145.

Pinõl, J., LLedó, M.J. and A. Escarré. 1991. Hydrological balance of two Mediterranean forested catchments (Prades, northeast Spain). *Hydrol. Sci. J. 36, 95-107.*

Reid, P.C.M., 1981. Energy aspects of water use efficiency. Msc. Thesis, University of the Orange Free State, Bloemfontein.

Reginato, R. & Nakayama, F.S. 1987. Plastic standards for transferring neutron probe calibrations. Procedings of the international conference on Measurement of Soil and Plant Water status. Vol. I.

Rogler, G.A. & Haas, H.J., 1947. Range production as related to soil moisture and precipitation on the northern Great Plains. *j. Am. Soc. Agron.***39**:378-389.

Rosenberg, N.J., Blad B.L. & Verma, S.B., 1983. *Microclimate: the biological environment.* 2nd ed., John Wiley and Sons, New York.

Tarboton, K.C. & Shulze, R.E., 1993. Hydrological consequences of develoment scenarios for the Mgeni catchment. *Proceedings, 6th South African National Hydrological Symposium.* University of Natal, Pietermaritzburg, Department of Agricultural Engineering. 297-304.

Savage, M.J., C.S. Everson & B.R. Metelerkamp, 1995. Evaporation measurement comparisons and advective influences using Bowen ratio, lysimetric and eddy correlation methods. Proceeding of the South African Irrigation Symposium, June 1991, pp 160-166.

Rasmussen, V.P. & Hanks, R.J., 1978. Spring wheat yield model for limited moisture conditions. *Agron. J.* **70**: 940-944.

Schulze, R.E. 1994.Hydrology and Agrohydrology : A text to accompany the *ACRU 3.00* agrohydrological modelling system. Water Research Commission, Pretoria, Report TT69/95.

Schulze, R.E. 1995. Hydrology and Agrohydrology: A text to accompany the *ACRU 3.00* agrohydrological modelling system. Water Research Commission, Pretoria, Report.

Schulze, R.E. 1996. The *ACRU* model for agrohydrological decision making : Structure, options and application. *Proceedings, Hydrological Sciences Symposium,*Rhodes University Grahamstown, Department of Geography. 1-19.

Schulze, R.E., Schafer, N.W. & Lynch, S.D. 1990. An assessment of regional runoff production in Qwa Qwa : A GIS aplication of the *ACRU* modelling system. *South African Journal of Photogrammetry, Remote sensing and Cartography,* **15**:141-148.

Slatyer, R.O., & McIlroy, I.C. 1967. Practical micrometeorology. CSIRO, Melbourne, Australia.

Smith, M. 1991. Report on the expert consultation on procedures for revision of FAO guidelines for predicting of crop water requirements. Food and Agriculture Organization of the United Nations, Rome, Italy.

Smoliak, S., 1956. Influence of climatic conditions on forage production of shortgrass rangeland. *J. Range Management* **32**:89-91.

Sneva, F.A. & Hyder, D.N., 1962. Estimating herbage production on semiarid ranges in the intermountain region. *J. Range Management* **15**:88-93.

Thiessen, A.H. 1911. Precipitation for large areas. *Mon. Weath. Rev*, **39**, 1082-1084.

Thom, A.S., 1975. Momentum, mass and heat excahnge of plant communities. *Vegatation and the Atmosphere* (J.L. Monteith, ed.), Academic Press, pp. 57-109.

Tyson, P.D., Preston-Whyte, R.A. & Schulze, R.E., 1976. The climate of the Drakensberg. Town and Regional Planning Commission, Natal, Vol **31**.

Ward R.C. & Robinson M., 1980. *Principles of Hydrology*. McGraw-Hill, Maidenhead, UK.

Wight, J.R. & Hanks, R.J., 1987. A water-balance climate model for range herbage production. *J. Range management* **64** (4):307-311.

Appendix A

Calibration of the Troxler neutron probe for a hutton soil at Cathedral Peak

Regression analyses were carried out using GENSTAT statistical procedures (Clarke pers. comm.). The following relationships were tested using volumetric water content as the response variate:

1. Linear regression (all data)
2. Linear regression for each access tube separately and their interactions with the count ratio.
3. Linear regression for each depth separately and their interactions with the count ratio.
4. Quadratic regression (all data)
5. Quadratic regression for each tube separately and their interactions with the count ratio.
6. Quadratic estimates for each depth separately and their interactions with the count ratio.
7. Quadratic regression with depths 1 to 4 and 5 to 8 pooled.
8. As above but removing outliers.
9. Quadratic regression for each tube separately.
10. Quadratic regression excluding tubes 7 and 8.
11. As above but removing outliers.
12. Quadratic regression on tubes 7 and 8 only.
13. Quadratic regression grouping tubes 1 2 3 4 7 8 12 13 and 5 6 9 10 11 14 in another group.
14. As above but removing outliers.
15. Quadratic analysis by depth excluding tubes 7 and 8 plus outliers
16. Quadratic analysis excluding tubes 7 and 8, plus outliers for depths 1 and 2 combined, and depths 4 5 6 7 combined.
17. As above excluding extra outliers.
18. Exponential regression on all data excluding tubes 7 and 8 plus outliers.

Summary of findings:

Generally the regressions were variable both across sites and for varying depths. The best fit was with the quadratic regression equations. Regression was stronger for shallow depths, particularly depth 1 (0-0.25 m). This is probably a function of the greater variation in water content experienced at the surface, which produces a wider range of possible values.

With VOL the volumeteric water content of moisture per unit volume of soil (expressed as a percentage), and X the count ratio (measured count/standard count) determined from the neutron moisture meter, the most meaningful regression equations were the following:

(a) **Quadratic over all depths:**

$$VOL = -50.9 + 134.0\ (X) - 44.3\ X^2 \quad \text{.....(a)}$$

	d.f.	s.s.	m.s.
Regression	2	7169	3584.66
Residual	302	12251	40.57
Total	304	9421	63.88

$p=<0.001$

percentage variance accounted for =36.5

(a) **Quadratic for depths 1 & 2 only:**

$$VOL = -53.6 + 129.6\ (X) - 40.0\ X^2 \quad \text{.....(b)}$$

	d.f.	s.s.	m.s.
Regression	2	3336	1667.95
Residual	302	4611	41.92
Total	304	7947	70.96

p=<0.001

percentage variance accounted for =40.9

(c) **Exponential regression over all depths.**

$$VOL = 55.59 - 258\ (0.0654)^{x} \quad \text{.....(c)}$$

	d.f.	s.s.	m.s.
Regression	2	7348	3673.81
Residual	298	11011	36.95
Total	300	18358	61.19

p=<0.001

percentage variance accounted for =39.6

Actual volumeteric soil water and count ratio values, together with the predictive form of the exponential regression are presented in Figure A1.

Conclusion:

The most useful fit is given by equation (c) where the volume of soil water may be estimated from the neutron probe by means of the following expression:

$$VOL = 55.59 - 258\ (0.0654)^{x}$$

The calibration of the neutron probe is typified by a high level of unexplained variance. Close fits are sometimes found in very homogenous soils (eg. sands) or on well mixed sites (agricultural soils). The variance experienced in this calibration is typical of field calibration methods.

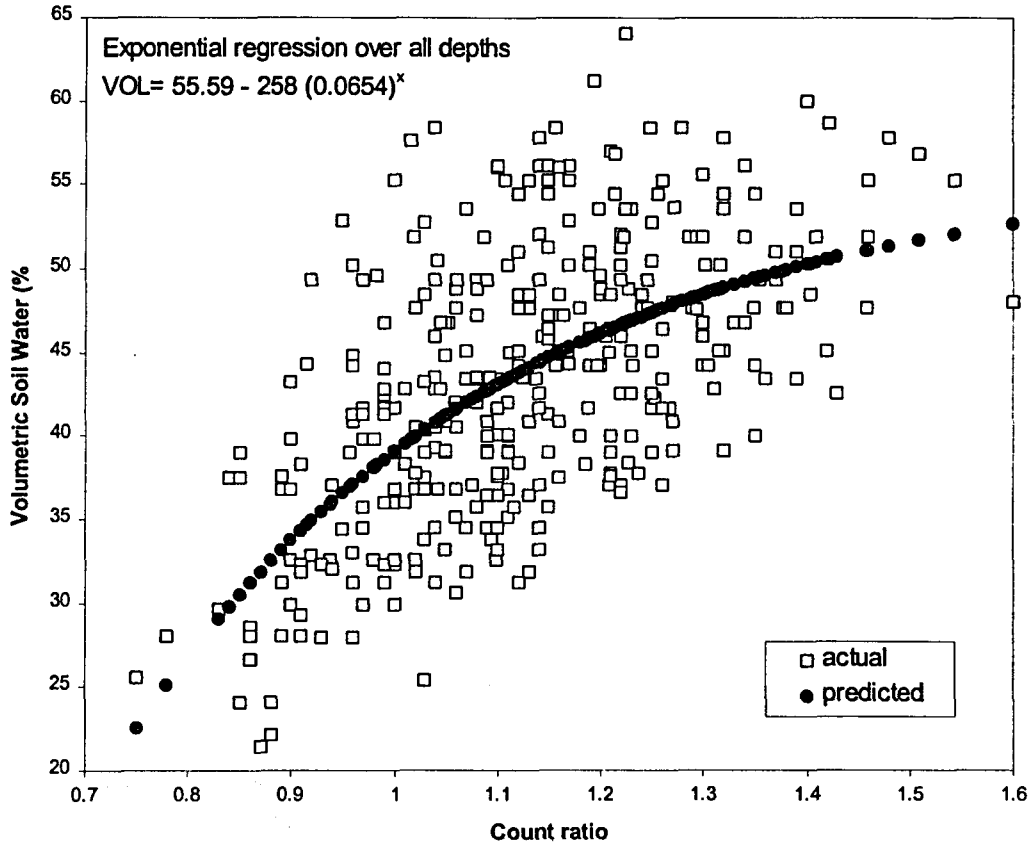

Figure A1 A plot of the volumetric water content determined gravimetrically versus the count ratio recorded with a Troxler neutron probe.

Appendix B

Calibration of the Capacitance probe

A capacitance soil moisture probe (type IH1, Didcot Instruments Co. Ltd., Oxford, UK) was used to measure profiles of the volumetric soil moisture content of the soils in catchment VI. The frequency output of the probe is influenced by variations in temperature and these can therefore not be used directly for the calculation of volumetric soil moisture content. A universal frequency (*UF*) is calculated from frequency readings taken in the soil (F_s) using the frequency measured in the access tube extension, which is read at the start and end of each measurement and represents the frequency measured in air (F_a), and that measured in an access tube fully submerged in water (F_w):

$$UF = \frac{F_a - F_s}{F_a - F_w}$$

For the probe sensor used in the present study F_a ranged from 17 748 to 17 941 kHz. F_w was measured on two occasions and was 14 189 kHz (17 April 93) and 13 368 kHz (24 March 94).

As the capacitance moisture probe is very sensitive to small variations in soil properties and water content (Bell, Dean & Hodnett 1987) it was not possible to calibrate the probe using samples collected in the vicinity of the access tube. The capacitance probe was therefore calibrated on volumetric water potential obtained from soil samples removed during installation of the access tube. Readings were taken at 2 cm intervals over the length of the 2 m tube. This was an extremely time-consuming and labourious procedure. The presence of rocks and stones in the soil resulted in numerous aborted attempts to install the access tube after considerable time and effort had already been expended.

As the volume of each sample was known (78.5 m^3) the water content and bulk density could be determined from the wet and oven-dried samples. Instrumental drift during the measurements was determined by taking readings of F_a before and after measuring the profile. It has been shown that the probe is sensitive to moisture volume fractions below 0.35 $m^3 m^{-3}$. The porosity of the catchment VI soil was high (66-70%) due to the large proportions of clay and silt.

The plot of the Universal Frequency versus volumetric water content showed no clear relationship (Figure B1). This necessitated separate calibrations for four different depths (40 -240 mm, 340 - 540mm, 580 - 1 020 mm and 1 180 - 1700 mm). Linear regressions have been fitted to these with correlation coefficients between 0.696 and 0.866 (Figure B2). However, the regressions generally showed a large scatter in the data caused by the small range in *UF* and volumetric water content. A plot of the volumetric water content over depth showed that the capacitance probe was not sensitive to moisture content changes over depth when compared with the neutron probe and gravimetric sampling techniques (Figure B3). Since the variation in volumetric water content was small throughout the profiles of this study a satisfactory calibration could not be obtained.

References

Bell, Dean & Hodnett 1987. Soil moisture measured by an improved capacitance technique: Part II, field techniques, evaluation and calibration. User manual.

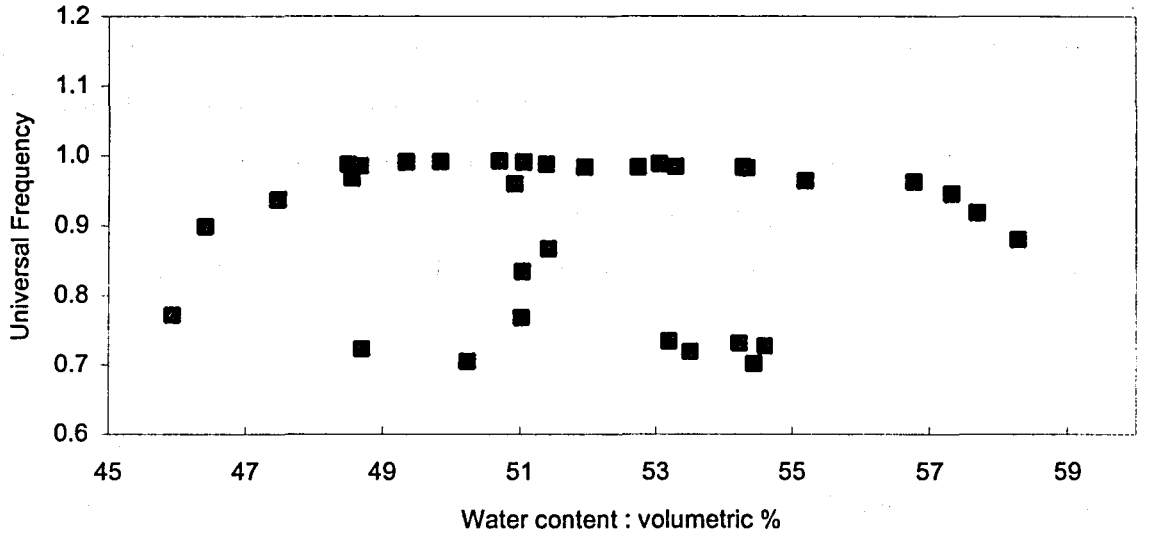

Figure 31. Capacitance Probe Calibration : Universal Frequency vs volumetric water content (%).

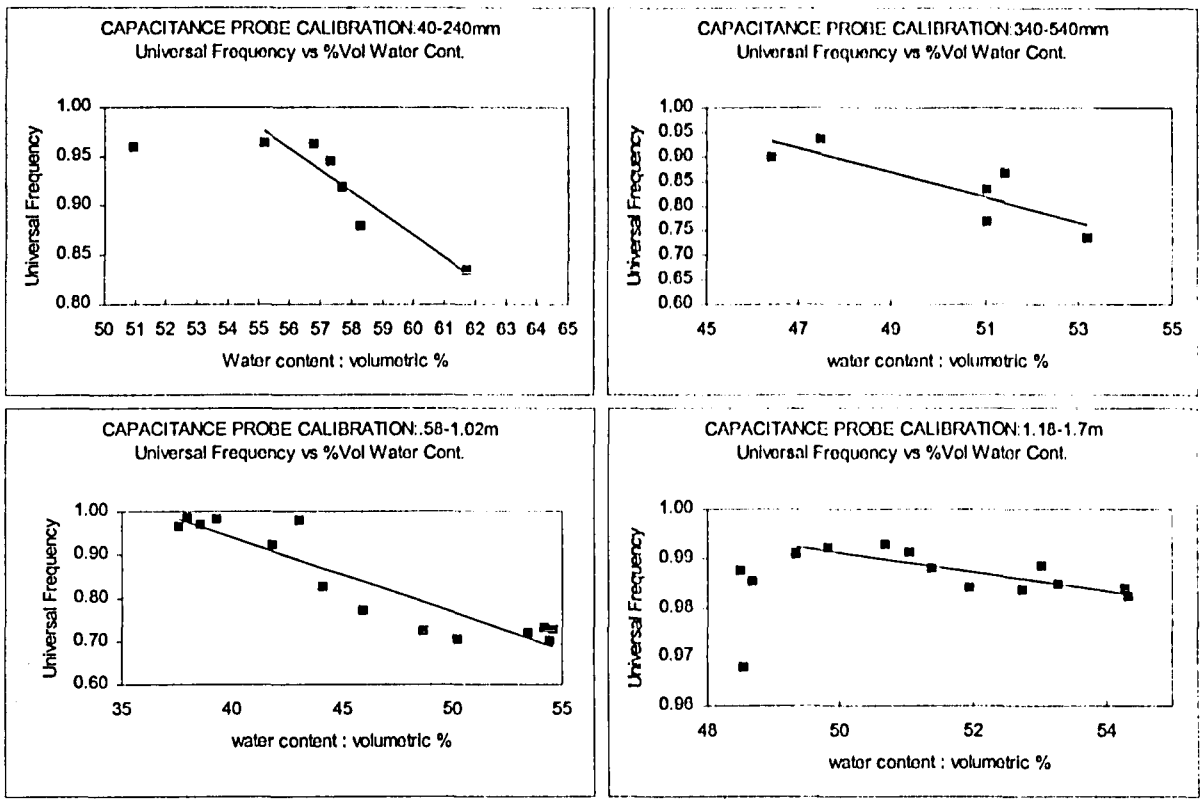

Figure B2. Calibration of the Capacitance probe (universal frequency versus volumetric water content) at four different depths in the soil profile).

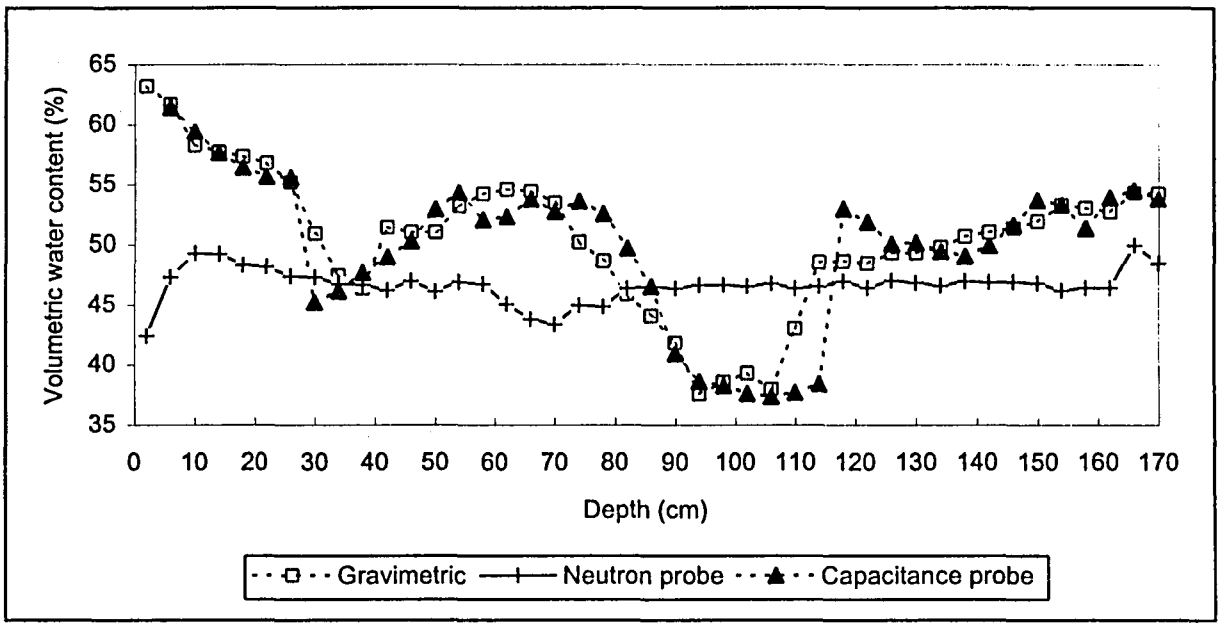

Figure B3. Comparison of the volumatric water content over a 1.7m soil profile using three different measuring techniques.

Appendix C:

TIME DOMAIN REFLECTOMETRY : A REVIEW OF THEORY, INSTRUMENTATION AND METHOD

INTRODUCTION

Soil water content is a critical variable in many processes, and its determination is of vital importance in efforts to improve plant growth and water use efficiency. In catchment hydrology the modelling of infiltration, flux and redistribution of water in catchments are dependent on accurate measurements of *in situ* water content. There are many direct and indirect methods available for soil water measurement (Gardner 1965; Gurr 1962). These include gravimetric and psychometric techniques, gypsum blocks, lysimetry, neutron moderation and various capacitance techniques. These techniques have several disadvantages in the accurate collection of data in the field. By contrast the time-domain reflectometry (TDR) approach which was originally described for use in earth materials by Davis & Annan (1977) is promising for *in situ* measurements. Time-domain reflectometry is a relatively new tool for determining volumetric soil moisture and overcomes some of the problems associated with more traditional methods (Topp, Davis & Annan 1980, 1982a,b; Topp & Davis 1981).

Conventional methods for determining soil water content are discussed briefly to enable comparison with the time-domain reflectometry technique. One of the techniques longest in use is the ***gravimetric method*** (Gardner 1987) whereby soil samples are collected and weighed before and after drying. Since the measurement needs conversion to a volumetric basis, an independent measure of soil bulk density is necessary. The destructive nature of sampling, the time delay for drying of samples and the intensive labour required are drawbacks of the gravimetric method.

The installation of ***resistive blocks*** is an alternative technique for measurement of soil water. However, this requires the calibration of the resistive blocks for each site, and the difference in hysteresis characteristics between blocks and soil seriously limits their use in varying environments (Topp, Davis, Bailey & Zebchuk 1984).

A nondestructive method for measuring the water content of soil is ***neutron moderation*** (Reginato & Nakayama 1987). This method is based on the fact that the hydrogen nucleus has the same mass as a neutron. When the two collide there is a transfer of energy which slows down the neutron. This change in energy is measured with a neutron probe. Besides its non-destructive attribute, one of the main advantages of this method is its precision. However, since the instrument responds to total hydrogen and not just the hydrogen component of the available water in soil, there is a need for calibration for every situation. Faulty calibration curves may cause bias in the result. Since the neutron method requires a relatively large sampling volume, one of its limitations is the inability to measure close to the soil surface (Greacen 1981). The radiation hazard is an added disadvantage (Gardner 1987).

Lysimeters measure water content directly, but are expensive, fixed in space and yield no information about the distribution of water-content changes (Baker & Allmaras 1990).

Another direct method is that of ***thermocouple psychrometry*** by which the chemical potential of water is measured and which provides a direct indication of the energy moving water from place to place. The main disadvantage of thermocouple psychrometers is their susceptibility to *in situ* thermal gradients (Savage 1982).

Preliminary work on the potential of electrical conductivity methods of determining soil moisture was carried out by a number of authors (Edlefsen 1933; Fletcher 1939; Wallihan 1945). Numerous laboratory studies have shown that the dielectric constant of soil is primarily related to its water content (Thomas 1966, Selig & Mansukhani 1975, Okrasinski, Koerner & Lord 1978, Topp, Davis & Annan 1980). The *capacitance technique* provides rapid in situ measurements of the dielectric constant (real and apparent parts) of the contact medium (Wobschall 1978, Brisco & Pultz, 1992). If the medium is soil, then the volumetric soil water content (θ) may be calculated using the empirical relationship to convert the real part of the dielectric constant (ϵ'_r) to θ. This approach was used by Wang & Schmugge (1980) and by Hallikainen *et al.* (1985), and is possible because of the large dielectric constant of water at microwave frequencies ($\approx$60-80) compared to the dielectric constant of dry soil ($\approx$2-5). One of the problems with this technique is that it depends upon specific electrode configurations and detailed calibration (Topp, Davis & Annan 1982b). In some instances the electrodes may measure extraneous capacitance.

Measurement of the ***dielectric constant in the time domain***, by measuring the propagation velocity of a voltage pulse was introduced by Fellner- Feldegg (1969). The general applicability of this method for measuring the volumetric water content of soils and other porous materials has been shown by Topp, Davis & Annan (1980).

PRINCIPLES OF TDR

The physical principles that form the basis of the time domain reflectometry method have been described by Dalton & Van Genuchten (1986). This section gives a brief summary of the principles that relate to the dielectric constant.

When an instantaneous voltage V is applied across an ideal air-filled parallel plate capacitor with capacitance C_0, the electrical charge Q stored on the capacitor is given by:

$$Q = C_0 V \tag{1}$$

If an insulating material is placed between the parallel plates, the electric charge will increase, and hence also the capacitance C. One can give an operational definition of the dielectric constant of the material in terms of the capacitance of the air-filled and material-filled capacitors:

$$C = C_0 \quad \epsilon' / \epsilon_0 = C_0 \, \epsilon \tag{2}$$

where ϵ' and ϵ_0 are the dielectric constant of the material and the air, respectively, and ϵ is the relative dielectric constant, or alternatively termed the relative permittivity. When the applied voltage is sinusoidal in time, i.e. of the form:

$$V = V_0 e^{i\omega t} \tag{3}$$

where complex notation is used ($i^2 = -1$) and is the angular frequency, then the charging current I_c represents the time rate of change of the stored charge:

$$I_c = \mathrm{d}Q/\mathrm{d}t = C_0 \, \mathrm{d}V/\mathrm{d}t = i\omega C_0 V \tag{4}$$

which will be 90 degrees out of phase with the applied voltage.

If the material between the capacitor plates is not a perfect insulator, as would be the case for a saline soil, then there will be a conduction or loss of current I_l proportional to the material conductance G and applied voltage V such that $I_l = GV$. The conductance current I_c is said to be in phase with the applied voltage. Both the loss current and the charge current are key properties that ultimately allow one to measure the electrical conductivity and dielectric constant simultaneously. The ratio of the loss current to the conductance current is called the dissipation factor D, or loss tangent (tan δ):

$$D = \tan \delta = I_l/I_c \tag{5}$$

The total current I_t (charging current + loss current) becomes:

$$I_t = I_l + I_c = (G + i\omega C)V \tag{6}$$

which shows that the total current can be viewed as a complex variable consisting of real and imaginary components. Since the loss current may be due to any energy consuming process and not just to conduction losses, it is convenient to introduce in analogy to equation 6 a complex dielectric constant (von Hippel 1953):

$$\epsilon^* = \epsilon' - i\epsilon'' \tag{7}$$

Using equations 2 and 7, the total current (equation 6) can now be expanded into a form that does not specifically include the loss current:

$$I_t = i\omega CV = i\omega\epsilon C_0 V/\epsilon_0 = (i\omega\epsilon' + \omega\epsilon'')\, C_0 V/\epsilon_0 \tag{8}$$

The parameter ϵ'' is called the loss factor, whereas $\omega\epsilon''$ is equivalent to the dielectric conductivity. As was shown by Fellner-Feldegg (1969), it is possible to obtain in one measurement the frequency-dependent dielectric properties of a medium. Topp, Davis & Annan (1980) further demonstrated that the low-frequency or static component of the dielectric constant can be used to correlate with the soil water content.

TDR MEASUREMENTS OF THE DIELECTRIC CONSTANT

Time domain reflectometry involves measurements of the propagation of electromagnetic waves or signals. The propagation constants (such as velocity and attenuation), depend on the soil properties, especially on its water content and electrical conductivity. In the TDR technique a step voltage pulse or signal is propagated down a transmission line. Parallel pair transmission lines, as depicted in Figure C1a, are usually used for measurement in soil. The parallel rods or wires serve as conductors, and the soil in which the rods are installed, serves as the dielectric medium. The pair of rods act as a wave guide, and the signal propagates as a plane wave in the soil. The signal is reflected from the end of the transmission line in the soil back to the TDR receiver. The reflected signal of the TDR pulse is analyzed with an oscilloscope to estimate the dielectric constant of the medium (Reeves & Smith 1992).

The timing device in TDR (Fig. C1 b.) measures the time between sending a signal from point

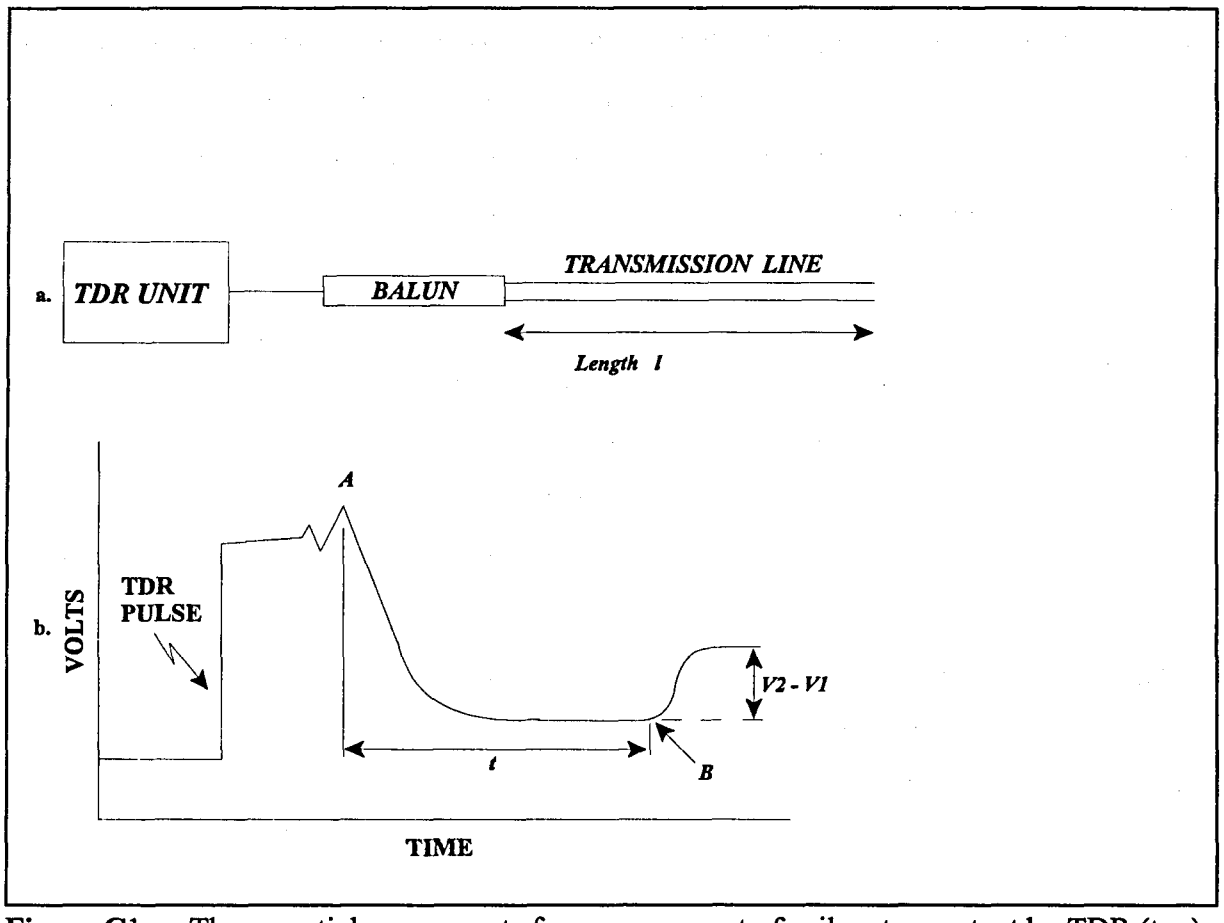

Figure C1. a. The essential components for measurement of soil water content by TDR (top). b. Idealised TDR output trace showing how the propagation time is determined (from Topp & Davis, 1985c).

A and receiving the reflected signal at point B (Topp 1987). The time interval relates directly to the propagation velocity of the signal in the soil since the line length is known. The mode of propagation is similar to the way radio and television signals propagate through space. The propagation velocity is indicative of the volumetric water content, being smaller as water content increases. The TDR signal's propagation velocity is linked to the soil dielectric constant. The dielectric constant is an electrical property that represents the ratio of the dielectric permittivity of the media being measured to the dielectric permittivity of the free space (Hoekstra & Delaney 1974). Water, the component which governs the dielectric constant of the soil, has a dielectric constant of 80 as contrasted with values of 2-5 for soil solids. The theoretical relationship between the dielectric constant and water content is described by Ansout, De Baker & Declercq (1985).

For soil there is a simple approximate relationship between signal propagation velocity, V, and the dielectric constant:

$$V = c/\sqrt{\epsilon} \qquad (9)$$

where c is the propagation velocity of an electromagnetic wave in free space ($3 \times 10^8 ms^{-1}$):

The velocity, V, is obtained from knowledge of the length of the transmission line, l, in the soil (the travel distance is $2l$) and by measurement of signal travel time, t, in the soil using a time-domain reflectometer (Fig. C1). The dielectric constant, ϵ, results from substitution into equation (1) and re-arrangement to

$$\epsilon = (ct/2l)^2 \qquad (10)$$

Once an estimate for ϵ is obtained with equation 10, the dielectric constant must still be correlated with the volumetric soil water content (θ_v). Topp *et al.* (1980) found that ϵ was primarily a function of volumetric water content θ_v, and most soil types can be represented by the following empirical relationship between ϵ and θ_v :

$$\theta_v = -530 + 292\,\epsilon - 5.5\,\epsilon^2 + 0.043\,\epsilon^3)/10000 \qquad (11)$$

Dalton, Herkelrath, Rawlins & Rhoades (1984) took this one step further and proposed that the attenuation of the reflected TDR signal be used to infer soil water electrical conductivity (σ). These authors demonstrated the attenuation of the electromagnetic pulse in a saline solution. Measurements of transit time and attenuation are sufficiently independent to measure conductivity and the dielectric constant simultaneously. As the signal propagates in the soil, the voltage is decreased by the attenuation factor *f*, which has the following relation to the soil's electrical conductivity:

$$f = \exp(-al) \tag{12}$$

where a is the attenuation constant of the soil.

Electrical conductivity is estimated from the TDR trace using the signal amplitude from the TDR device v_0, the signal after the partial reflection from the start of the probe v_1, and the amplitude of the signal after the reflection from the end of the probe v_2 (Fig. C1). Thus calculation of electrical conductivity is as follows:

$$(v^2-v^1)/v_0 = (1-p^2)f^2 \tag{13}$$

The symbol, p, is the reflection of voltage signals at points A and B. The reflection at B is assumed to be a perfect reflection having a reflection coefficient of 1.

Rhoades (1984) demonstrated the simultaneous measurement of soil water and conductivity with a single probe. This was tested in field conditions by Dasberg & Dalton (1985), and good correlations were found between gravimetric determinations, and neutron probe estimates. While the potential of TDR for measuring soil electrical conductivity has been shown by several authors (Dalton & Van Genuchten 1986, Dasberg & Nadler 1987, Zegelin, White & Jenkins 1989), the present review is limited to the application of the technique for measurement of soil water content.

TDR EQUIPMENT

Instrumentation for determining TDR has been described by various authors (Topp *et al.* 1984;

Zegelin, White & Jenkins 1989; Reeves & Smith 1992). The basic design is a probe comprising parallel rods or wave guides which act as a balanced transmission line and are connected to an oscilloscope (Fig. C2). When the probe is inserted into the soil, the soil around and between the wave guides also becomes part of the transmission line. The dielectric constant of the soil is determined by interpreting the reflected signal on the oscilloscope of the Time Domain Reflectometer (Topp *et al.* 1982).

One of the disadvantages of the first TDR system was that the coaxial transmission line used in the laboratory situation was unsuitable for the field. A later development was the use of the more convenient and practical parallel pair transmission lines, consisting simply of two parallel rod conductors embedded in the soil. This resulted in signal and information loss at the coaxial cable/probe interface. To overcome this, shielded twin lead TV antenna cable was connected from each soil transmission line to a common plug-in board or switching apparatus mounted on a post. This impedance matching transformer, called a balun, is situated between the balanced TDR lines and the unbalanced line. The Anzac model TP103 balun has been used successfully for this purpose (Topp & Davis 1985: Patterson & Smith 1985: Stein & Kane 1983) The balun is connected to coaxial cable on its unbalanced side and to about 100mm length of balanced cable

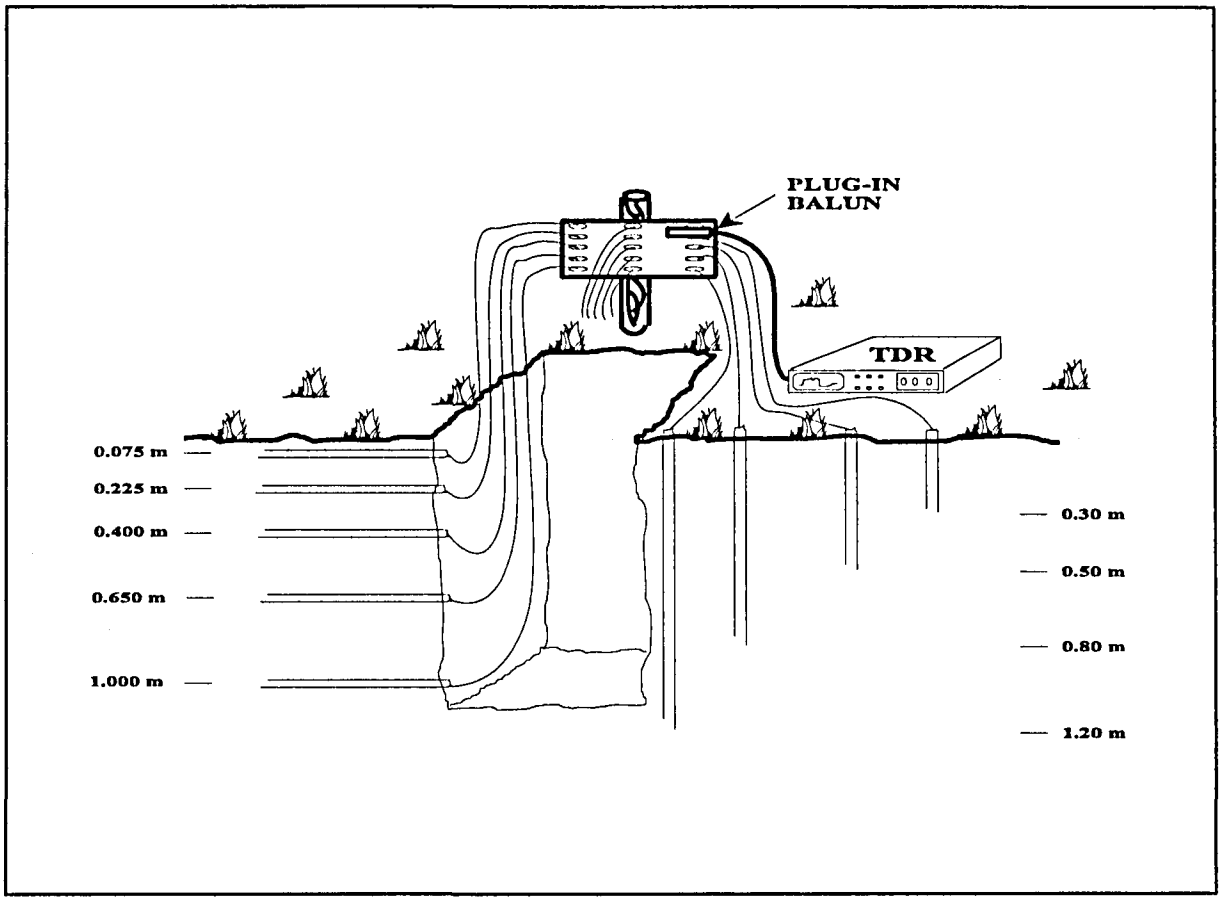

Figure C2. A diagrammatic representation of the TDR transmission line installations. (From Topp *et al.* 1983.

on the other side. After the electrical connections are made, this apparatus is encased in resin for water proof protection. The other end of the balanced cable is connected to a pair of pin plugs for attachment to the plug-in board.

While the balun solves the problem of information loss, the transformer itself could be a source of noise. This led to the development of improved three and four-wire probes by Zegelin, White & Jenkins (1989). These probes emulate coaxial transmission line cells and minimize impedance mismatch which occurred with the two-wire probes. These authors found that the improved probes were more precise, less noisy and enabled soil sample diameters to be extended to at least 0.2 metres.

A number of TDR instruments that are battery powered and portable for easy use in field measurements are now available commercially. One of the most commonly used is the Tektronix model 1502 cable tester described by Topp (1987). The cable tester produces a low-frequency analog output that can be plotted on an X-Y plotter, transmitted to a computer for analysis or displayed on a cathode ray tube screen and photographed. Travel times have usually been determined by graphical interpretation as described by Topp *et al* (1982a) and Hayhoe, Topp & Bailey 1983. From the travel times one can calculates the water content using equations (9) and (10).

Foundation Instruments of Ottowa, Canada have developed a convenient TDR field instrument, the IRAMS (Instrument for Reflectometry Analysis of Moisture In Soil), which automatically measures the travel times, solves equations (9) and (10) and displays θ_v (Topp 1987). The unit is battery operated, has data storage and downloading capability, and can accommodate a variety of operator-selected TDR line lengths.

TDR TRANSMISSION LINE INSTALLATION

Installation of transmission lines may be either vertical or horizontal lines (Fig. 2). Baker & Lascano (1989) found that the spatial resolution of TDR using horizontal lines is confined to an area of 1000mm^2 surrounding the wave guides, while the perpendicular plane is narrow (30mm). Thus a good resolution is obtained when the waveguides are horizontal. However, in areas where

frost is frequent, seasonal frost may displace horizontal probes. Topp (1987) recommends horizontal lines for water content profiles and vertical lines for total water estimates in the rooting zone. While vertical probes have less disturbance and involve less time to install, there can be a problem with preferential water movement along the vertical lines. Topp & Davis (1985) showed that both transmission lines have equivalent values, with horizontal lines having less variation. Ultimately, the choice of vertical versus horizontal depends on the application, type of information required and the period of observation (Patterson & Smith 1985).

Since soil water content usually exhibits considerable spatial variability, reliable measurements may be required at a number of sites each time. Topp & Davis (1981) demonstrated how this problem can be overcome by using transmission lines with electrical discontinuities. The lines are constructed with electrical impedance discontinuities filled with a dielectric material. The discontinuities provide the opportunity to measure water content profiles from a single transmission line rather than from a number of transmission line of various lengths at slightly different locations in the soil. However, some difficulties were encountered by Topp & Davis (1981) when using vertical lines with discontinuities in the field. The peaks on the TDR trace which corresponded to the 0.50- and 0.75-m discontinuities were not always detectable. In addition, the construction of lines with the discontinuities filled with dielectric material was labour intensive and time-consuming.

In many studies the change in water content with respect to time requires repeated measurements at the same site. A single unattended time-domain reflectometer can be used to obtain measurements of water content at multiple sites through automation and by multiplexing (Heimovaara & Bouten 1990, Reeves & Elgezawi 1992). Baker & Allmaras (1990) developed a system using a digital TDR apparatus (Tektronix Model 1502B) which interfaces with a microcomputer to control the TDR, operate the multiplexing system, and record and analyze the waveforms. The system comprises a 50-ohm coaxial cable which carries microwave pulses from the TDR and is connected through an impedance-matching transformer, or balun, to 186-ohm fully shielded TV-antenna wire. The antenna wire is connected to the input side of a 12-position, dual pole, rotary switch. The switches are turned by stepping solenoids that are activated by a datalogger and computer. The microwave pulse is carried along the antenna wire from each of the 11 pairs of output poles to waveguide pairs embedded at different locations in the soil. The

system uses software to automatically analyse the incoming waveforms and calculate volumetric water content.

One factor that has been open to debate in TDR transmission line installation is the spacing and diameter of rods. The volume measured by TDR can be varied by changing the separation of the wires making up the transmission lines (Keng & Topp 1983). The transmission lines associated with most TDR instruments are the coaxial or unbalanced type. The standard sizes of rods used in early studies were 6.4 mm or 12.7 mm in diameter (Topp *et al.* 1982). Although Topp & Davis (1985) used 12.7 mm diameter rods for vertical transmission lines, they found that it was unnecessary to use pilot holes if smaller diameter rods were used. They suggest using 3 mm diameter rods for lines up to 0.5 m long and 6 mm diameter rods for lengths greater than 0.5 m.

Reeves & Elgezawi (1992) used two stainless steel rods 10 cm long (6.4 mm diameter) mounted parallel with 4 cm spacing in a PVC plastic block. Stainless steel and PVC were used as the major construction materials because of their resistance. The balun transformer was mounted as close as possible to the top of the rods to minimize voltage loss after the electronic pulse was converted from an unbalanced to a balanced signal by the balun transformer. Concurrently, short waveguides (8.7 cm) extending beyond the PVC block) were used to further minimise the risk of complete voltage attenuation at high water contents. The use of short waveguides decreases the relative time base of the measurement. With a small time base the determination of breakpoints on the TDR trace and the calculation of ϵ are very sensitive to small errors.

If the wire diameter is small compared to the spacing between the electrodes, then a high-energy density develops around the wire (Knight 1992). This means that any local non-uniformities around the wires will have a great effect on the apparent measured water content of the sample. In order to minimize this the wire diameter should be as large as possible compared to the electrode spacing. This poses a dilemma as probes constructed of thin wire minimize soil compaction and disturbance. In addition, for probes embedded horizontally in a field soil Philip, Knight & Waechter (1989) show that the probe wires should be thin to avoid too much disturbance to downward flow and any consequent water build up on the upper surface. Knight (1992) recommends that the ratio of electrode spacing to wire diameter should not be greater than about 10. The design of a practical probe must be a compromise between these conflicting

requirements. Although there has been much debate over the pros and cons of horizontal and vertical lines, Topp, Davis & Annan (1982b) showed that the installation method & design of rods did not affect water content values if there was good electrical contact with the soil. In addition, TDR is not confined to shallow soil depths.

LIMITATIONS OF TDR

One of the critical factors that affects the accuracy of TDR measurements is that it is sensitive to the air gap effect, i.e. any air gap between probe and soil. To ensure good electrical contact with the soil, Patterson and Smith (1985) recommended the use of narrow pilot poles to prevent gaps between the soil and line resulting from probe installation. The air gap effect can also be minimized by the use of smaller diameter rods or tapered rods (Reeves & Smith 1992) Topp, Davis & Annan (1982) evaluated three methods of installation and several types of transmission line. They confirmed the necessity of good electrical contact between the rods and the soil. However, Dalton & Van Genechten (1986) found that TDR is not suitable for media with a high electrical conductivity, unless the path length is reduced.

Another limitation of TDR is that insertion of the horizontal probes disturbs the soil. Once installed, however, there is minimal disturbance.

A crucial question which arises when using the TDR technique is that of the volume of the surrounding soil for which the soil water content is sampled. Knight (1992) investigated the effect of spatial variation in the water content of a sample on the measured value of the water content for both the 'coaxial cylinders' probe and the 'two parallel wires' probe types. For coaxial probes most of the energy (and hence most of the measurement sensitivity) is concentrated around the inner cylinder in a "skin effect" if the ratio of the radii of the inner and outer cylinders is too small. For parallel wire probes, most of the measurement sensitivity is close to the wires if the wire diameter is too small compared to the spacing between them. This can cause significant errors if there is an air gap close to the wires or if the soil around the wires has been compacted by the process of inserting them into the soil.

One of the drawbacks of TDR is that the equipment is expensive (approximately R50 000), and

a high level of competence is required when setting up the system. However, once the system is in place, routine monitoring can be carried out by technical staff.

VALIDATION AND APPLICATION OF TDR

Several studies have shown that the accuracy of TDR measurements of soil water are comparable to that of standard techniques. For example, TDR measurements of soil water, using probes 100 mm or more in length, were as accurate and precise as those from gravimetric samples (Topp *et al.* 1984). Similarly, water content measurements obtained with TDR showed a good relationship to both gravimetric determinations ($r^2 = 0.84$) and neutron measurements (Dasberg & Dalton 1985). The accuracy of the technique for measuring *in situ* soil water in processed oil shale waste was demonstrated by Reeves & Elgezawi (1992).

Comparison between capacitance probes and TDR showed comparable and accurate results (Brisco & Pultz 1992). In general the TDR is suitable for 0-50 mm or deeper layers while the capacitance probe can be used for measuring layers of the order of 10 mm in thickness.

TDR is particularly useful in hydrological applications. Murphy & Black (1987) demonstrate its use in the characterization of moisture conditions and spatial variability on natural and simulated rainfall-runoff plots. TDR was used with an accuracy of +- 0.02 $cm^3.cm^{-2}$ to measure volumetric water content in soil columns in the laboratory (Keng & Topp 1983). Baker & Allmaras (1990) describe the application of the automated TDR system for measuring water profiles at 26 sites on an hourly basis. Since a TDR trace shows the impedance difference between wet and dry soil, TDR has also been successfully used in infiltration experiments. Topp, Davis & Annan (1982) show how it is possible to measure both the distance to the wetting front and the amount of water behind the wetting front during infiltration experiments. TDR has also been used successfully for detecting infiltration of water through soil cracks (Topp & Davis 1981). The TDR response in non-uniformly wet soils has been found to be as accurate as that in uniformly wet soils (Topp, Davis & Annan 1982a). TDR is therefore a viable method for detecting and monitoring the progression of wetting front advance through a soil. In addition, TDR is not confined to shallow soil depths. Topp, Davis, Bailey & Zebchuk (1984) describe the use of a hand probe and portable TDR instrument in the measurement of water content of soil in pits to a depth of greater than one

meter.

Another useful application of TDR is the measurement of moisture storage of the woody part of trees (Constantz & Murphy 1990). Wave guides driven into parallel pilot holes drilled into the woody parts of trees were used to determine the apparent dielectric constant. The method proved rapid and reliable and could be used where precise water balance calculations are required for forested watersheds. These authors also recommend TDR for the estimation of moisture stress for a given tree species.

In summary there are a number of features which suggest advantages to TDR:
1) non-destructive *in-situ* measurement of soil moisture and electrical conductivity (Dalton 1987),
2) the ability to take rapid readings (Reeves & Smith 1992 report that the measurement of the volumetric content of water in soil can be estimated in less than one minute),
3) calibration for different soil types is not necessary,
4) the sampling equipment is mobile and easy to use,
5) soil density, texture, salt content and temperature do not affect TDR,
6) real time measurements are possible because sampling by TDR is time efficient,
7) infiltration measurements enable wetting fronts to be followed very accurately, and
8) measurements of volumetric water content can be made from dry to nearly saturated conditions.

Given these features TDR is not surprisingly percieved more and more as the most viable and accurate option for measuring volumetric water content of *in situ* soils in the field.

References

Ansoult, M., De Baker, L.W. & Declercq, M. 1985. Statistical relationship between apparent dielectric constant and water content in porous media. *Soil Sci. Soc. Am. J.* 49:47-50.

Baker, J.M. & Allmaras, R.R. 1990. System for automating and multiplexing soil moisture

measurement by time-domain reflectometry. *Soil Sci. Soc. Am. J.* 54:1-6.

Baker, J.M. & Lascano, R.J. 1989. The spatial sensitivity of time-domain reflectometry. *Soil Sci.* 147:378-384.

Brisco, B. & Pultz, T.J. 1992. Soil moisture measurement using portable dielectric probes and time domain reflectometry. *Water Resources Research* 28:1339-1346.

Dalton, F.N. 1987. Measurement of soil water content and electrical conductivity using time-domain reflectometry. Proceedings of international conference on Measurement of Soil and Plant Water status. Vol. I.

Dalton, F.N., Herkelrath, W.N., Rawlins, D.S. & Rhoades, J.D. 1984. Time-domain reflectometry: Simultaneous measurement of soil water content and electrical conductivity with a single probe. *Science* 224:989-990.

Dalton, F.N. & Van Genuchten, M.T. 1986. The time-domain reflectometry method for measuring soil water content and salinity. *Geoderma* 38:237-250.

Dasberg, S. & Dalton, F.N. 1985. Time-domain reflectometry field measurements of soil water content and electrical conductivity with a single probe. *Soil Sci. Soc. Am. Jour.* 49:293-297.

Dasberg, S & Nadler, A. 1987. Field sampling of soil water content and bulk electrical conductivity with time domain reflectrometry. Proceedings of international conference on Measurement of Soil and Plant Water Status. Vol. I.

Davis, J.L. & Annan, A.P. 1977. Electromagnetic detection of soil moisture: Progress Report I, *Can. Jour. Remote Sensing* 3(1):76-86.

Edelefsen, N.E. 1933. A review of results of dielectric methods for measuring moisture present in materials. *Agr. Eng.* 14:243.

Fellner-Feldegg, H.R. 1969. The measurement of dielectrics in the time-domain. *J. of Phys. Chem.* 73(3):616-623.

Fletcher, J.R. 1939. A dielectric method of measuring soil moisture. *Soil Sci. Soc. Am. Proc.* 4:84-88.

Gardner, W.R. 1965. Water Content. In Methods of Soil Analysis I. Chpt. 7. pp. 82-127. Ed by Black, Evans, White, Ensminger and Clark. Number 9 in the series Agronomy. American Society of Agronomy Incc., Madison, Wisconsin, U.S.A.

Gardner, W.R. 1987. Water content: an overview. Proceedings of international conference on Measurement of Soil and Plant Water status. Vol. I.

Greacen, E.L. 1981. Soil water assessment by the neutron method. CSIRO, East Melbourne, Victoria, Australia.

Gurr, C.G. 1962. Use of gamma-ray in measurement of wter content and permeability in unsatureated columns of soil . *Soil Sci.* 94:224-229.

Hallikainen, M., Ulaby, F.T., Dobson, M.C. El-Rayes, M. & Wu, L.K. 1985. Microwave dielectric behaviour of wet soil I. Empirical models and experimental observations. *IEEE Trans. Geosci. Remote Sens.* 23:25-34.

Hayhoe, H.N., Topp, G.C. & Bailey, W.G. 1983. Measurement of soil water contents and frozen soil depth during a thaw using time-domain reflectometry. *Atmosphere-Ocean* 21: 1077-1084.

Heimovaara, T.J. & Bouten, W. 1990. A computer-controlled 36-channel time domain reflectometry for monitoring soil water contents. *Water Resour. Res.* 26(10):2311-2316.

Hoekstra, P. & Delaney, A.J. 1974. Dielectric properties of soils at VHF and microwave frequencies. *Jour. of Geophys. Res.* 79(11):1699-1708.

Keng, J.C.W. & Topp, G.C. 1983. Measuring water contents of soil columns in the laboratory: A comparison of gamma ray attenuation and TDR techniques. *Can. J. of Soil Sci.* 63(1):37-43.

Knight, J.H. 1992. Sensitivity of time domain reflectometry measurements to lateral variations in soil water content. *Water Resour. Res.* 28(9):2345-2352.

Murphy, M.R. & Back, L.B. 1987. Use of time domain reflectometry in a hydrological study. Proceedings of international conference on Measurement of Soil and Plant Water Status. Vol.3.

Patterson, D.E. & Smith, M.W. 1985. Unfrozen water content in saline soils: Results using time-domain reflectometry. *Can. Geotech. J.* 22(1):95-101.

Philip, J.R., Knight, J.H. & Waechter, R.T. 1989. Unsaturated seepage and subterranean holes: Conspectus, and exclusion problem for circular cylindrical cavities. *Water Resour. Res.* 25: 16-28.

Reeves, T.L. & Smith, M.A. 1992. Time domain reflectometry for measuring soil water content in range surveys. *J. Range Manage.*, in press.

Reeves, T.L. & Elgezawi, S.M. 1992. Time domain reflectometry for measuring volumetric water content in processed oil shale waste. *Water Resources Research* 28(3):769-776.

Reginato, R. & Nakayama, F.S. 1987. Plastic standards for transferring neutron probe calibrations. Proceedings of international conference on Measurement of Soil and Plant Water status. Vol. I.

Rhoades, J.D. 1984. Time-domain reflectometry: Simultaneous measurement of soil water content and electrical conductivity with a single probe. *Science* 224:989-990.

Savage M.J. 1982. Measurement of water potential using thermocouple hygrometers. PhD.

Thesis, University of Natal.

Topp, G.C. 1987. The application of time-domain reflectometry (TDR) to soil water content measurement. Proceedings of international conference on Measurement of Soil and Plant Water status. Vol. I.

Topp, G.C., Davis, J.L. 1981. Detecting the infiltration of water through soil cracks by time-domain reflectometry. *Geoderma* 26(1-2):13-23.

Topp, G.C., Davis, J.L. 1985. Measurement of soil water content using time-domain reflectometry (TDR): A field evaluation. *Soil Sci. Soc., Am. J.* 49::19-24.

Topp, G.C., Davis, J.L. & Annan, A.P. 1980. Electromagnetic determination of soil water content: Measurements in coaxial transmission lines. *Water Resources Research.* 16(3):574-582.

Topp, G.C., Davis, J.L. & Annan, A.P. 1982. Electromagnetic determination of soil water using TDR: I. Applications to wetting fronts and steep gradients. *Soil. Sci. Soc. Am. J.* 46(4):672-678.

Topp, G.C., Davis, J.L. & Annan, A.P. 1982. Electromagnetic determination of soil water using TDR: II. Evaluation of installation and configuration of parallel transmission lines. *Soil. Sci. Soc. Am. J.* 46(4):678-684.

Topp, G.C., Davis, J.L., Bailey, W.G. & Zebchuk, W.D. 1984. The measurement of soil water content using a portable TDR hand probe. *Can. J. Soil Sci.* 64:313-321.

von Hippel, A. 1953. Dielectrics. In: Candon and Odishaw (Editors), Handbook of Physics. McGraw-Hill, New York.

Wallihan, E.F. 1945. Studies of the dielectric method of measuring soil moisture. *Soil Sci. Soc. Am. Proc.* 10:39-40.

Wang, J.R. & Schmugge, T.J. 1980. An empirical model for the complex permittivity of soil as a function of water content. *IEEE Trans. Geosci. Remote Sens.* 18:288-295.

Wobschall, D. 1978. Afrequency shift dielectric soil moisture sensor. *IEEE Trans. On Geoscience Electronics.* 16: 112-118.

Zegelin, S.J., White, I. & Jenkins, D.R. 1989. Improved field probes for soil water content and electrical conductivity measurement using time domain reflectometry. *Water Resour. Res.* 25: 2367-2376.

Appendix D:

THE ACRU MENU USED FOR STREAMFLOW SIMULATIONS

```
 Mode of simulation (point/lumped vs distributed)
   -------------------------------------------------
ICELL
,,,,I
  0
    Distributed model specifications
   ----------------------------------
 ISUBNO MINSUB MAXSUB LOOPBK
,,,,III,,,,III,,,,III,,,,,,I
    1    1    1    0
   Hydrograph routing options
   ---------------------------
 IROUTE DELT
,,,,,,I,FFFF.F
    0 1440.0
     Subcatchment configuration information
   ----------------------------------------
ICELLN IDSTRM PRTOUT
,,,III,,,,III,,,,,,F
   0    0    0                                    1
     Rainfall file organisation
   ---------------------------
IRAINF
AAAAAAAAAAAAAAAAAAAAAAAAAAAAAAAAAAAAAAAAAAAAAAAAAAAAAAAAAAAAAAAAAAAAAAAAAAAAAAA
AAAAAAAA
c:\acru323\compo.dat                                  1

    Rainfall information
   ----------------------
 FORMAT PPTCOR   MAP
,,,,,,F,,,,,,F,,IIIII
    1    1  1299                                  1

    Monthly rainfall adjustment factors, CORPPT(i)
   ------------------------------------------------
 JAN FEB MAR APR MAY JUN JUL AUG SEP OCT NOV DEC
,F.FF,F.FF,F.FF,F.FF,F.FF,F.FF,F.FF,F.FF,F.FF,F.FF,F.FF,F.FF
 1.06 1.06 1.06 1.06 1.06 1.06 1.06 1.06 1.06 1.06 1.06 1.06              1

    Availability of observed streamflow data
   ------------------------------------------
IOBSTQ IOBSPK IOBOVR
,,,,,I,,,,,,I,,,,,,I
   1    0    0                                    1

    Streamflow file organisation
   ------------------------------
ISTRMF
AAAAAAAAAAAAAAAAAAAAAAAAAAAAAAAAAAAAAAAAAAAAAAAAAAAAAAAAAAAAAAAAAAAAAAAAAAAAAAA
AAAAAAAA
                                                1
```

```
 Dynamic file option
    --------------------
DNAMIC
F
0                                              1

    Dynamic file organisation
    --------------------------
IDYNFL
AAAAAAAAAAAAAAAAAAAAAAAAAAAAAAAAAAAAAAAAAAAAAAAAAAAAAAAAAAAAAAAAAAAAAAAAA
AAAAAAAA
fdg                                            1

    General heading of simulation
    ------------------------------
HEAD
AAAAAAAAAAAAAAAAAAAAAAAAAAAAAAAAAAAA
C6 - composite file                                1

    Locational information
    -----------------------
 CLAREA   ELEV  ALAT ALONG IHEMI IQUAD
FFFFF.FF,FFFF.F,FF.FF,FF.FF,,,,,I ,,,,I
   .68 1950.0 29.00 29.25    2    1                   1

    Period of record for simulation
    ---------------------------------
IYSTRT IYREND
,,IIII,,,IIII
   0    0                                      1

    Simulation printout options
    ----------------------------
WRIDY WRIMO
,,,,F,,,,,F
  0    1                                       1

    Statistical output options (I)
    -------------------------------
SUMMRY ICOMPR
,,,,FF,,,,,,I
  1    0                                       1

    Statistical output options (II)
    --------------------------------
ICOMPV LOGVAL
,,,,,,I,,,,,,I
   0    0                                      1

    Monthly means of daily max temperature, TMAX(i)
    ------------------------------------------------
 JAN  FEB  MAR  APR  MAY  JUN  JUL  AUG  SEP  OCT  NOV  DEC
,FFF.F,FFF.F,FFF.F,FFF.F,FFF.F,FFF.F,FFF.F,FFF.F,FFF.F,FFF.F,FFF.F,FFF.F
 26.0 25.6 24.6 22.3 19.9 17.3 17.6 19.7 22.0 23.1 24.0 25.6    1
```

```
   Monthly means of daily min temperature, TMIN(i)
   -----------------------------------------------
  JAN  FEB  MAR  APR  MAY  JUN  JUL  AUG  SEP  OCT  NOV  DEC
,FFF.F,FFF.F,FFF.F,FFF.F,FFF.F,FFF.F,FFF.F,FFF.F,FFF.F,FFF.F,FFF.F,FFF.F
 13.9 13.7 12.4  9.0  5.5  2.6  2.4  4.5  7.5  9.7 11.4 13.0     1

#   Reference potential evaporation control variables
   -------------------------------------------------
EQPET
,,FFF
 102                                          1

   Evaporation input availability control flags
   --------------------------------------------
 IEIF ILRF IWDF IRHF ISNF IRDF IPNF
,,,,,I,,,,,I,,,,,I,,,,,I,,,,,I,,,,,I
   1    0    0    0    0    0    0                  1

   Means of monthly totals of pan evaporation, E(i)
   ------------------------------------------------
  JAN  FEB  MAR  APR  MAY  JUN  JUL  AUG  SEP  OCT  NOV  DEC
,FFF.F,FFF.F,FFF.F,FFF.F,FFF.F,FFF.F,FFF.F,FFF.F,FFF.F,FFF.F,FFF.F,FFF.F
 187.3 158.8 147.0 122.3 105.8  95.5 107.0 134.4 159.9 176.4 175.9 198.5     1

   Temperature adjustment for altitude
   -----------------------------------
 TELEV LRREG
FFFF.F,,,,II
1040.0    0                                    1

   Mean lapse rates for min and max temperatures
   ---------------------------------------------
 TMAXLR  TMINLR
FFFF.FF,FFFF.FF
  7.00    5.50                                  1

   Mean daily windspeed (m/s)
   --------------------------
WNDSPD
,,FF.F
  1.6                                          1

   Windspeed region number
   -----------------------
LINWIN
,,,III
   1                                           1

   Monthly means of daily windrun (km/day), WIND(i)
   ------------------------------------------------
  JAN  FEB  MAR  APR  MAY  JUN  JUL  AUG  SEP  OCT  NOV  DEC
,FFF.F,FFF.F,FFF.F,FFF.F,FFF.F,FFF.F,FFF.F,FFF.F,FFF.F,FFF.F,FFF.F,FFF.F
 160.0 187.0 185.0 150.0 180.0 179.0 185.0 240.0 228.0 235.0 185.0 183.0     1
```

Monthly means of daily average relative humidity, RH(i)

```
 JAN FEB MAR APR MAY JUN JUL AUG SEP OCT NOV DEC
,FF.F,FF.F,FF.F,FF.F,FF.F,FF.F,FF.F,FF.F,FF.F,FF.F,FF.F,FF.F
 79.0 81.0 76.0 69.0 58.0 52.0 49.0 51.0 60.0 69.0 77.0 79.0          1
```

Monthly means of daily hours of sunshine, ASSH(i)

```
 JAN FEB MAR APR MAY JUN JUL AUG SEP OCT NOV DEC
,FF.F,FF.F,FF.F,FF.F,FF.F,FF.F,FF.F,FF.F,FF.F,FF.F,FF.F,FF.F
  .70   0   0                                          1
```

Penman equation control variables

```
ALBEDO ICONS ISWAVE
,,F.FF,,,,,I,,,,,I
  .0  .0  .1  .1  .0  .0  .0  .0  .0  .0  .0  .0          1
```

"A" coefficient in Penman equation, ACONS(i)

```
 JAN FEB MAR APR MAY JUN JUL AUG SEP OCT NOV DEC
,F.FF,F.FF,F.FF,F.FF,F.FF,F.FF,F.FF,F.FF,F.FF,F.FF,F.FF,F.FF
 .27 .27 .28 .24 .24 .25 .24 .21 .23 .23 .22 .24          1
```

"B" coefficient in Penman equation, BCONS(i)

```
 JAN FEB MAR APR MAY JUN JUL AUG SEP OCT NOV DEC
,F.FF,F.FF,F.FF,F.FF,F.FF,F.FF,F.FF,F.FF,F.FF,F.FF,F.FF,F.FF
 .52 .49 .52 .52 .51 .50 .51 .55 .57 .56 .58 .54          1
```

Monthly means of daily incoming radiation, RADMET(i)

```
 JAN FEB MAR APR MAY JUN JUL AUG SEP OCT NOV DEC
,FF.F,FF.F,FF.F,FF.F,FF.F,FF.F,FF.F,FF.F,FF.F,FF.F,FF.F,FF.F
 12.0 12.0 12.0 12.0 12.0 12.0 12.0 12.0 12.0 12.0 12.0 12.0          1
```

Penman equation option for either S-tank or A-pan equivalent evaporation

```
SAPANC
,,,,,I
   1                                          1
```

Smoothed mean monthly A-pan/S-pan ratios, SARAT(i)

```
 JAN FEB MAR APR MAY JUN JUL AUG SEP OCT NOV DEC
,F.FF,F.FF,F.FF,F.FF,F.FF,F.FF,F.FF,F.FF,F.FF,F.FF,F.FF,F.FF
 1.25 1.26 1.27 1.27 1.31 1.34 1.36 1.37 1.35 1.32 1.28 1.27          1
```

Pan adjustment option

```
PANCOR
,,,,,F
   0                                          1
```

```
   Monthly pan adjustment factors, CORPAN(i)
   ----------------------------------------
 JAN FEB MAR APR MAY JUN JUL AUG SEP OCT NOV DEC
,F.FF,F.FF,F.FF,F.FF,F.FF,F.FF,F.FF,F.FF,F.FF,F.FF,F.FF,F.FF
 1.25 1.26 1.27 1.27 1.31 1.34 1.36 1.37 1.35 1.32 1.28 1.27          1

#    Level of soils information
   ---------------------------
PEDINF
,,,,,F
   1                                          1

   Soils texture information
   -------------------------
 ITEXT
,,,,II
   11                                         1

   Soil physics based infiltration/soil water redistribution option
   ----------------------------------------------------------------
REDIST
,,,,,F
   0                                          1

   Rainfall intensity distribution type
   ------------------------------------
IRDIST
,,,,,I
   1                                          1

   Soil thickness information
   --------------------------
 PEDDEP
,,,,,,F
   2                                          1

   Soils information (adequate)
   ----------------------------
DEPAHO DEPBHO  WP1  WP2  FC1  FC2  PO1  PO2 ABRESP BFRESP
,FF.FF,,FF.FF,.FFF,.FFF,.FFF,.FFF,.FFF,.FFF,,FF.FF,,FF.FF
  .25    .25 .250 .245 .420 .420 .550 .550    .65    .50          1

   Shrink-swell soils option
   -------------------------
ICRACK
,,,,,I
   0                                          1

   Initial values of soil water retention constants
   ------------------------------------------------
 SMAINI SMBINI
,FFF.FF,FFF.FF
  80.00  80.00                                    1
```

```
    Option for statistical analysis of soil water regime
    ----------------------------------------------------
SWLOPT
,,,,,F
    0                                          1

    Soil water content thresholds for A horizon, SWLAM(i)
    -----------------------------------------------------
  1    2    3    4    5    6
,,F.FFF,,F.FFF,,F.FFF,,F.FFF,,F.FFF,,F.FFF
  .018  .050  .100  .150  .200  .300                    1

    Soil water content thresholds for B horizon, SWLBM(i)
    -----------------------------------------------------
  1    2    3    4    5    6
,,F.FFF,,F.FFF,,F.FFF,,F.FFF,,F.FFF,,F.FFF
  .018  .050  .100  .150  .200  .300                    1

#    Level of land cover information
    --------------------------------
LCOVER
,,,,,I
    1                                          1

    Land cover number information
    -------------------------------
   CROPNO
,,,FFFFFFF
  2030306                                        1

    Determination of canopy interception loss
    -----------------------------------------
INTLOS
,,,,,I
    1                                          1

    Leaf area index information
    ---------------------------
 LAIND
,,,,,I
    0                                          1

    Monthly means of crop coefficients, CAY(i)
    ------------------------------------------
 JAN FEB MAR APR MAY JUN JUL AUG SEP OCT NOV DEC
,F.FF,F.FF,F.FF,F.FF,F.FF,F.FF,F.FF,F.FF,F.FF,F.FF,F.FF,F.FF,F.FF
 .70 .70 .65 .50 .20 .20 .20 .20 .35 .45 .55 .65             1

    Monthly means of leaf area index, ELAIM(i)
    ------------------------------------------
 JAN FEB MAR APR MAY JUN JUL AUG SEP OCT NOV DEC
,F.FF,F.FF,F.FF,F.FF,F.FF,F.FF,F.FF,F.FF,F.FF,F.FF,F.FF,F.FF,F.FF
 .00 .00 .00 .00 .00 .00 .00 .00 .00 .00 .00 .00             1
```

Canopy interception loss (mm) per rainday, VEGINT(i)

```
 JAN FEB MAR APR MAY JUN JUL AUG SEP OCT NOV DEC
,F.FF,F.FF,F.FF,F.FF,F.FF,F.FF,F.FF,F.FF,F.FF,F.FF,F.FF,F.FF
 1.30 1.30 1.30 1.30 1.30 1.30 1.30 1.30 1.30 1.30 1.30 1.30          1
```

Fraction of active root system in topsoil horizon, ROOTA(i)

```
 JAN FEB MAR APR MAY JUN JUL AUG SEP OCT NOV DEC
,F.FF,F.FF,F.FF,F.FF,F.FF,F.FF,F.FF,F.FF,F.FF,F.FF,F.FF,F.FF
  .92  .92  .92  .95 1.00 1.00 1.00 1.00  .95  .92  .92  .92          1
```

Effective total rooting depth

```
EFRDEP
FFF.FF
  .00                                                  1
```

Total evaporation control variables

```
 EVTR FPAW
,,,,F,,,,F
   1   0                                               1
```

Fraction of PAW at which plant stress sets in

```
CONST
FF.FF
 .40                                                   1
```

Critical leaf water potential

```
 CRLEPO
FFFFF.F
   .0                                                  1
```

Option for enhanced wet canopy evaporation

```
FOREST
,,,,,F
   0                                                   1
```

Option for simulation under enhanced atmospheric CO2 levels

```
CO2TRA
,FFF.F
   .0                                                  1
```

Mean temperature threshold (°C) for active growth to take place

```
TMPCUT
,,FF.F
 10.0                                                  1
```

Unsaturated soil moisture redistribution

IUNSAT

,,,,,I

1 1

Option for lysimeter routine

LYSIM

,,,,I

0 1

Streamflow sim

Appendix E

DAY OF YEAR CALENDAR

	1	2	3	4	5	6	7	8	9	10	11	12	13	14	15	16	17	18	19	20	21	22	23	24	25	26	27	28	29	30	31
JAN	1	2	3	4	5	6	7	8	9	10	11	12	13	14	15	16	17	18	19	20	21	22	23	24	25	26	27	28	29	30	31
FEB	32	33	34	35	36	37	38	39	40	41	42	43	44	45	46	47	48	49	50	51	52	53	54	55	56	57	58	59	60		
MAR	*60*	*61*	*62*	*63*	*64*	*65*	*66*	*67*	*68*	*69*	*70*	*71*	*72*	*73*	*74*	*75*	*76*	*77*	*78*	*79*	*80*	*81*	*82*	*83*	*84*	*85*	*86*	*87*	*88*	*89*	*90*
APR	*91*	*92*	*93*	*94*	*95*	*96*	*97*	*98*	*99*	*100*	*101*	*102*	*103*	*104*	*105*	*106*	*107*	*108*	*109*	*110*	*111*	*112*	*113*	*114*	*115*	*116*	*117*	*118*	*119*	*120*	
MAY	*121*	*122*	*123*	*124*	*125*	*126*	*127*	*128*	*129*	*130*	*131*	*132*	*133*	*134*	*135*	*136*	*137*	*138*	*139*	*140*	*141*	*142*	*143*	*144*	*145*	*146*	*147*	*148*	*149*	*150*	*151*
JUN	*152*	*153*	*154*	*155*	*156*	*157*	*158*	*159*	*160*	*161*	*162*	*163*	*164*	*165*	*166*	*167*	*168*	*169*	*170*	*171*	*172*	*173*	*174*	*175*	*176*	*177*	*178*	*179*	*180*	*181*	
JUL	*182*	*183*	*184*	*185*	*186*	*187*	*188*	*189*	*190*	*191*	*192*	*193*	*194*	*195*	*196*	*197*	*198*	*199*	*200*	*201*	*202*	*203*	*204*	*205*	*206*	*207*	*208*	*209*	*210*	*211*	*212*
AUG	*213*	*214*	*215*	*216*	*217*	*218*	*219*	*220*	*221*	*222*	*223*	*224*	*225*	*226*	*227*	*228*	*229*	*230*	*231*	*232*	*233*	*234*	*235*	*236*	*237*	*238*	*239*	*240*	*241*	*242*	*243*
SEP	*244*	*245*	*246*	*247*	*248*	*249*	*250*	*251*	*252*	*253*	*254*	*255*	*256*	*257*	*258*	*259*	*260*	*261*	*262*	*263*	*264*	*265*	*266*	*267*	*268*	*269*	*270*	*271*	*272*	*273*	
OCT	*274*	*275*	*276*	*277*	*278*	*279*	*280*	*281*	*282*	*283*	*284*	*285*	*286*	*287*	*288*	*289*	*290*	*291*	*292*	*293*	*294*	*295*	*296*	*297*	*298*	*299*	*300*	*301*	*302*	*303*	*304*
NOV	*305*	*306*	*307*	*308*	*309*	*310*	*311*	*312*	*313*	*314*	*315*	*316*	*317*	*318*	*319*	*320*	*321*	*322*	*323*	*324*	*325*	*326*	*327*	*328*	*329*	*330*	*331*	*332*	*333*	*334*	
DEC	*335*	*336*	*337*	*338*	*339*	*340*	*341*	*342*	*343*	*344*	*345*	*346*	*347*	*348*	*349*	*350*	*351*	*352*	*353*	*354*	*355*	*356*	*357*	*358*	*359*	*360*	*361*	*362*	*363*	*364*	*365*

Add 1 to italic values during leap years.